Gas/Solid and Gas/Particle Partitioning of Polychlorinated Dibenzodioxins,
Polychlorinated Dibenzofurans and Polycyclic Aromatic Hydrocarbons to
Filter Surfaces and Ambient Atmospheric Particulate Material
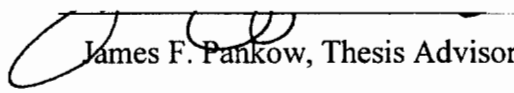
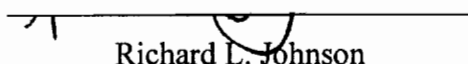Brian T. Mader

B.S. University of Minnesota, 1993
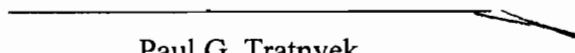
M.S., University of Minnesota, 1996

A dissertation presented to the faculty of the

Oregon Graduate Institute of Science and Technology

in partial fulfillment of the

requirements for the degree

Doctor of Philosophy

in

Environmental Science and Engineering

April, 2000

The dissertation "Gas/Solid and Gas/Particle Partitioning of Polychlorinated Dibenzodioxins, Polychlorinated Dibenzofurans and Polycyclic Aromatic Hydrocarbons to Filter Surfaces and Ambient Atmospheric Particulate Material" by Brian T. Mader has been examined and approved by the following Examination Committee:

James F. Pankow, Thesis Advisor
Department Chairman, Professor

Richard L. Johnson
Associate Professor

Paul G. Tratnyek
Associate Professor

Dr. Willam Asher
University of Washington

ii

ACKNOWLEDGEMENTS

The time I have spent at OGI has been one of tremendous scientific and personal growth, in which my advisor Jim Pankow has played a very important role. I would like to thank him for helping mold me into a better scientist and technical writer. I would also like to thank him for his financial support, professional and personal advice as well as his insightful suggestions both in the lab and on the mountain! Jim provided me with opportunities, too numerous to mention here. I truly enjoy and value his friendship.

I would like to thank my thesis committee, Rick Johnson, Paul Tratnyek and William Asher for their insightful comments. Specifically I would like to thank Rick for sharing his GC/MS, Paul for his help regarding statistical analysis and for providing me with several speaking opportunities and William Asher for his help regarding optimization routines and the Solver option in Excel.

I would like to thank the staff who make OGI such a friendly and efficient place to conduct research: Lorne Isabelle is such an important part of OGI, his resourcefulness helped keep my project moving along and his humor always brightened my day. Wentai Luo gave me several helpful suggestions regarding the design and construction of my air sampler and frequently let me bounce ideas off of him. Linda Wolf guided me through the OGI administration system, Donna Reid made sure all my sampling equipment was delivered on time and in one piece and Carol Resco performed numerous Chemical Abstracts searches for me.

I would like to thank the graduate students who enriched my OGI experience. My labmates, Cikui Liang and Andrea Pavlick provided helpful discussions regarding my research. Jay Hollingsworth introduced me to nighttime single track mountain biking (I enjoyed our rides on the Wildwood trail) as well as the art of scrumpy brewing. Michelle Scherer gave me insight into the academic world and also helped coordinate my sampling trip to the University of Iowa. Jeff Darland provided many free computer consultations

TABLE OF CONTENTS

LIST OF TABLES

LIST OF FIGURES

xv

NOTATION

p_S^o (torr)	partial pressure over a pure solid phase compound
p_L^o (torr)	sub-cooled liquid vapor pressure of a compound
#Cl	number of chlorines present on molecule
ξ	a compound's solid phase activity coefficient
γ	activity coefficient of a compound in a GC column stationary phase
ζ_{om}	activity coefficient of a compound of interest in OM on a mole fraction scale
ΣPAH c_p(ng/μg)	sum of the particle-phase concentration of fluorene, phenanthrene, anthracene, fluoranthene, pyrene, benz(a)anthracene and chrysene
ACU	air conditioning unit
a_f (m^2/g)	filter specific surface area
A_{filter} (cm^2)	filter face area of a filter
a_{tsp} (m^2/g)	surface area of particle phase
b_L	intercept of a log p_L^o vs. 1/T plot
b_r	intercept of log K_p vs. log p_L^o plot
$b_{r,s}$	intercept of log $K_{p,s}$ vs. log p_L^o plot
CF	conversion factor relating OM to OC
c_g (ng/m^3)	gas-phase concentration of a compound
$c_{g,corrected}$ (ng/m^3)	corrected measured gas-phase concentration of a compound
$c_{g,eq}$ (ng/m^3)	equilibrium gas phase concentration of a compound
c_p (ng/μg)	particle-phase concentration of a compound
$c_{p,corrected}$ (ng/μg)	corrected measured particle-phase concentration of a compound
$c_{p,measured}$ (ng/μg)	measured particle-phase concentration of a compound

c_p^{g-1} (kJ/mole °C)	a compound's heat capacity as a liquid phase
c_{TMF} (ng /µg)	TMF-sorbed concentration of a compound
EC	particle-phase elemental carbon
ECU	environmental chamber unit
ETS	environmental tobacco smoke
$F_{adsorbent}$ (ng)	mass of a compound collected on a sorbent material
F_{filter} (ng)	mass of an individual compound adsorbed on the filter surface
f_{oc} (µg OC/µg)	weight fraction of particle phase OC
f_{om} (µg OM/µg)	weight fraction of particle phase OM
$F_{particle}$ (ng)	mass of an individual compound present in/on collected particles
FTE	flow-through extraction
GC-RI	gas chromatograph retention index
GFF	glass fiber filter
$\Delta H_{vap}(T_m))$ (kJ/mole)	a compound's enthalpy of vaporization from it's liquid phase at the melting point
$\Delta H_{vap,}$ (kJ/mol)	a compound's enthalpy of vaporization from it's liquid phase
K_p (m³/µg)	gas/particle partitioning coefficient of a compound
$K_{p,corrected}$ (m³/µg)	corrected measured gas/particle partition coefficient a compound
$K_{p,exchangeable}$ (m³/µg)	gas/particle partition coefficient of a compound for partitioning to a completely exchangeable particle
$K_{p,measured}$ (m³/µg)	measured gas/particle partition coefficient a compound
$K_{p,non-exchangeable}$ (m³/µg)	gas/particle partition coefficient of a compound for partitioning to a particle having a non-exchangeable fraction
$K_{p,oc}$ (m³/µg OC)	K_p value normalized by f_{oc}
$K_{p,om}$ (m³/µg OM)	K_p value normalized by f_{om}
$K_{p,s}$ (m³/m²)	surface-area-normalized gas/solid partition coefficient of a compound
$K_{p,x}$ (m³/cm²)	partition coefficient of a compound expressed as [ng sorbed/cm² of filter face] / [ng/m³ in gas phase]

m_{eq} (ng)	total mass of a compound found on the two filters at apparent equilibrium
M_{filter} (μg)	mass of the filter
m_L	slope of log p_L^o vs. 1/T plot
$M_{PAH,exchangeable}$ (ng)	mass of a compound present in/on a particle that is exchangeable
$M_{PAH,non-exchageable}$ (ng)	mass of a compound present in/on a particle that is non-exchangeable
$M_{particle}$ (μg)	mass of particulate material
m_r	slope of log K_p vs. log p_L^o plot
$m_{r,s}$	slope of log $K_{p,s}$ vs. log p_L^o plot
MW_{om} (g/mol)	mean molecular weight of OM
n	moles of compound
OC	particle-phase organic carbon
OM	particle-phase organic matter
PAH	polycyclic aromatic hydrocarbon
PCDD	polychlorinated dibenzodioxin
PCDF	polychlorinated dibenzofuran
p_{gc} (torr)	vapor pressure measured using GC-RI method
p_{gen} (atm)	absolute pressure at the exit of the generator cartridge
PUF	polyurethane foam plug
p_{water} (atm)	partial pressure of water vapor at the relative humidity and temperature of interest
Q_d (kJ/mol)	a compound's enthalpy of desorption from a solid surface
QFF	quartz fiber filter
Q_v (kJ/mol)	a compound's enthalpy of vaporization from it's liquid phase
$Q_v(T_b)$ (kJ/mol)	a compound's enthalpy of vaporization from it's liquid phase at the boiling point
R (atm L/mole K)	gas constant of 0.0821
RH	relative humidity
SA (m²)	surface area

SOA	secondary organic aerosol
SOC	semivolatile organic compound
T (°C)	temperature
TGFF	Teflon-coated glass fiber filter
T_m (K)	melting point of a compound
TMF	Teflon membrane filter
TSP (μg /m^3)	total suspended particulate material
UPM	urban particulate material
V (m^3)	volume
V_t (m^3)	total air sample volume
$V_{t,min}$ (m^3)	minimum air sample volume required to reach gas/filter sorption equilibrium for a given compound and sampler configuration
$V_{t,filter}$ (m^3)	minimum air sample volume required to reach gas/filter sorption equilibrium on a single filter for a given compound
x	mole fraction of a compound in a mixture
x_{ne}	percent of a particle that is non-exchangeable

ABSTRACT

Gas/Solid and Gas/Particle Partitioning of Polychlorinated Dibenzodioxins, Polychlorinated Dibenzofurans and Polycyclic Aromatic Hydrocarbons to Filter Surfaces and Ambient Atmospheric Particulate Material

Brian T. Mader

Oregon Graduate Institute of Science and Technology, 2000

Supervising Professor: James F. Pankow

Atmospheric transport has been considered to be the dominant process responsible for the movement of polychlorinated dibenzodioxins (PCDDs), polychlorinated dibenzofurans (PCDFs), polycyclic aromatic hydrocarbons (PAHs) from combustion sources to remote receptors such as lake sediments, soils, and grasses. PCDD/Fs and PAHs are considered semi-volatile organic compounds (SOCs) and are distributed between the gas (G) and particle (P) -phases in the atmosphere. A G/P partition coefficient (K_p) is defined as the ratio of the concentration of compound associated with the P-phase (c_p) to the concentration of the compound in the gas phase (c_g). The c_g and c_p of a given SOC are obtained from field measurements. Sampling artifacts can bias these values and preclude a mechanistic level understanding of the G/P partitioning process.

Controlled field experiments (CFEs) represent a new approach, which minimizes sampling artifacts. Results are presented from field trials of CFEs conducted in Beaverton, OR Denver, CO and Hills, IA. The adsorptive affinity of two types of filters for gaseous PCDD/Fs and PAHs was compared and a model developed to predict the

magnitude of the influence of gas adsorption artifacts on measurements of c_g, c_p and K_p. The vapor pressures of 13 PCDD/Fs and 6 PAHs were measured and several vapor pressure prediction techniques were evaluated using the new vapor pressure data. Parameters are given for calculating the p_L^o value of each of the 210 PCDD/F congeners as function of temperature. K_p values were normalized by the weight fraction of P-phase organic carbon (f_{oc}) and organic matter phase (f_{om}). There was less variation in the $K_{p,oc}$ and $K_{p,om}$ values of compounds with similar p_L^o values among locations than for K_p values. Among the three field locations and three studies from the literature, the K_p values of PAHs with similar p_L^o values varied by over 2.5 orders of magnitude; the $K_{p,om}$ and $K_{p,oc}$ values varied by one order of magnitude. Variation in the $K_{p,om}$ values of a given compound among locations may be due to error in the conversion factor relating f_{oc} to f_{om} and/or differences in the chemical composition of particulate organic matter phases among locations and/or sources of particles.

CHAPTER 1

INTRODUCTION

1.1 Overview

The term semi-volatile organic compounds (SOCs) refer to organic compounds having vapor pressures between 10^{-11} and 10^{-4} atm (Bidleman, 1988). In the presence of suspended atmospheric particulate matter, SOCs will be distributed between the gas (G) and (P) particle phases. The extent to which an SOC is associated with the P phase will be controlled in large part by the concentration of total suspended particle (*TSP*) concentration and the compound's subcooled liquid vapor pressure (p_L^o) (Pankow, 1987).

Many organic contaminants of interest are considered semi-volatile, examples are; polycyclic aromatic hydrocarbons (PAHs), the polychlorinated dibenzodioxins and dibenzofurans (PCDD/Fs), polychlorinated biphenyls (PCBs), organic pesticides such as lindane, malathion and DDT, components of tobacco smoke such as nicotine, and finally many aromatic organic compounds comprising secondary organic aerosols present in urban smog (Odum, Hoffman *et al.* (1996). In order to understand the environmental behavior of these contaminants, it is important to quantify the extent to which an SOC is distributed between the G and P phases: the processes affecting the fate and transport of these phases differ significantly. For example, compounds in the G phase will be able to undergo direct air/water exchange, whereas a particle bound compound cannot. Moreover, it has been suggested that for PCDD/Fs degradation via OH radicals can occur for congeners present in the G phase whereas compounds in the P phase react more slowly (Brubaker and Hites, 1997). The physiological activity of a compound may also be affected its G/P distribution. Compounds present on particles greater than 4.0 µm are typically deposited in the bronchial tree of the upper respiratory tract and are removed to

the stomach (Lippmann and Albert, 1969). In contrast, G-phase compounds reach the alveolar region of the lung.

1.2 Theory

At a given temperature, the distribution of a compound between the G and P phases has been well parameterized using the G/P partition coefficient, K_p ($m^3/\mu g$) (Yamasaki, Kuwata et al. 1982; Bidleman, Billings et al., 1986; Bidleman and Foreman, 1987; Pankow, 1991; Pankow and Bidleman, 1992):

$$K_p = (F/TSP) / A \qquad (1.1)$$

Where: F = concentration of compound associated with the P phase (ng/m^3);

TSP = the total suspended particle concentration ($\mu g/m^3$); and A = the G phase concentration of the compound (ng/m^3). When based on sampling results, the G and P phase concentrations are operationally defined. Thus, F gives the portion of the compound that is retained on a filter, and A gives the portion which passes through the filter and is collected on a sorbent material.

When G/P partitioning occurs by the *ad*sorption of an SOC to the surface of a particle, K_p is as follows (Pankow (1987):

$$K_p = N_s \, a_{tsp} \, T \exp \left[(Q_d - Q_v) / RT \right] / 1600 \; p_L^o \qquad (1.2)$$

where: N_s is the number of surface sites per cm^2 of particulate surface area; a_{tsp} is the specific surface area of the atmospheric particulate material (m^2/g); T is the temperature (K); Q_d (kcal/mole) is the compound's enthalpy of desorption directly from the surface; Q_v (kcal/mol) the compound's enthalpy of vaporization as a liquid; R is the gas constant; and p_L^o is the sub-cooled liquid vapor pressure (torr).

When an SOC partitions from the G phase into an organic matter phase (OM) present on a particle, K_p is as follows (Pankow (1994):

$$K_p = f_{om} \, 760 \, RT / \zeta_{om} \, MW_{om} \; p_L^o \; 10^6 \qquad (1.3)$$

where: f_{om} = weight fraction that is absorbing organic material phase; ζ_{om} = the activity coefficient of the compound of interest in the organic material on a mole fraction scale; MW_{om} = the mean molecular weight of the absorbing organic material phase (g/mol).

1.3 Rationale

Compound-dependent values of K_p can usually be correlated using the corresponding values of p_L^o (torr) (Pankow, 1987; 1994a; 1994b). In the general case, we have:

$$\log K_p = m_r \log p_L^o + b_r \qquad adsorptive\ or\ absorptive\ partitioning \qquad (1.4)$$

Values of the slope m_r are frequently close to -1. A major goal of environmental chemists is to predict the environmental fate of an organic compound. Correlations of the form of Equation 1.4 have been used to predict the G/P partitioning behavior of SOCs of environmental concern. To construct a correlation of $\log K_p$ vs. $\log p_L^o$, the K_p value of a given compound is calculated from field measurements of F and A for that compound at a given location (reference location). Field measurements are made over a period of time ranging from 6 hours to one month. In typical studies, K_p values are determined for a series of compounds of a certain class of SOCs (i.e PAHs, PCDD/Fs, PCBs) spanning a three order of magnitude range of p_L^o. The value of p_L^o for a given compound at the average T observed during field sampling is obtained from the literature.

When a correlation of $\log K_p$ vs. $\log p_L^o$ is used to predict the G/P partitioning behavior of a given compound at a given location (test location) the accuracy of the prediction depends in part on 1) the accuracy of the F and A measurements of the given SOC. 2) The similarity of the chemical composition of the particle phase between the test and reference locations and 3) if the T at the test and reference locations is different, the accuracy of the p_L^o value of a given SOC as a function of T. (Note when evaluating the mechanisms of G/P partitioning, the accuracy of the p_L^o value of a given SOC̄ at the T observed at the reference location is also important)

Pankow and Bidleman (1991) and Hart and Pankow (1994) have shown that measurements of the F and A values of a given compound can be affected by sampling artifacts caused by T and RH fluctuations during sampling, and the adsorption of gaseous SOC to filter surfaces. For SOCs that are absorbed into OM, if the OM content and/or chemical composition of the test and reference P phases is/are different, there will be error in the K_p estimates for the test location (Equation 1.3). For many classes of SOCs, only predicted or indirect measurements of p_L^o as a function of T are available; and for

compounds such as PCDD/Fs these data are not known for the majority of the congeners. When measurements of the p_L^o value of a given SOC do exist, it is not uncommon to find order of magnitude variation among the literature values. If the source of the p_L^o values is different for the test and reference locations error in the predicted K_p values may result. The overall goal of this research project was to gain a better understanding of how the physical-chemical properties of an SOC and a P-phase affect the G/P distribution of an SOC and to improve the accuracy and universality of the log K_p vs. log p_L^o correlations of the PCDD/Fs and PAHs.

1.4 Experiments

The G/P partitioning behavior of two classes of SOCs were studied. Due to their significant human toxicity and in the case of the PCDD/Fs, a lack of G/P partitioning data, the SOCs studied were the PCDD/Fs and PAHs. To improve the accuracy of K_p measurements a new air sampler was constructed which minimizes T and RH fluctuations during air sampling. Backup filters were used to correct for gas adsorption artifacts. Furthermore, the adsorptive affinity of two commonly used filters (Teflon membrane and quartz fiber) for gaseous PCDD/Fs and PAH was compared and a model developed which can be used to predict the magnitude of the bias in F, A and K_p values as caused by the adsorption of gaseous SOCs to filter surfaces. The vapor pressures of several PAH and PCDD/Fs were directly measured and this data used to evaluate current vapor pressure estimation techniques. For the PCDD/Fs a correlation between p_L^o and gas chromatographic retention index (RI) was observed. This correlation and predicted values of the enthalpy of evaporation (H_{vap}) and the heat capacity (c_p^{l-g}) were used to determine the p_L^o values of all 210 PCDD/Fs as a function of T. Field experiments were conducted at a number of locations to determine the K_p values of PAH and PCDD/F, the organic (OC), elemental (EC) and inorganic carbon (IC) content of particle phases collected during these field experiments was also measured. Values of f_{om} were estimated using measured OC values and an assumption regarding the chemical composition of OM. Measured K_p values were normalized by f_{om} to account for differences in the OM content of the particulate material among the different locations.

1.5 Format of thesis

The format the thesis is that of a compilation of six individual manuscripts suitable for publication.

1.6 References

Bidleman, T. F. 1988. Atmospheric processes- wet and dry deposition of organic compounds are controlled by their water vapor partitioning. *Environmental Science and Technology* 22, 361-367.

Bidleman, T. F. *et al.* 1986. Vapor-particle partitioning of semivolatile organic compounds: estimates from field collections. *Environmental Science and Technology* 20, 1038-1043.

Bidleman, T. F., Foreman, W. T. 1987. Vapor-particle partitioning of semivolatile organic compounds. In *Sources and Fates of Aquatic Pollutants*. Eds. R. A. Hites and S. J. Eisenreich. New York, ACS. pp. 27-56.

Brubaker, W. W., Hites, R. A. 1997. Polychlorinated dibenzo-p-dioxins and dibenzofurans: gas-phase hydroxyl radical reactions and related atmospheric removal. *Environmental Science and Technology* 31, 1805-1810.

Hart, K. M., Pankow, J. F. 1994. High volume air sampler for particle and gas sampling 2. Use of backup filters to correct the adsorption of gas phase polycylic aromatic hydrocarbons to the front filter. *Environmental Science and Technology* 28, 655-661.

Lippmann, M., Albert, R. 1969. The effect of particle size on the regional deposition of inhaled aerosols in the human respiratory tract. *American Industrial Hygiene Journal* 30, 257-275.

Odum, J. R. *et al.* 1996. Gas/particle partitioning and secondary organic aerosol yields. *Environmental Science and Technology* 30, 2580-2585.

Pankow, J. F. 1987. Review and comparative analysis of the theories on partitioning between the gas and aerosol particulate phases in the atmosphere. *Atmospheric Environment* 21, 2275-2283.

Pankow, J. F. 1991. Common y-intercept and single compound regressions of gas-particle partitioning data vs. 1/T. *Atmospheric Environment* 25A, 2229-2239.

Pankow, J. F. 1994. An absorption model of gas/particle partitioning of organic compounds in the atmosphere. *Atmospheric Environment* 28, 185-188.

Pankow, J. F. 1994. An absorption model of the gas/aerosol partitioning involved in the formation of secondary organic aerosol. *Atmospheric Environment* 28, 189-193.

Pankow, J. F., Bidleman, T. F. 1991. Effects of temperature, TSP, and percent non-exchangeable material in determining the gas-particle partitioning of organic compounds. *Atmospheric Environment* 25, 2241-2249.

Pankow, J. F., Bidleman, T. F. 1992. Interdependence of the slopes and intercepts from log-log correlations of measured gas-particle partitioning and vapor pressure: Part 1 theory and analysis of available data. *Atmospheric Environment* 26A, 1071-1080.

Yamasaki, H. *et al.* 1982. Effects of ambient temperature on aspects of airborne polycyclic aromatic hydrocarbons. *Environmental Science and Technology* 16, 189-194.

CHAPTER 2
GAS/SOLID PARTITIONING OF POLYCHLORINATED DIBENZODIOXINS, POLYCHLORINATED DIBENZOFURANS AND POLYCYCLIC AROMATIC HYDROCARBONS TO FILTER SURFACES: TEFLON MEMBRANE FILTERS

2.1 Introduction

Semivolatile organic compounds (SOCs) have been classified as compounds with vapor pressures between $\sim10^{-11}$ and $\sim10^{-4}$ atm. SOCs of interest include the polychlorinated dibenzodioxins (PCDDs), polychlorinated dibenzofurans (PCDFs), polycyclic aromatic hydrocarbons (PAHs), polychlorinated biphenyls (PCBs), organic pesticides (*e.g.*, lindane, malathion, DDT), and the compounds which condense to form secondary organic aerosols (Pankow, 1994; Odum *et al.*, 1996, 1997). When sampling atmospheric SOCs, a variety of types of filters are commonly used to separate the particle- and gas-phase portions of these compounds, including Teflon membrane filters (TMFs), Teflon-coated glass fiber filters (TGFF), and quartz fiber filters (QFFs). Unfortunately, the adsorption of gaseous SOCs to filter surfaces can cause positive biases in measured particle-phase concentration values (c_p, ng/µg), and negative biases in measured gas-phase concentration values (c_g, ng/m^3) (McDow and Huntzicker, 1990; Hart and Pankow, 1994; Turpin and Huntzicker, 1994; Mader and Pankow, 2000a). Gas/particle partitioning can be parameterized using the coefficient K_p (m^3/µg):

$$K_p = c_p / c_g \qquad (2.1)$$

For PAHs, biases in the measured c_p and c_g values caused by gas/filter adsorption have been found to be capable of causing K_p values to be overestimated by factors of 1.2 to 1.6 (Hart and Pankow, 1994). As in gas/particle partitioning, gas/filter partitioning can be characterized by a K_p coefficient. By definition, gas/filter adsorption artifacts will be small when the amounts of SOCs adsorbed on the filters are small compared to the amounts in/on the collected particles. This condition will be achieved when the gas/filter K_p values for the compounds of interest are low, and/or the particle loading on the filter is

7

high. When gas/filter partitioning occurs by adsorption, normalizing gas/filter K_p by the specific surface area a_f (m^2/g) of the filter yields

$$K_{p,s} \ (m^3/m^2) \ = \ K_p \ (m^3/\mu g) \ / \ [10^{-6} \ (g/\mu g) \cdot a_f \ (m^2/g)] \qquad (2.2)$$

For a given sampling event, predicting the compound-dependent magnitudes of the artifact for gaseous SOCs adsorbing to filters requires knowledge of the gas/particle K_p values, the level of total suspended particulate material (TSP, μg/m) in the atmosphere, the length of time over which sampling takes place, the gas/filter $K_{p,s}$ values for the compounds and filter type of interest. For TMF a predictive analysis of the magnitude of this artifact is currently not possible since there are few data for the gas/solid partitioning of SOCs to TMFs. The goal of the present work was to measure $K_{p,s}$ values for a range of PAHs, PCDDs, and PCDFs adsorbing to TMFs. We note that $K_{p,s}$ for Teflon will also be useful for predicting the magnitudes of wall losses of SOCs in Teflon bag experiments such as those conducted by Kamens, J.R.Odum *et al.* (1995), Odum et al. (1996) and Liang, Pankow *et al.* (1997).

2.2 Experimental

2.2.1 TMFs. The TMFs (2 μm pore size, 100 mm diameter) were obtained from Pall-Gelman Sciences (Ann Arbor, MI). Each TMF was precleaned by washing three times with 50 mL of methylene chloride. For each experiment, two TMFs were held overnight at a relative humidity (RH) of 65%, then weighed and loaded into a filter holder. Blank TMFs sent to Micrometrics (Norcross, GA) yielded a specific surface area value of 0.21 m^2/g. A typical TMF weighed about 1.3 g.

2.2.2 Clean TMF Experiments - Specifics. Ambient, outdoor air was first cleaned of particles and gaseous SOCs by passage through a glass fiber filter (GFF) then through a 178 mL polyurethane foam (PUF) plug (Figure 2.1). The cleaned air was then drawn into a air conditioning unit (ACU) in which the air passed through a 45 cm long, 0.95 cm i.d. stainless steel tube in a water bath; the temperature sensor governing the heating/cooling of the water bath was located in the stainless steel filter holder containing the TMFs. The expected mean outdoor temperature for the experimental period was selected as the set-point temperature for the experiment, *i.e.* for the water bath. The air
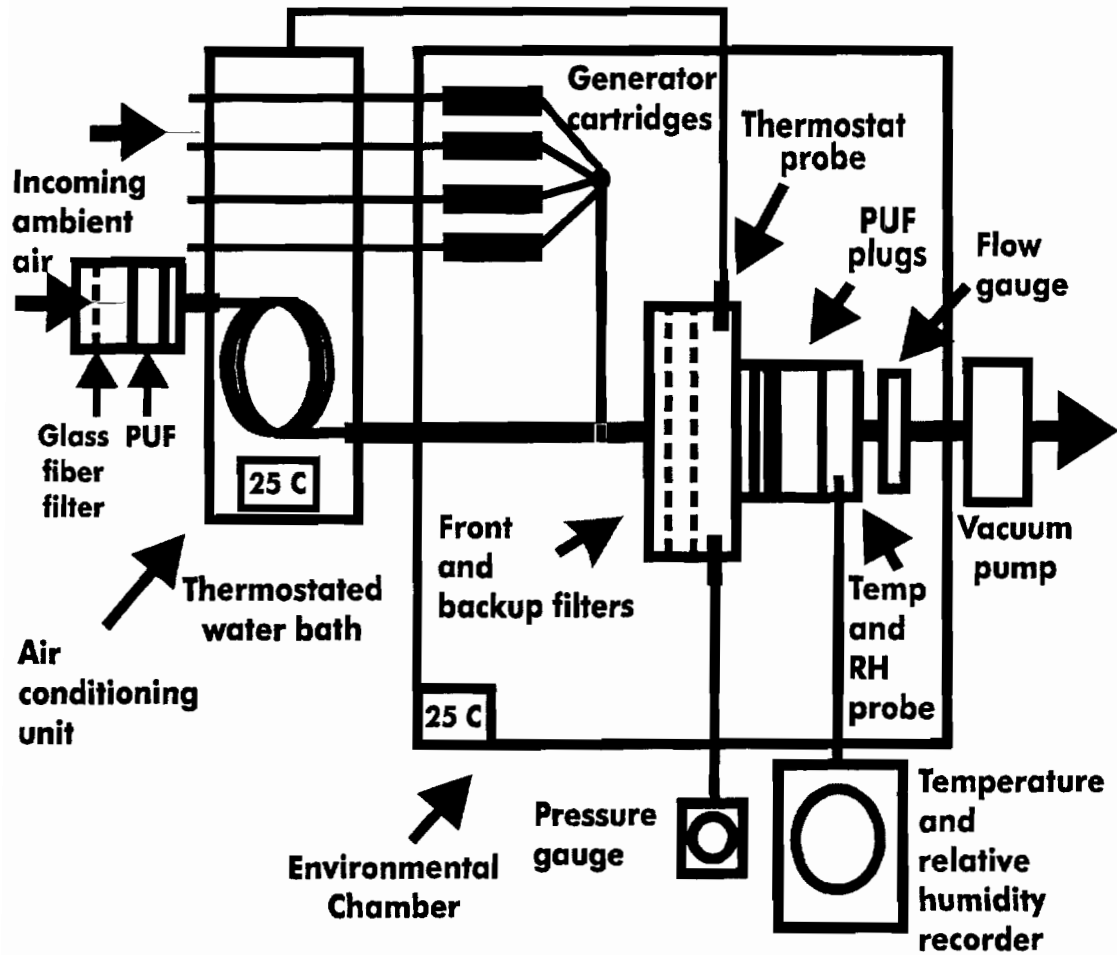
Figure 2.1 Apparatus used to study PAH and PCDD/F gas/solid partitioning.

produced by the ACU was characterized by that temperature, and by a nearly-constant RH. (During stable meteorological conditions, air parcels do not tend to mix vertically, and the water content expressed in ppmV will generally stay constant. Under these conditions, adjusting the air temperature to a constant value will maintain a near-constant RH.) The RH was measured using an Omega CTH89 temperature/humidity recorder (Omega Engineering, Stamford, CT). The air produced by the ACU was drawn into an environmental chamber unit (ECU) in which SOCs were added; the air was then equilibrated with the TMFs. The ECU was set at the same temperature as the CTU. SOCs were added to the air flow in the ECU by routing a small portion (5 L/min) of the incoming air through SOC "generator cartridges". This flow was then mixed back into the main flow at a point upstream of the filter holder. After the filter holder, the air was directed through a 24 mL front PUF plug, followed by a 178 mL backup PUF plug (PUF density = 0.022 g/mL).

2.2.3 Ambient Backup TMF Experiments - Specifics. Ambient atmospheric particles were first collected using a 20.32 cm × 25.4 cm front/backup TMF combination located in the filter holder of a conventional high-volume air sampler for a period of 11-430 hours. The three sampling sites used were located as follows: University of Colorado at Denver (urban), Oregon Graduate Institute, Beaverton, OR (suburban), and Hills Observatory, Hills, Iowa (rural/farm). Once an adequate amount of particulate material had been collected to allow gas/particle K_p values to be measured using the ACU/ECU apparatus, particle collection on the TMFs was halted. A 100 mm diameter punch of the front/backup filter pair was then loaded into the filter holder of the ECU. A GFF was placed in front of the TMF filter holder as in the clean TMF experiments, and T/RH regulation of the air was begun using the ACU. In contrast to the clean TMF experiments, PUF plugs were not placed after the GFF; the gaseous organic compounds passing through the GFF were allowed to continue on to the TMF thereby minimizing the desorption "stripping" of organic compounds from the particles. Once it entered the ECU, the air flow was handled as in the clean TMF experiments: SOCs were added upstream of the filter holder, and PUF plugs were positioned downstream of the filter holder for purposes of determining the c_g values to which the collected particles and

TMFs were exposed. (The data on sorption to the collected particles will be presented elsewhere.)

2.2.4 Clean and Ambient Backup TMF Experiments – General. The total air flow rate through the TMFs was constant within every experiment, but ranged from 11 to 72 L/min among the different experiments depending on the particle loading of the front filter. A flow rate was chosen such that the pressure drop across the filters was less than 0.1 atm (40 inches of H_2O). The duration of each experiment depended on the air temperature and front filter particle loading, lasting from 1.5 days to 21 days, using a total air volume V_t between 55 and 920 m^3. Colder temperatures required longer experimental times because the gas/TMF partition coefficients (and gas/particle partition coefficients for the ambient backup TMF experiments) were correspondingly larger.

The PUF plugs behind the TMFs were changed at intervals that ranged from 10 minutes to 20 hours; the sample volumes for those intervals ranged from 0.6 to 70 m^3. At the point that an experiment was ended, for each SOC of interest, it was considered likely that gas/TMF equilibrium had been achieved if: 1) the gas phase concentration exiting the filter (as measured with the PUF plugs) had approached an asymptotic equilibrium value (designated as $c_{g,eq}$); and 2) V_t was at least twice the volume required to deliver the total mass that was found sorbed on the two TMFs, *i.e.*,

$$V_t \geq 2 m_{eq} / c_{g,eq} \tag{2.3}$$

Where: m_{eq} is the sum of the mass found on the two filters at apparent equilibrium. Equation 2.3 assumes that the gas concentration entering the filter equaled $c_{g,eq}$ for the entire duration of the experiment

2.2.5 Extractions. Immediately after an experiment, each TMF was spiked with four surrogate standard solutions: 4 μL of 250 ng/μL perdeuterated fluorene in hexane; 4 μL of 250 ng/μL perdeuterated pyrene in hexane; 16 μL of 50 ng/μL fully-^{13}C labeled 1234 F in toluene; and 16 μL of 50 ng/μL fully-^{13}C labeled 2,7+2,8 D in toluene. Each filter was then extracted four times; 25 mL of methylene chloride and 10 minutes of sonication was used each time. The four extracts were combined, and concentrated to 2 mL using rotoevaporation. Each 2 mL extract was transferred to a precleaned 4 mL mini-vial and stored at -20 °C. Immediately before analysis by GC/MS, each extract was gently blown down to 200 μL using a stream of ultra-clean N_2, then spiked with 2000 ng

of perdeuterated phenanthrene. All deuterated and ^{13}C-labeled compounds were obtained from Cambridge Isotope Labs (Andover, MA). No cleanup was necessary.

The extracts were analyzed on a Hewlett Packard 5890/5971 GC/MS using a 30 m × 0.25 mm DB-5 fused silica capillary column (J&W Scientific Folsom, Ca). Each extract was injected "splitless" with the injector at 280 °C. The GC temperature program was: 100 to 200 °C at 4 °C/min; 200 to 250°C at 5 °C/min; hold isothermal at 250°C for 5 min. The MS was operated in electron impact mode. The PAH standard solution contained fluorene, fluorene-d$_{10}$, phenanthrene, phenanthrene-d$_{10}$, anthracene, fluoranthene, pyrene, pyrene-d$_{10}$, benz(a)anthracene, and chrysene. The PCDD/F standard solution contained the compounds 2 F, 28 F, 246 F, 238 F, 1378 F, 2378 F, 12378 F, 23478 F, 1 D, 2 D, 23 D, 28 D, 124 D, 1234 D, 2378 D, 12478 D, 12378 D, and the two fully-^{13}C-labeled internal standard compounds (all from Cambridge Isotopes Labs). Response factors for the PAHs and PCDD/Fs were determined as a function of mass injected. The internal standard compound for the PAHs was phenanthrene-d$_{10}$. The internal standard compounds for the PCDD/Fs were the ^{13}C-labeled PCDD/Fs.

Each PUF plug was extracted using a flow-through extraction (FTE) method (Maddalena *et al.*, 1998). In this method, each PUF plug was first compressed into a glass syringe that was about half the volume of the non-deformed plug. After being spiked with the surrogate standard solutions, each PUF plug was then extracted with a volume of methylene chloride that was twice the volume of the non-deformed PUF plug (40 to 200 mL). Each extract was concentrated to 4 mL using rotoevaporation. Analysis proceeded as with the TMF extracts.

2.2.6 QA/QC. Blank filters and PUF plugs were extracted regularly. Except for chrysene, the blank levels were always less than 5% of the total mass measured for each compound on the filters and PUF plugs. For chrysene, when the blank amount corresponded to more than 10% of the sample amount, a $K_{p,s}$ value was not computed for that experiment. For the PAHs, absolute recoveries from the PUF plugs and TMFs averaged 111% and 107% respectively. For the PCDD/Fs, they averaged 65% and 92% respectively. For the PUF plugs behind the TMF filter holder, at the warmest experimental temperature used (26 °C), breakthrough from the front to backup plug averaged 60, 5, and 7% for fluorene, phenanthrene, and anthracene, respectively, and 15,

8, and 9% for 1 F, 1 D and 2 D, respectively. Breakthrough was negligible for the other compounds at 26 °C. Since the volume of the 178 mL backup PUF plug was over seven times that of the 24 mL front PUF plug, when combined, both plugs provided essentially quantitative recoveries for all compounds at all experimental temperatures.

2.3 Theory

Compound-dependent values of log K_p can usually be correlated using the corresponding values of the sub-cooled liquid vapor pressure p_L^o (torr) (Pankow, 1987, 1994a, 1994b). In the general case, we have

$$\log K_p = m_r \log p_L^o + b_r \qquad \text{adsorptive or absorptive partitioning} \qquad (2.4)$$

Values of the slope m_r are frequently close to -1. When the partitioning takes place by adsorption, consideration of Equation 2.2 leads to

$$\log K_{p,s} = m_{r,s} \log p_L^o + b_{r,s} \qquad \text{adsorptive partitioning} \qquad (2.5)$$

where $m_{r,s} = m_r$. Equation 2.5 has been applied in studies of the gas/solid partitioning of n-alkanes and PAHs to quartz (Storey et al., 1995), and of aromatic volatile organic compounds (VOCs) to soot carbon (Goss and Eisenreich, 1997).

For adsorptive partitioning, within a given compound class, the slope m_r will be close to -1 when there is compound-to-compound constancy in $(Q_d - Q_v)$, which is the difference between the enthalpy of desorption from the surface and the enthalpy of vaporization from the pure liquid. Although Pankow (1987), Pankow and Bidleman (1992), Pankow and Bidleman (1991) have provided detailed discussions of how measured values of m_r can come to be different from -1, such deviations have been incorrectly interpreted by some as being necessarily indicative of non-equilibrium biases in the corresponding measured values of K_p (or $K_{p,s}$). Goss and Schwarzenbach (1998) recently revisited some of the reasons why true equilibrium values of m_r can differ from -1. Using data for VOCs, Goss and Schwarzenbach (1998) derived a semi-empirical equation to predict $K_{p,s}$ values of organic compounds based primarily on the van der Waals and Lewis acid-base properties of the sorbing compound and solid surface. However, the ability of this equation to predict the gas/solid partitioning of SOCs to Teflon surfaces has not been tested.

2.4 Results

2.4.1 Gas/TMF Partitioning Equilibrium.

As equilibrium between each TMF and the gaseous SOCs was approached, the gas-phase concentration of each SOC in the air exiting the filter approached an asymptotically constant value of $c_{g,eq}$ (*e.g.*, see Figure 2.2). For the PAHs, $c_{g,eq}$ was computed as the average of the measured c_g values once c_g varied by no more than $\pm 10\%$. For the PCDD/Fs, the criterion was variation by no more than $\pm 20\%$. Values of K_p are reported here only for those cases when the Equation 2.3 criterion was satisfied.

2.4.2 Sorption Isotherms.

Sorption isotherms of the TMF-sorbed concentration c_{TMF} (ng/m^2) *vs.* $c_{g,eq}$ were constructed at 25 °C for five of the six PAHs and eight of the twelve PCDD/Fs. Isotherms could not be constructed for the most non-volatile PAH and PCDD/Fs since a sufficiently wide range of c_g values could not be measured for these compounds with the current experimental methodology. For the compounds tested isotherms covered at least a factor two, and in some cases up to three orders of magnitude in $c_{g,eq}$ (Figures 2.3a and b). All six PAHs and eight PCDD/Fs exhibited isotherm r^2 values of ≥ 0.99. The slopes of the isotherms for the PAHs and for 2 F, 238 F, and 1 D were not statistically different from 1.0. For 28 F, 246 F, 2 D, 28 D, and 124 D, although the slopes of the isotherms (1.14, 1.07, 1.08, 1.15, and 1.13 respectively) were statistically different from 1.0 (95% confidence level), the deviations were small.

2.4.3 Effects of RH on Partitioning.

The measured $K_{p,s}$ values for TMFs exhibited little dependence on RH in the range RH = 21 to 52% (25 °C, Figures 2.4, 2.5a and b). In contrast, for partitioning of PAHs to QFFs, Storey *et al.*, (1995) observed a factor of two decrease in the $K_{p,s}$ values over the same RH range, and increasing RH has been observed to decrease the partitioning of SOCs (and VOCs) to other mineral surfaces (Goss, 1992, 1993; Storey *et al.* 1995; Goss and Eisenreich, 1996, 1997). The mechanism underlying this effect for mineral surfaces is believed to be a displacement/blocking by water molecules of non-polar SOCs from polar sorption sites as the RH increases. The fact that an RH effect was not observed for the TMFs is probably due to the fact that water does not interact in any specific manner with the hydrophobic Teflon surface. Thus, at low to intermediate RH values, water is less likely
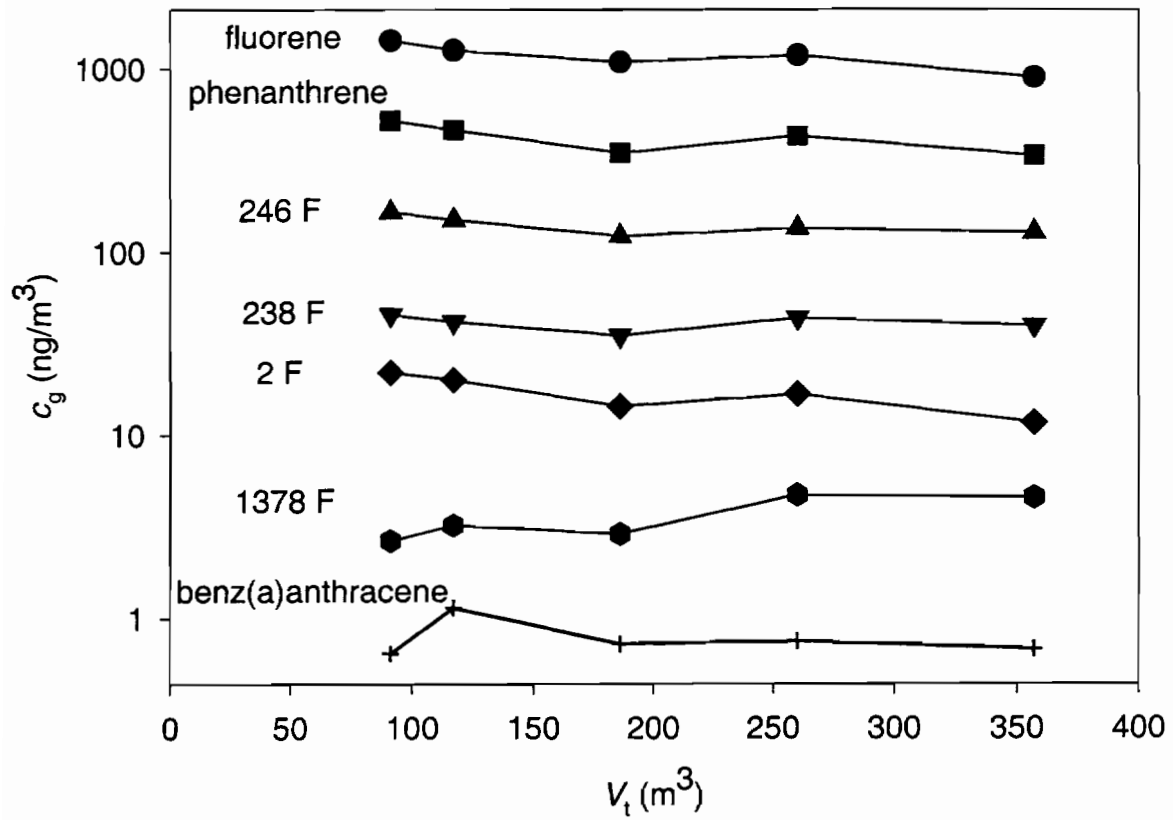
Figure 2.2 Gas phase concentration (c_g) of selected PAH and PCDD/Fs as a function of the volume (V_t) of air passed through the TMF filters.

to displace SOC molecules from a Teflon surface. At very high RH values approaching 100%, however, condensation of water onto a Teflon surface will become unavoidable, and the sorption properties of a Teflon surface might become different from what was observed in the RH range studied here.

2.4.4 Effects of Temperature on Partitioning. The effects of temperature T (K) on the measured $K_{p,s}$ values were studied over the range 285 K to 299 K. A 10 degree increase in T resulted in decreases in the $K_{p,s}$ values of the PAHs, PCDFs and PCDDs by factors of 2.4, 3.1 and 3.4, respectively. As seen in Figures 2.6a and b, the sorption data display typical van't Hoff behavior, and are correlated according to:

$$\log K_{p,s} = m_{p,s} / T + b_{p,s} \qquad (2.6)$$

Values of $m_{p,s}$ and $b_{p,s}$ were evaluated using the common y-intercept regression (CYIR) method of Pankow (1991). Briefly, Pankow (1991) has shown that it is likely that values of $b_{p,s}$ will be the similar within a given class of compounds. The Solver option in Excel (Microsoft, Redmond WA) was used to perform the CYIR. Table 2.1 gives the measured values of $m_{p,s}$ and $b_{p,s}$. Table 2.2 gives the compound-dependent values of Q_v, along with the enthalpies of desorption Q_d (kJ/mol) calculated according to:

$$Q_d = 2.303 \text{ R } m_{p,s} \qquad (2.7)$$

where R is the gas constant. For physical adsorption, Goss and Eisenreich (1996) have discussed that a generally linear relationship can be expected between $K_{p,s}$ and Q_d. Such a relationship was observed in this study, with the highest values of $K_{p,s}$ observed for those compounds with the largest values of Q_d.

The data in Table 2.1 indicate that $Q_d < Q_v$ for all of the PAHs and PCDD/Fs. When $Q_d < Q_v$ for a compound, the attractive interactions between the compound and the surface are weaker than the interactions within the pure compound as a subcooled liquid. This is the behavior that was expected for the non-interacting Teflon surface.

2.4.5 log $K_{p,s}$ vs. log p_L^o Correlations. The measured values of log $K_{p,s}$ were well correlated with the corresponding log p_L^o values (Figures 2.7a and b). For the PAHs, the temperature-dependent log p_L^o values used were based on the data set of Yamasaki *et al.*(1984); for the PCDD/Fs, the data set of Mader and Pankow (2000b) was used to provide the temperature-dependent log p_L^o values. The slope and intercept
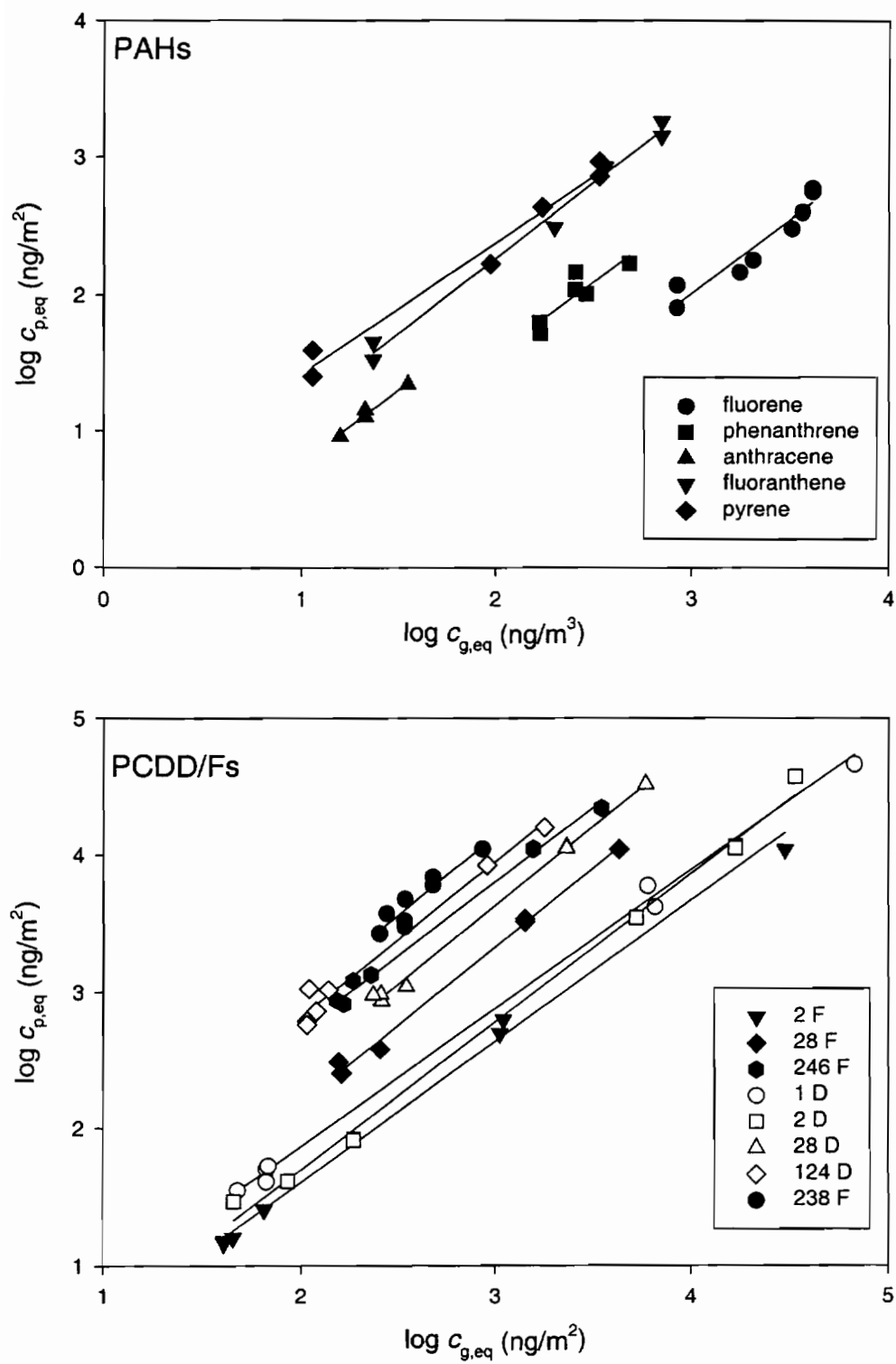
Figure 2.3 Sorption isotherms of selected compounds at 25 °C **a.** PAHs **b.** PCDD/Fs
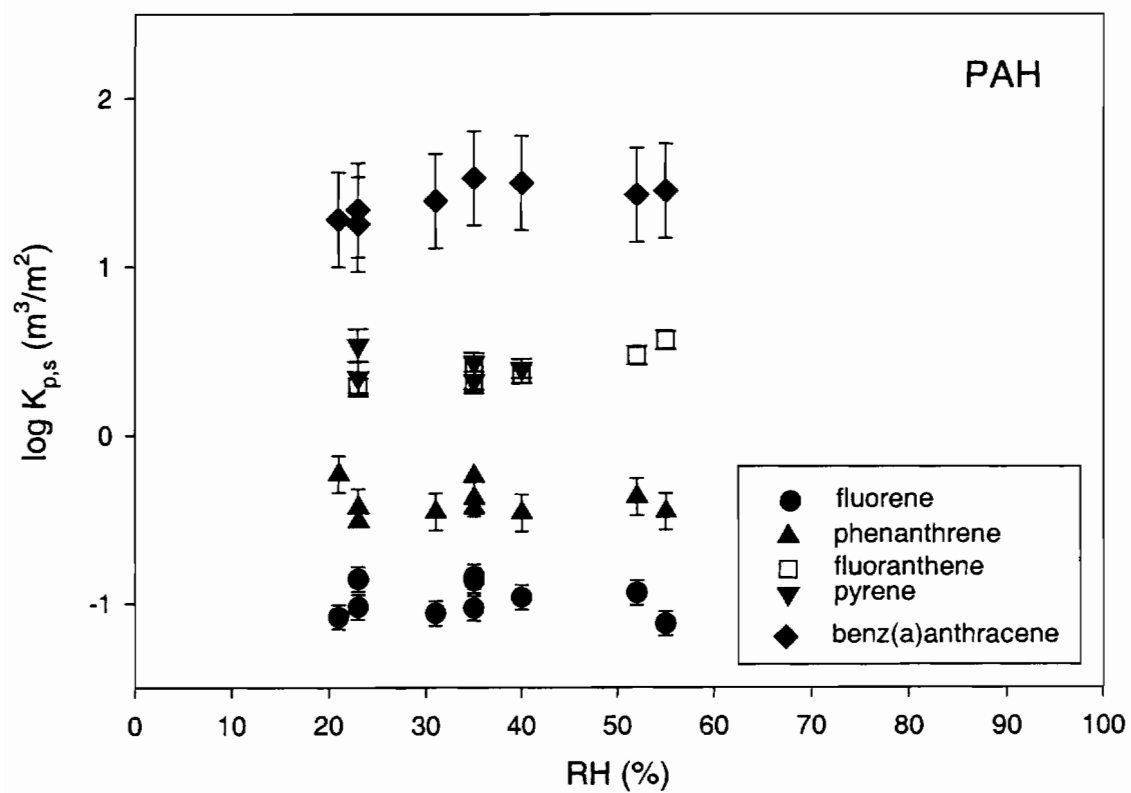
Figure 2.4 Log $K_{p,s}$ values of PAHs as a function of percent relative humidity (%RH).
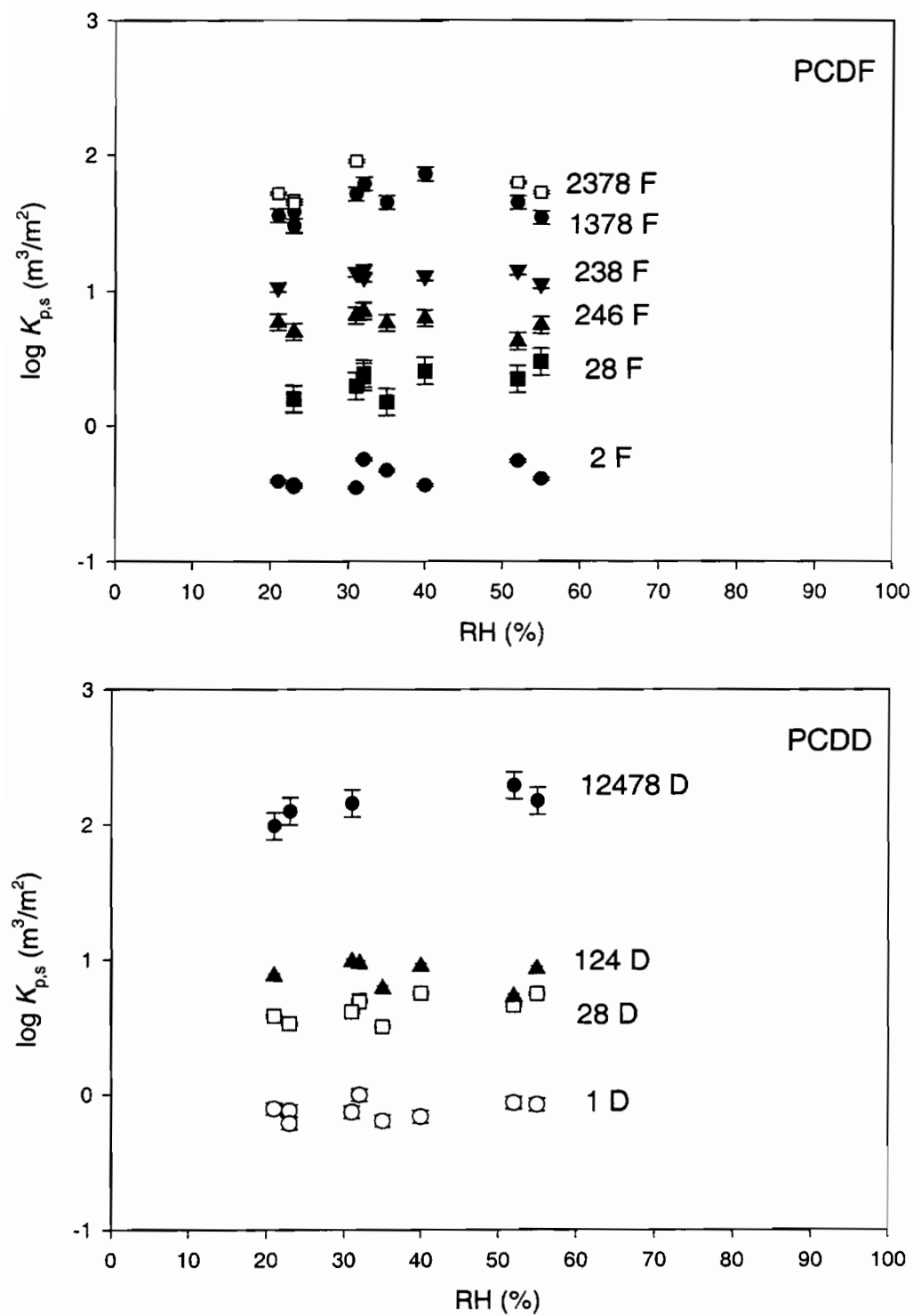
Figure 2.5 Log $K_{p,s}$ values of PCDD/Fs as a function of percent relative humidity (%RH) **a**. PCDD **b.**PCDF

values (presented on Figures 2.7a and b) for the correlation for the PAHs are similar to those observed in the correlation for the PCDD/Fs. This result is consistent with: 1) the presumption that adsorption to Teflon is non-specific in nature and depends primarily on van der Waals interactions between the compound and the surface; 2) the view that the strength of an adsorbing compound's van der Waals interactions with such a surface is proportional to that compound's p_L^o value (Goss, 1997); and 3) the use of a single, pooled log $K_{p,s}$ vs. log p_L^o correlation for both classes of compounds.

One can extend the above consideration of Teflon as an inert adsorbent surface by examining the log $K_{p,s}$ values obtained here together with the values of Goss and Schwarzenbach (1998) for non-polar and polar VOCs sorbing to Teflon. In the resulting plot (Figure 2.8), which spans 10 orders of magnitude in p_L^o, the slope is -1.13, and all of the data points fall within 0.4 log units of the regression line. This is much less variability than was observed by Goss and Schwarzenbach (1998) for the adsorption of non-polar and polar VOCs to quartz, where there was 4.5 order of magnitude difference in the $K_{p,s}$ values of alkanes and ethers with similar p_L^o values. We conclude that the correlation represented in Figure 2.8 will be useful in predicting log $K_{p,s}$ values to Teflon for a wide range of VOCs and SOCs. Unfortunately equation 11 from Goss and Schwarzenbach (1998) did not accurately predict the $K_{p,s}$ values of the PAH and PCDD/Fs on Teflon. To ensure that predictions made using the correlation in Figure 2.8 were not biased an anaylsis of variance was done according to Scherer at al. (1998); the error term was found to be insignificant.

2.4.6 Comparison of partitioning to clean and ambient backup TMF. The log $K_{p,s}$ values of the PAHs and PCDD/Fs are plotted versus log p_L^o for partitioning to TMFs in Figures 2.7a and b respectively. Data labeled clean refers to experiments using TMFs free of particles, and not placed behind a particle-loaded filter nor exposed to SOCs present in ambient air. Ambient backup refers to data from particle-free filters that had been placed behind particle-loaded TMFs and exposed to ambient air. In Figure 2.7a, Hart backup refers to data from ambient backup TMFs used during the conventional high volume air sampling experiments of Hart (1990). As illustrated in Figures 2.7a and b there was no significant difference in the partitioning behavior of clean and ambient
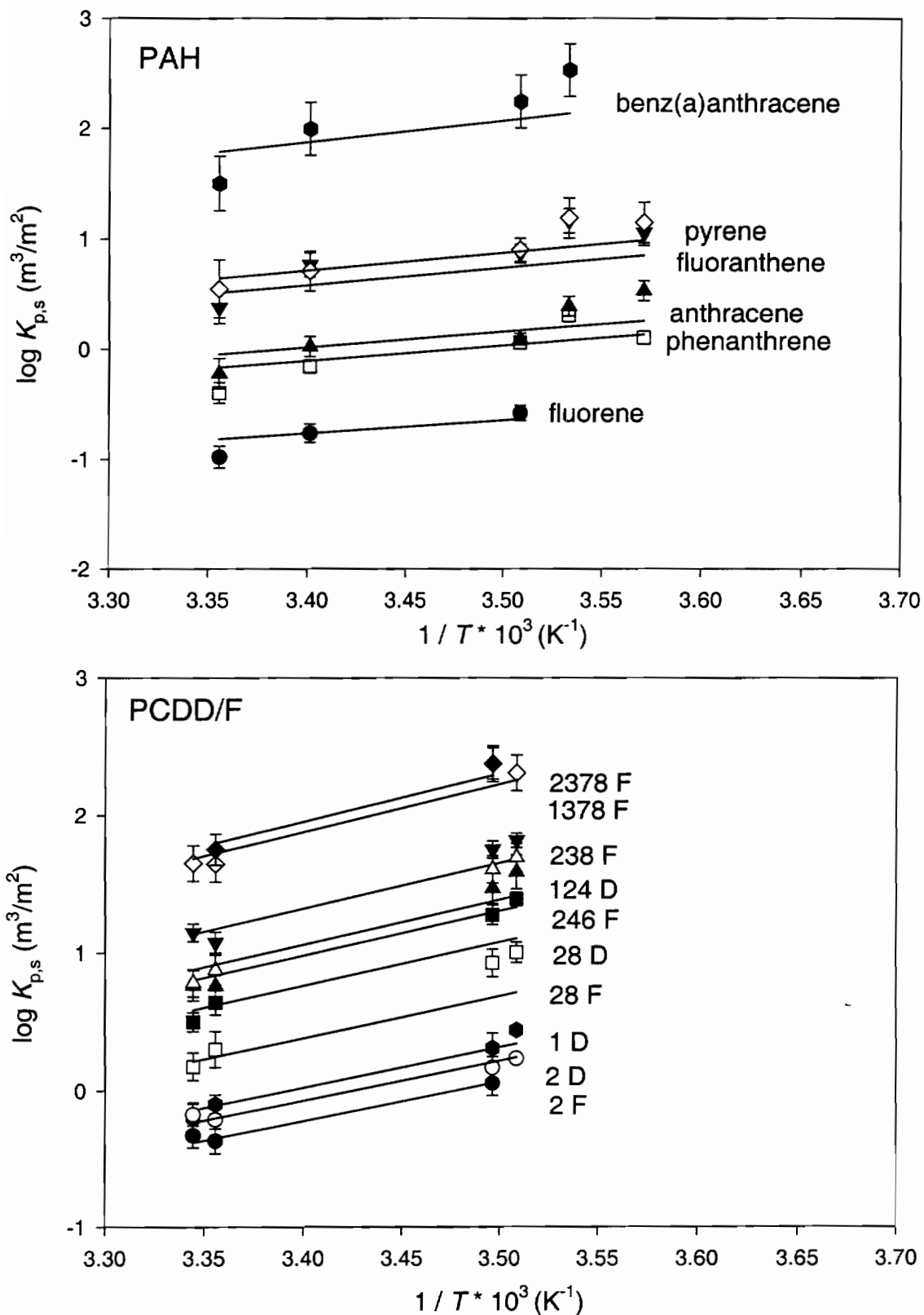
Figure 2.6 Log $K_{p,s}$ vs. 1/T plots for the partitioning of selected compounds to TMF. **a.** PAHs **b.** PCDD/Fs

Table 2.1 Values of $m_{p,s}$ and $b_{p,s}$ for the equation $\log K_{p,s} = m_{p,s} / T \ (K^{-1}) + b_{p,s}$ and values of $\log K_{p,s}$ at 20 °C.

Compound	$m_{p,s}$	$b_{p,s}$	r^2	$\log K_{p,s}$ (m^3/m^2) @ 20 °C
fluorene	1180	-4.773	0.99	-0.75 (±0.08)
phenanthrene	1373	-4.773	0.99	-0.09 (±0.02)
anthracene	1408	-4.773	0.99	0.03 (±0.13)
fluoranthene	1575	-4.773	0.99	0.60 (±0.13)
pyrene	1613	-4.773	0.99	0.7 (±0.2)
benz(a)anthracene	1955	-4.773	0.99	2 (±0.2)
2 F	2873	-9.989	0.99	-0.2 (±0.1)
28 F	3051	-9.989	0.99	0.42 (±0.11)
246 F	3227	-9.989	0.99	1.0 (±0.07)
238 F	3327	-9.989	0.99	1.4 (±0.07)
1378 F	3491	-9.989	0.99	1.9 (±0.11)
2378 F	3513	-9.989	0.99	2.0 (±0.11)
1 D	2945	-9.989	0.99	0.06 (±0.06)
2 D	2917	-9.989	0.99	0 (±0.1)
28 D	3163	-9.989	0.99	0.81 (±0.08)
124 D	3250	-9.989	0.99	1.1 (±0.09)
1234 D	3474	-9.989	0.99	2 (±0.1)

Table 2.2 Values of Q_d and Q_v for selected compounds at 25 °C.

Compound	ΔQ_d (kJ/mole)	ΔQ_v (kJ/mole[1])[a]	$\Delta Q_d - \Delta Q_v$ (kJ/mole)
fluorene	23	69	-46
phenanthrene	26	76	-50
anthracene	27	77	-50
fluoranthene	30	85	-55
pyrene	31	87	-56
benz(a)anthracene	37	99	-62
2 F	55	82	-27
28 F	58	87	-29
246 F	62	91	-29
238 F	64	91	-27
1378 F	67	NA	NA
2378 F	67	95	-28
1 D	56	85	-29
2 D	56	85	-29
28 D	61	97	-36
124 D	62	94	-32
1234 D	67	102	-35

[a]Values at 20 °C for PAH from Yamasaki *et al.* (1984) and PCDD/F calculated from Rordorf (1989)
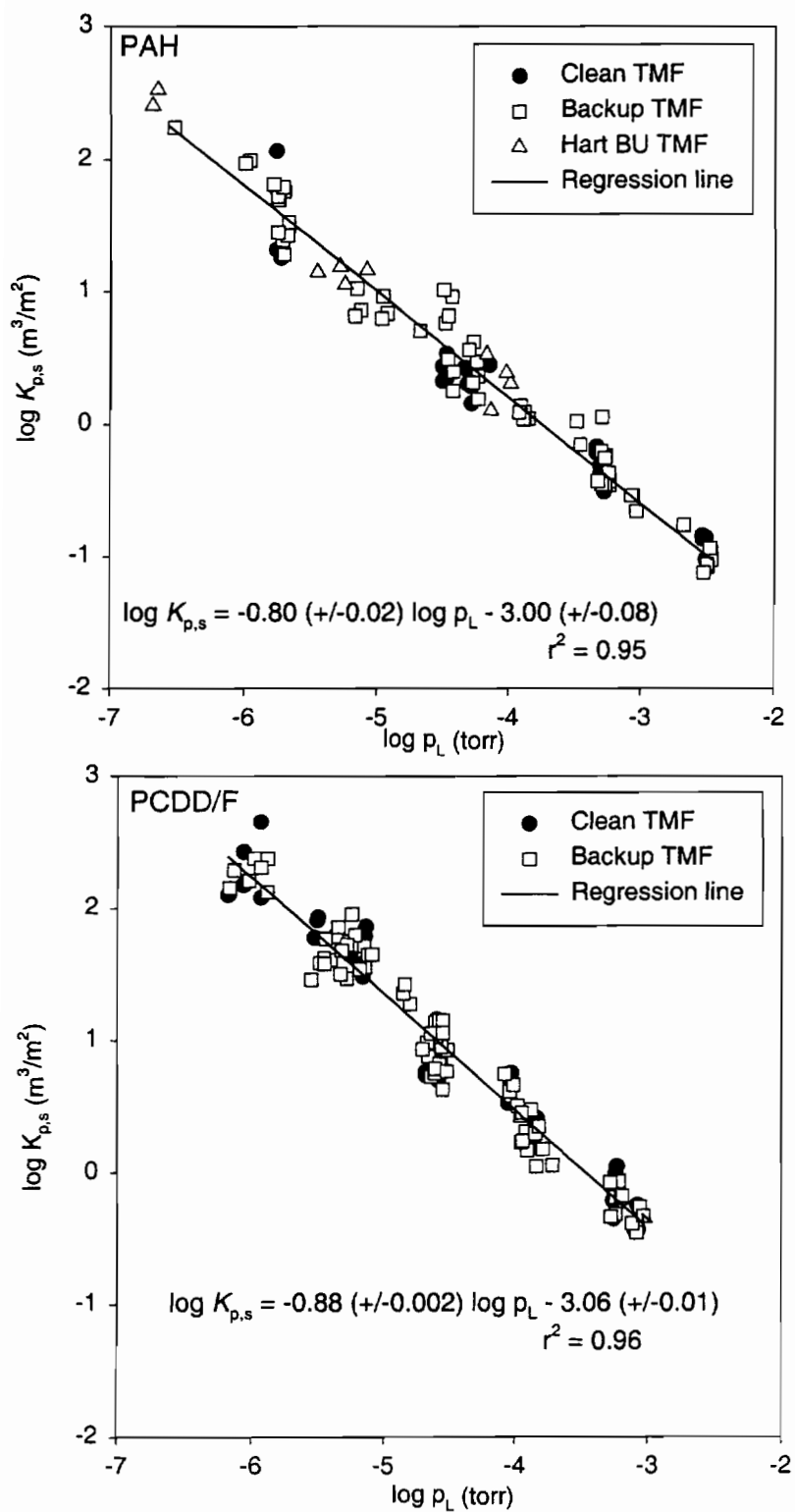
Figure 2.7 Log $K_{p,s}$ versus log p_L^o plots for selected compounds on TMFs. **a**. PAH **b**. PCDD/Fs
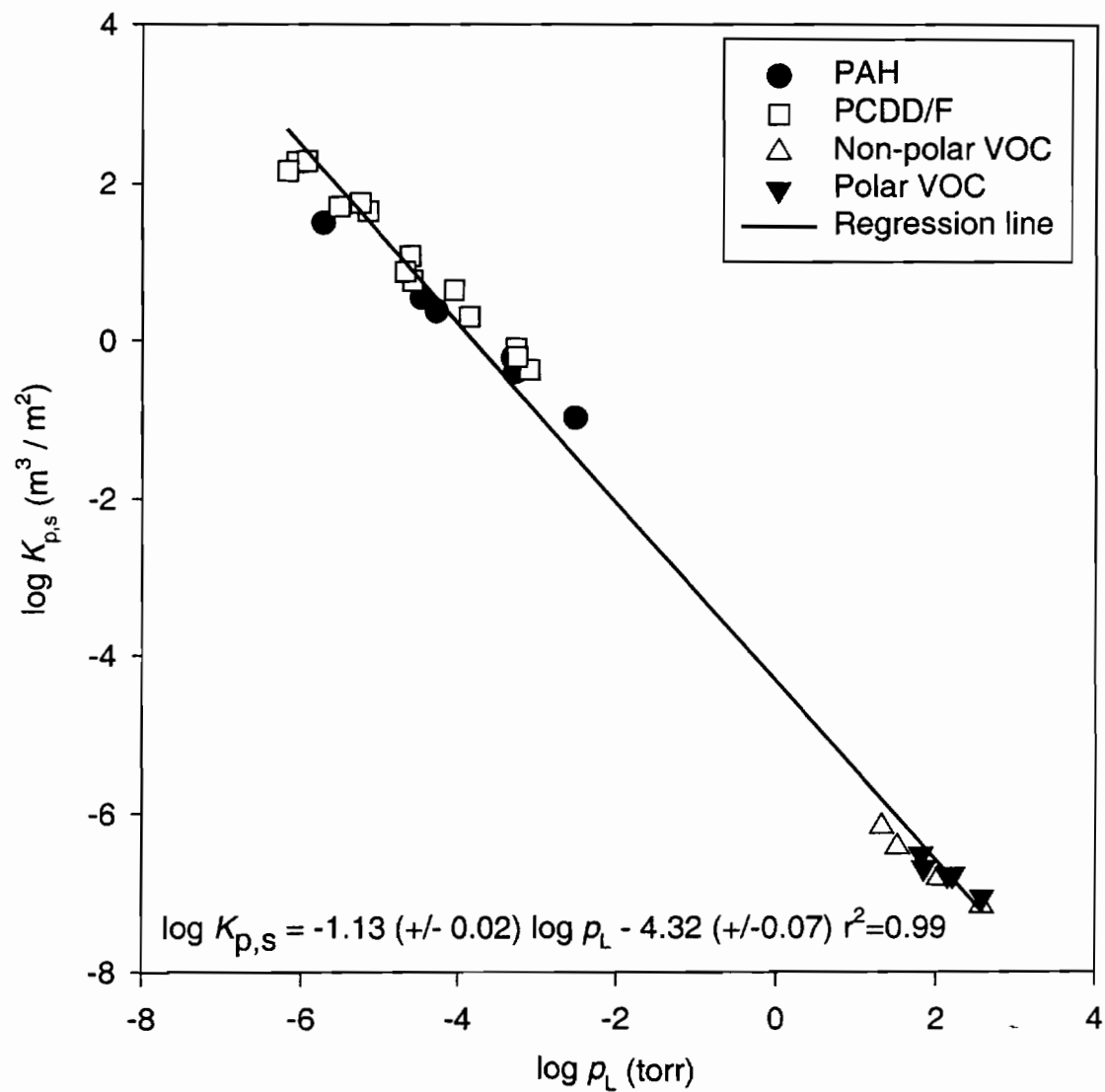
Figure 2.8 Plot of log $K_{p,s}$ versus log p_L^o for PAHs, PCDD/F, polar and non-polar VOC on Teflon.

backup filters. This observation is in contrast to what Cotham and Bidleman (1992) observed for partitioning of organochlorine compounds (OCs) to glass fiber ambient backup filters. These authors observed enhanced partitioning of OCs to filters placed behind particle loaded filters compared to filters placed behind clean glass fiber filters. The enhanced partitioning was attributed to the partitioning of OCs into organic films. The organic films are formed when organic material from particles on the front filter is stripped off and re-adsorbed from the gas phase onto the backup filter surface. This organic film is more hydrophobic than the glass surface and thus more sorptive for the OCs. The reason enhanced partitioning is not observed for TMF could be that such filters are inherently less adsorptive than glass surfaces for organic compounds and hence such organic films are not formed on Teflon surfaces. An additional explanation is that significant desorption "stripping" of organic material from the particle loaded front filters did not occur in these experiments. These results indicate that the $K_{p,s}$ values measured in this study on clean TMF filters can be used to assess the potential for gas adsorption artifacts in field measurements. In future work the $K_{p,s}$ values measured in this study will be combined with typical K_p values for SOCs on ambient particles to assess the potential for sampling artifacts during the sampling of ambient gas and particle phase SOCs.

2.5 References

Cotham, W. E., Bidleman, T. F. 1992. Laboratory investigations of the partitioning of organochlorine compounds between the gas phase and atmospheric aerosols on glass fiber filters. *Environmental Science and Technology* 26, 468-478.

Goss, K. U. 1992. Effects of temperature and relative humidity on the sorption of organic vapors on quartz sand. *Environmental Science and Technology* 26, 2287-2294.

Goss, K. U. 1993. Effects of temperature and relative humidity on the sorption of organic vapors on clay minerals. *Environmental Science and Technology* 27, 2127-2132.

Goss, K. U. 1997. Conceptual model for the adsorption of organic compounds from the gas phase to liquid and solid surfaces. *Environmental Science and Technology* 31, 3600-3605.

Goss, K. U., Eisenreich, S. J. 1996. Adsorption of VOCs from the gas phase to different minerals and a mineral mixture. *Environmental Science and Technology* 30, 2135-2142.

Goss, K. U., Eisenreich, S. J. 1997. Sorption of volatile organic compounds to particles from a combustion source at different temperatures and relative humidities. *Atmospheric Environment* 31, 2827-2834.

Goss, K. U., Schwarzenbach, R. P. 1998. Gas/solid and gas/liquid partitioning of organic compounds: critical evaluation of the interpretation of equilibrium constants. *Environmental Science and Technology* 32, 2025-2032.

Hart, K. M. 1990. *A study of atmospheric n-alkanes and PAHs and their distributions between the gaseous and particulate phases.* Ph.D. Thesis, Department of Environmental Science and Engineering, Oregon Graduate Institute.

Hart, K. M., Pankow, J. F. 1994. High volume air sampler for particle and gas sampling Part 2. Use of backup filters to correct the adsorption of gas phase polycylic aromatic hydrocarbons to the front filter. *Environmental Science and Technology* 28, 655-661.

Kamens, R. *et al.* 1995. Some observations on times to equilibrium for semivolatile polycyclic aromatic hydrocarbons. *Environmental Science and Technology* 29, 43-50.

Liang, C. *et al.* 1997. Gas/particle partitioning of semi-volatile organic compounds to model inorganic, model organic and ambient smog aerosols. *Environmental Science and Technology* 31, 3086-3092.

Maddalena, R. L. *et al.* 1998. Simple and rapid extraction of polycyclic aromatic hydrocarbons collected on polyurethane foam adsobent. *Atmospheric Environment* 32, 2497-2503.

Mader, B. T., Pankow, J. F. 2000a. Gas/solid partitioning of polychlorinated dibenzodioxins (PCDDs), polychlorinated dibenzofurans (PCDFs) and polycyclic aromatic hydrocarbons (PAHs) to filter surfaces: Part 3. Comparison of the gas adsorption artifact potential of Teflon membrane vs. quartz fiber filters and prediction of the magnitude of gas adsorption artifacts. *Environmental Science and Technology* submitted March 15, 2000.

Mader, B. T., Pankow, J. F. 2000b. Vapor pressures of polychlorinated dibenzodioxins, polychlorinated dibenzofurans and polycylic aromatic hydrocarbons: measurements and evaluation of estimation techniques. *Environmental Science and Technology* submitted March 15, 2000.

McDow, S. R., Huntzicker, J. J. 1990. Vapor adsorption artifact in the sampling of organic aerosol: face velocity effects. *Atmospheric Environment* 24, 2563-2571.

Odum, J. R. *et al.* 1996. Gas/particle partitioning and secondary organic aerosol yields. *Environmental Science and Technology* 30, 2580-2585.

Odum, J. R. *et al.* 1997. The atmospheric aerosol-forming potential of whole gasoline vapor. *Science* 276, 96-100.

Pankow, J. F. 1987. Review and comparative analysis of the theories on partitioning between the gas and aerosol particulate phases in the atmosphere. *Atmospheric Environment* 21, 2275-2283.

Pankow, J. F. 1991. Common y-intercept and single compound regressions of gas-particle partitioning data vs. 1/T. *Atmospheric Environment* 25A, 2229-2239.

Pankow, J. F. 1994. An absorption model of gas/particle partitioning of organic compounds in the atmosphere. *Atmospheric Environment* 28, 185-188.

Pankow, J. F. 1994. An absorption model of the gas/aerosol partitioning involved in the formation of secondary organic aerosol. *Atmospheric Environment* 28, 189-193.

Pankow, J. F., Bidleman, T. F. 1991. Effects of temperature, TSP, and percent non-exchangeable material in determining the gas-particle partitioning of organic compounds. *Atmospheric Environment* 25, 2241-2249.

Pankow, J. F., Bidleman, T. F. 1992. Interdependence of the slopes and intercepts from log-log correlations of measured gas-particle partitioning and vapor pressure Part 1. Theory and analysis of available data. *Atmospheric Environment* 26A, 1071-1080.

Rordorf, B. F. 1989. Prediction of vapor pressures boiling points and enthalpies of fusion for twenty-nine halogenated dibenzo-p-dioxins and fifty-five dibenzofurans by a vapor pressure correlation method. *Chemosphere* 18, 783-788.

Storey, J. M. *et al.* 1995. Gas/solid partitioning of semivolatile organic compounds to model atmospheric solid surfaces as a function of relative humidity: Part 1. Clean quartz. *Environmental Science and Technology* 29, 2420-2428.

Turpin, B. J., Huntzicker, J. J. 1994. Investigation of organic aerosol sampling artifacts in the Los Angeles Basin. *Atmospheric Environment* 28, 3061-3071.

Yamasaki, H. *et al.* 1984. Determination of vapor pressure of polycyclic aromatic hydrocarbons in the supercooled liquid phase and their adsorption on airborne particulate matter. *The Chemical Society of Japan* 8, 1324-1329.

CHAPTER 3

GAS/SOLID PARTITIONING OF POLYCHLORINATED DIBENZODIOXINS, POLYCHLORINATED DIBENZOFURANS AND POLYCYCLIC AROMATIC HYDROCARBONS TO FILTER SURFACES: QUARTZ FIBER FILTERS

3.1 Introduction

When measuring the levels of atmospheric semivolatile organic compounds (SOCs) with filter/sorbent samplers, a variety of types of filters have been used to separate the gas- and particle-phase portions of these compounds. These include: Teflon membrane filters (TMFs); Teflon-coated glass fiber filters; and quartz fiber filters (QFFs). Unfortunately, the adsorption of gas phase SOCs to filter surfaces can cause positive biases in measured particle-phase concentration values (c_p, ng/μg), and negative biases in measured gas-phase concentration values (c_g, ng/m^3) (McDow and Huntzicker 1990; Hart and Pankow 1994; Turpin and Huntzicker 1994; Mader and Pankow 2000a). This adsorption will therefore also cause positive biases in measured values of the gas/particle partitioning coefficient K_p (m^3/μg)

$$K_p = c_p / c_g \tag{3.1}$$

As in gas/particle partitioning, gas/filter partitioning can be characterized by a K_p coefficient. When gas/filter partitioning occurs by adsorption, normalizing a gas/filter K_p by the specific surface area of the filter a_f (m^2/g) yields

$$K_{p,s} \text{ (m}^3\text{/m}^2\text{)} = K_p \text{ (m}^3\text{/}\mu\text{g)} / [10^{-6} \text{ (g/}\mu\text{g)} \cdot a_f \text{ (m}^2\text{/g)}] \tag{3.2}$$

As noted by Mader and Pankow (2000a), for a given sampling event, predicting the magnitudes of the artifact for gaseous SOCs adsorbing to filters requires knowledge of the gas/particle K_p values, the level of total suspended particulate material (TSP, μg/m^3) in the atmosphere, the length of time over which sampling takes place, and the gas/filter $K_{p,s}$ values for the compounds and filter type of interest. To accurately predict the magnitudes of gas adsorption artifacts, gas/filter $K_{p,s}$ values must be measured using

29

filters with adsorptive characteristics similar to filters used in ambient air sampling. Clean filters are free of particles and not placed behind a particle-loaded filter nor exposed to organic compounds in ambient air. Ambient backup filters are free of particles but placed behind a particle-loaded filter and exposed to ambient air. The adsorption of ambient organic compounds to QFF surfaces may at least partially block the direct adsorption of SOCs; gas/QFF $K_{p,s}$ values measured using ambient backup QFFs may be different than the values measured using clean QFFs. Since QFFs used to separate atmospheric gas- and particle-phase SOCs are exposed to ambient air; it may be that the gas/QFF $K_{p,s}$ values for ambient backup filters will be more similar to the values for filters used in ambient air sampling than gas/QFF $K_{p,s}$ values measured using clean filters. The goals of the present work were to: 1) measure gas/QFF $K_{p,s}$ values for PAH and PCDD/Fs partitioning to clean QFF; 2) measure gas/QFF $K_{p,s}$ values for PAH partitioning to ambient backup QFFs; and 3) determine whether the $K_{p,s}$ value of a given PAH on clean and ambient backup QFFs was the same at a given RH.

3.2 Experimental

3.2.1 General. The same methods used by Mader and Pankow (2000b) to study adsorption to TMFs were also employed here with QFFs; they are summarized briefly below. The field sampling site used was located at the Oregon Graduate Institute (Beaverton, OR)

3.2.2 QFFs. The QFFs were obtained from Pall-Gelman Sciences (Ann Arbor, MI). Micrometrics (Norcross, GA) measured the value of a_f for the QFFs to be 1.65 m^2/g. Each QFF was precleaned by baking for 4 h at 550°C. Before beginning an experiment, a pair of QFFs (100 mm diameter) were equilibrated overnight at room temperature with air at 65% relative humidity (RH), weighed, then loaded into a filter holder. Each 100 mm diameter QFF weighed about 0.3 g.

3.2.3 Clean Front/Backup QFF Experiments - Specifics. A schematic of the experimental apparatus is given in Mader and Pankow (2000b). A pump was used to draw ambient air first through a glass fiber filter (GFF) to remove the ambient particulate material, then through two polyurethane foam (PUF) plugs to remove ambient gas-phase SOCs. The cleaned air then entered an air conditioning unit (ACU) to adjust the air

temperature and RH. A small portion of the incoming air flow (5 L/min) was routed through generator cartridges containing solid PCDDs, PCDFs, and PAHs. Details concerning the design and operation of the generator cartridges are provided by Mader and Pankow (2000c). The generator cartridges and the filter holder were located inside an environmental chamber unit (ECU) which was maintained at the same temperature as the ACU. At a point upstream of the filter holder, the SOC-containing sub-flow was mixed back into the main air flow (57 L/min). That SOC-containing air was then passed through the pair of QFF filters in the filter holder. Downstream of the QFFs, the gas-phase SOCs leaving the QFFs were collected using a pair of PUF plugs. The PUF plugs were changed at sample volume intervals of between 2.4 to 54 m^3. Each experiment was terminated when it was considered that gas/QFF equilibrium had been achieved. The SOCs were then extracted from the filters and PUFs. Quantitation was by GC/MS.

3.2.4 Ambient Backup QFF Experiments - Specifics. Ambient atmospheric particles were first collected using front and backup 20.3 cm × 25.4 cm QFFs with a conventional high-volume air sampler for a period of 74 hours. Once an adequate amount of particulate material had been collected on the front filter to allow gas/particle K_p values to be measured, the high-volume air sampler was turned off. A 100 mm diameter punch of the front/backup filter pair was then taken and loaded into the filter holder in the ECU. As in the clean QFF experiments, a GFF was placed immediately after the air intake of the ACU. In contrast to the clean QFF experiments, however, PUF plugs were not placed after the GFF; the gaseous organic compounds passing through the GFF were allowed to continue on to the filter holder so as to minimize the desorption "stripping" of ambient organic compounds either from the particles on the front filter, or from the two filters themselves. Once it passed from the ACU into the ECU, the air flow was handled as in the clean QFF experiments: SOCs (PAHs only) were added upstream of the filter holder, and PUF plugs were positioned downstream of the filter holder for purposes of determining the c_g values to which the collected particles and QFFs were exposed. The data on sorption to the ambient backup QFF will be presented here; the data on sorption to the particles collected on the front QFF will be presented elsewhere.

3.2.5 Clean Front/Backup and Ambient Backup QFF Experiments – General. The total air flow rate through the QFFs was constant within every experiment,

but ranged from 57 to 85 L/min among the different experiments. The flow rate was always chosen such that the pressure drop across the filters was less than 0.1 atm. The duration of each experiment ranged from 2 to 7 days, using a total air volume V_t between 164 and 857 m^3. The PUF plugs behind the QFFs were changed at intervals that ranged from 40 minutes to 15 hours; the sample volumes for those intervals ranged from 2.4 to 54 m^3. As discussed by Mader and Pankow (2000b) for experiments conducted with TMFs, for each SOC of interest, it was considered likely that gas/QFF equilibrium had been achieved if: 1) the gas phase concentration exiting the filter (as measured with the PUF plugs) had approached an asymptotic equilibrium value (designated $c_{g,eq}$); and 2) V_t was at least twice the volume required to deliver the total mass found sorbed on the two filters, *i.e.*,

$$V_t \geq 2\, m_{eq} / c_{g,eq} \tag{3.3}$$

where: m_{eq} is the total mass found on the two filters at apparent equilibrium. Equation 3.3 assumes that the gas concentration entering the filter equaled $c_{g,eq}$ for the entire duration of the experiment.

3.2.6 Extractions and Analyses. The procedures used to extract and analyze the QFFs were the same as those employed by Mader and Pankow (2000b) to extract TMFs. Briefly, immediately after an experiment, each QFF was spiked with four surrogate standard compounds, namely perdeuterated fluorine (1000 ng), perdeuterated pyrene (1000 ng), fully-^{13}C labeled 1234 F (80 ng), and fully-^{13}C labeled 2,7+2,8 D (80 ng). Each filter was then extracted four times with 25 mL of methylene chloride. The four extracts were combined and concentrated to 2 mL, gently blown down to 200 μL, then spiked with 2000 ng of perdeuterated phenanthrene.

Each filter extract was analyzed by GC/MS using a 30 m × 0.25 mm fused silica capillary column. The PAH standard solution contained the PAH compounds of interest plus fluorene-d$_{10}$, phenanthrene-d$_{10}$, and pyrene-d$_{10}$. The PCDD/PCDF standard solution contained the PCDD/PCDF compounds of interest plus the two fully-^{13}C-labeled internal standard compounds. Response factors for the PAHs and PCDD/Fs were determined as a function of mass injected. The internal standard compound for the PAHs was phenanthrene-d$_{10}$. The internal standard compounds for the PCDD/Fs were the ^{13}C-labeled PCCD/Fs.

Each PUF plug was extracted using a flow-through extraction (FTE) method. After being spiked with the surrogate standard solutions, each PUF plug was then extracted with a volume of methylene chloride that was twice the volume of the non-deformed PUF plug. Each PUF extract was concentrated to 4 mL using rotoevaporation. Analysis proceeded as with the TMF extracts.

3.2.7 QA/QC. Blank filters and PUF plugs were extracted regularly. The blank levels were always less than 5% of the total mass measured for each compound on the filters and PUF plugs. For the PAHs, absolute recoveries from the PUF plugs and QFFs averaged 105% and 91% respectively. For the PCDD/Fs, recoveries from the PUF plugs and QFFs averaged approximately 63% and 92%, respectively. For the PUF plugs behind the QFF filter holder, at the warmest experimental temperature used (26 °C), breakthrough from the front to backup plug averaged 44, 6, and 7% for fluorene, phenanthrene, and anthracene, respectively, and 9, 3, and 5% for 1 F, 1 D and 2 D, respectively. Breakthrough was negligible for the other compounds at 26 °C. Since the volume of the 178 mL backup PUF plug was over seven times that of the 24 mL front PUF plug, it can be assumed the combination of the two plugs provided essentially quantitative recoveries for all compounds at all experimental temperatures.

3.3 Theory

Compound-dependent values of log K_p can usually be correlated using the corresponding values of the sub-cooled liquid vapor pressure p_L^o (torr) (Pankow 1987, 1994a, 1994b). In the general case, we have

$$\log K_p = m_r \log p_L^o + b_r \qquad \textit{adsorptive or absorptive partitioning} \qquad (3.4)$$

Values of the slope m_r are frequently close to -1. When the partitioning takes place by adsorption, consideration of Equation 3.2 leads to

$$\log K_{p,s} = m_{r,s} \log p_L^o + b_{r,s} \qquad \textit{adsorptive partitioning} \qquad (3.5)$$

where $m_{r,s} = m_r$. Equation 3.5 has been applied in studies of the gas/solid partitioning of n-alkanes and PAHs to quartz (Storey *et al.* 1995), and in studies of aromatic volatile organic compounds (VOCs) sorbing to soot carbon (Goss and Eisenreich 1997).

For adsorptive partitioning, within a given compound class, the slope m_r will be close to -1 when there is compound-to-compound constancy in $(Q_d - Q_v)$, which is the difference between the enthalpy of desorption from the surface and the enthalpy of vaporization from the pure liquid. Although Pankow (1987), Pankow and Bidleman (1991, 1992) have provided detailed discussions of how measured values of m_r can come to be different from -1, such deviations have been incorrectly interpreted by some as being necessarily indicative of non-equilibrium biases in the corresponding measured values of K_p (or $K_{p,s}$).

3.4 Results

3.4.1 Gas/QFF Partitioning Equilibrium.
Once equilibrium between the QFF and a gaseous SOC was approached, the gas-phase concentration of the SOC in the air exiting the filter achieved a constant value $c_{g,eq}$ (e.g., see Figure 3.1). For the PAHs, $c_{g,eq}$ was computed as the average of the measured c_g values once c_g varied by no more than $\pm 10\%$. For the PCDD/Fs, the criterion was variation by no more than $\pm 20\%$. Values of K_p are reported here only for those cases when the Equation 3.3 criterion was satisfied.

3.4.2 Log $K_{p,s}$ vs. Log p_L^o Correlations for Clean QFFs.
The data set of Yamasaki, Kuwata et al. (1984) was used to provide the p_L^o values of the PAHs at the temperatures of interest; the p_L^o values of the PCDD/Fs were determined from data presented by Mader and Pankow (2000c). A plot of log $K_{p,s}$ vs. log p_L^o for the partitioning of PAHs and PCDD/Fs to clean QFFs is presented in 3.2. The individual log $K_{p,s}$ values at 25 °C are tabulated in Tables 3.1 and 3.2. The partitioning of the PAHs to clean QFFs at RH = 25 % was similar to that observed by Storey et al. (1995) for QFFs at RH = 29%. Despite their structural differences, PAHs and PCDD/Fs with similar p_L^o values exhibited similar $K_{p,s}$ values for clean QFFs. For the PAHs and PCDD/Fs, the $m_{r,s}$, $b_{r,s}$, and r^2 values were -1.11, -3.61, 0.98 and -1.02, -3.29, 0.96, respectively.

3.4.3 Adsorptive Affinity of Clean QFFs vs. TMFs.
For each of the PAHs and PCDD/Fs studied, the $K_{p,s}$ values for clean QFFs at RH = 25% were found to be, on average, a factor of two larger than the corresponding $K_{p,s}$ values on TMFs (RH = 21-52%) reported by Mader and Pankow (2000b) (Figure 3.3). This may have been due to a
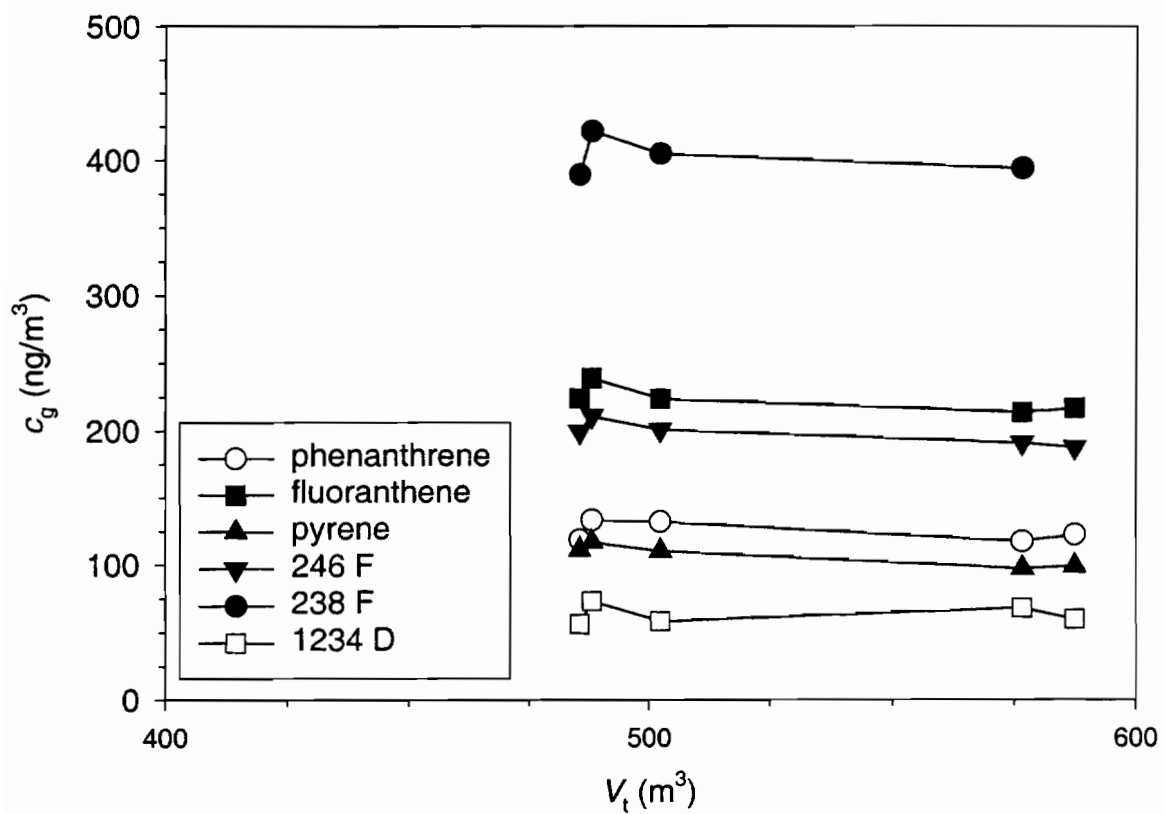
Figure 3.1 Equilibrium gas phase concentration ($c_{g,eq}$) of selected PAHs and PCDD/Fs as a function of the volume (V_t) of air passed through the QFFs.
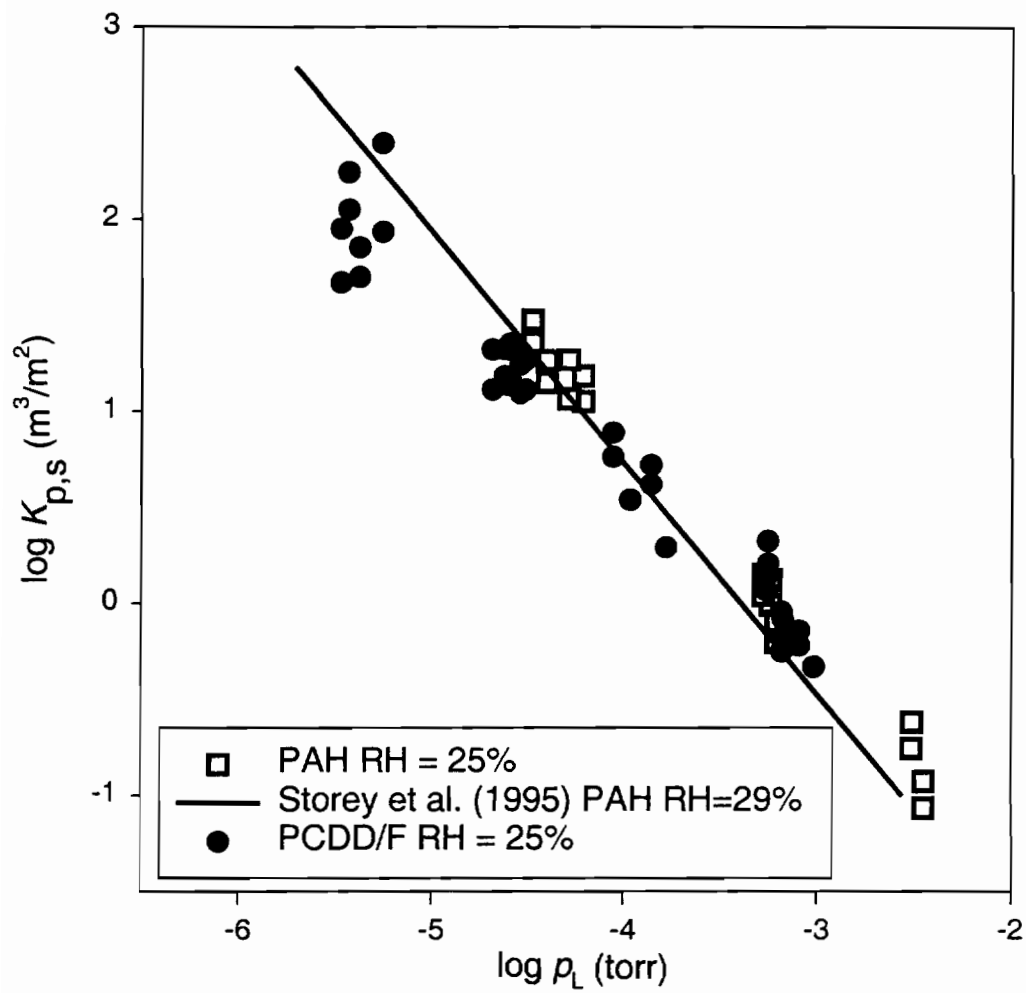
Figure 3.2 Plot of log $K_{p,s}$ versus log p_L^o for PAHs and PCDD/Fs on clean QFFs.

Table 3.1 Average values of log $K_{p,s}$ for PAHs at 25 (±1) °C.

Compound	log $K_{p,s}$ (m^3/m^2) clean QFFs RH = 25%	log $K_{p,s}$ (m^3/m^2) ambient backup QFFs, RH = 37%
fluorene	-0.69 (±0.16)	-2.1 (±0.08)
phenanthrene	0.09 (±0.11)	-0.95 (±0.15)
anthracene	0.3 (±0.2)	-0.82 (±0.09)
fluoranthene	1.1 (±0.09)	0.43 (±0.06)
pyrene	1.4 (±0.12)	0.43 (±0.10)
benz(a)anthracene	NA	2.0 (±0.08)
chrysene	NA	1.9 (±0.11)

Table 3.2 Average values of log $K_{p,s}$ for PCDD/Fs at 25 (±1) °C.

Compound	log $K_{p,s}$ (m^3/m^2) clean QFFs,RH=25%
2 F	-0.23 (±0.09)
28 F	0.4 (±0.2)
246 F	1.2 (±0.09)
238 F	1.2 (±0.09)
1378 F	1.8 (±0.11)
2378 F	2 (±0.2)
1 D	-0.01 (±0.13)
2 D	0.05 (±0.06)
28 D	0.6 (±0.2)
124 D	1.2 (±0.09)
1234 D	2.1 (±0.11)
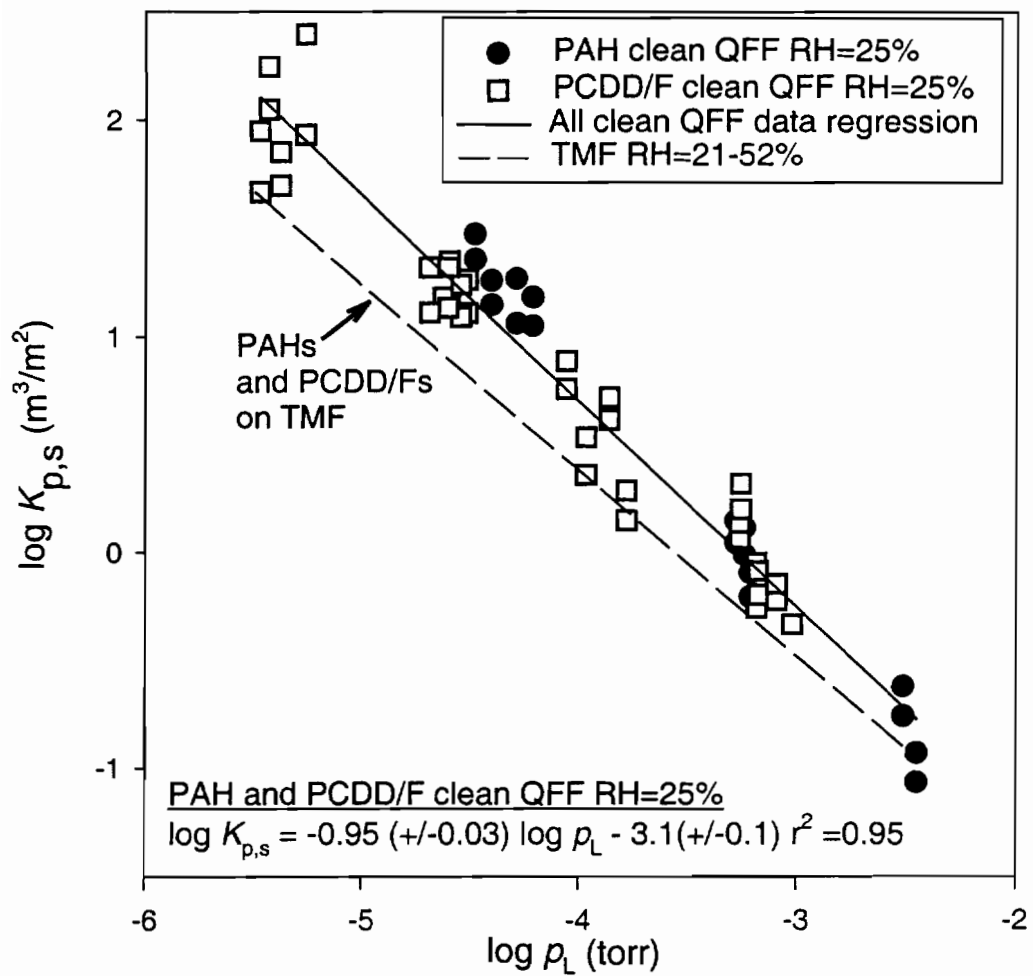
Figure 3.3 Comparison of the partitioning of PAHs and PCDD/Fs on clean QFFs vs. TMFs. PAH and PCDD/F data on TMF are from Mader and Pankow, (2000b).

partially active QFF surface at these RH values. Indeed, Goss (1992) observed monolayer coverage of water on quartz sand at RH = 26%, below this RH the quartz surface is not fully covered by water and direct interaction between an SOC and the SiO_2 groups is possible. If the water sorption isotherms of quartz sand and clean QFF are similar, it is possible that in this study (RH = 25%), clean QFF were not fully coated with water or perhaps the water film was not thick enough to eliminate the influence of the mineral surface on partitioning.

3.4.4 Log $K_{p,s}$ vs. Log p_L^o Correlations for Ambient Backup QFF Filters. A

plot of log $K_{p,s}$ vs. log p_L^o for the partitioning of PAHs to ambient backup QFFs at RH = 37% is presented in Figure 3.4. Data from Luo (1996) and Storey et al. (1995) for the partitioning of PAHs to clean QFFs at RH = 29% and RH = 48.5% are also included. Since the log $K_{p,s}$ values for PAHs sorbing to QFFs have been found to depend linearly on RH in this RH range (Storey et al., 1995), if PAHs sorbed to clean and ambient backup QFFs to the same extent, the line in Figure 3.4 for ambient backup QFFs at RH = 37% would lie approximately midway between the lines for clean QFFs at RH = 29% and RH = 48.5%. The line for ambient backup QFFs at RH=37% line however, is seen to lie *below* the line for clean QFFs at RH = 48.5%. Therefore at a given RH, the magnitude of the $K_{p,s}$ value of a PAH on ambient backup QFFs is less than on clean QFF. This may have been the result of the adsorption of ambient organic compounds on the QFF surface, and therefore the blocking of SOCs from those sites. Since QFFs used to separate atmospheric gas and particle phase SOCs are exposed to ambient air, an assessment of the magnitude of the compound-dependant gas adsorption artifact for QFF should only be carried out using $K_{p,s}$ values obtained with ambient backup QFFs. In future work $K_{p,s}$ values for PAHs partitioning to ambient backup QFFs will be combined with typical K_p values for PAHs on ambient particles to assess the potential for sampling artifacts during the sampling of ambient gas and particle phase PAHs.
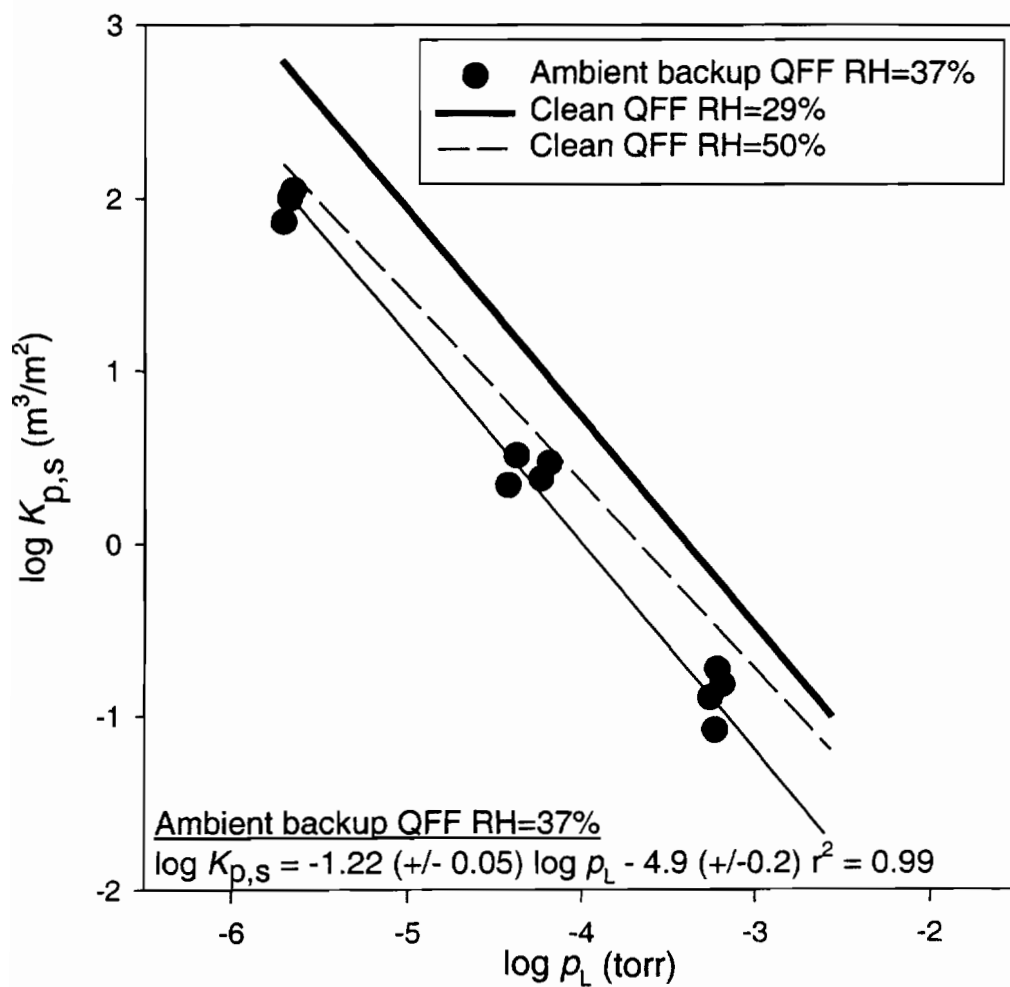
Figure 3.4 Plot of log $K_{p,s}$ versus log p_L^o for PAHs on ambient backup QFFs and clean QFFs.

3.5 References

Goss, K. U. 1992. Effects of temperature and relative humidity on the sorption of organic vapors on quartz sand. *Environmental Science and Technology* 26, 2287-2294.

Goss, K. U., Eisenreich, S. J. 1997. Sorption of volatile organic compounds to particles from a combustion source at different temperatures and relative humidities. *Atmospheric Environment* 31, 2827-2834.

Hart, K. M., Pankow, J. F. 1994. High volume air sampler for particle and gas sampling 2. Use of backup filters to correct the adsorption of gas phase polycyclic aromatic hydrocarbons to the front filter. *Environmental Science and Technology* 28, 655-661.

Luo, W. 1996. *Gas/Particle partitioning of semi-volatile organic compounds to two model atmospheric particulate materials: quartz and graphitic carbon.* Ph.D. Thesis, Environmental Science and Engineering, Oregon Graduate Institute of Science and Technology.

Mader, B. T., Pankow, J. F. 2000a. Gas/solid partitioning of polychlorinated dibenzodioxins (PCDDs), polychlorinated dibenzofurans (PCDFs) and polycyclic aromatic hydrocarbons (PAHs) to filter surfaces: Part 3. Comparison of the gas adsorption artifact potential of Teflon membrane vs. quartz fiber filters and prediction of the magnitude of gas adsorption artifacts. *Environmental Science and Technology* submitted March 15, 2000.

Mader, B. T., Pankow, J. F. 2000b. Gas/solid partitioning of polychlorinated dibenzodioxins, polychlorinated dibenzofurans and polycyclic aromatic hydrocarbons to filter surfaces: Part 1. Teflon membrane filters. *Atmospheric Environment* in press April 15, 2000.

Mader, B. T., Pankow, J. F. 2000c. Vapor pressures of polychlorinated dibenzodioxins, polychlorinated dibenzofurans and polycylic aromatic hydrocarbons: Measurements and evaluation of estimation techniques. *Environmental Science and Technology* submitted March 15, 2000.

McDow, S. R., Huntzicker, J. J. 1990. Vapor adsorption artifact in the sampling of organic aerosol: face velocity effects. *Atmospheric Environment* 24, 2563-2571.

Pankow, J. F. 1987. Review and comparative analysis of the theories on partitioning between the gas and aerosol particulate phases in the atmosphere. *Atmospheric Environment* 21, 2275-2283.

Pankow, J. F. 1994. An absorption model of gas/particle partitioning of organic compounds in the atmosphere. *Atmospheric Environment* 28, 185-188.

Pankow, J. F. 1994. An absorption model of the gas/aerosol partitioning involved in the formation of secondary organic aerosol. *Atmospheric Environment* 28, 189-193.

Pankow, J. F., Bidleman, T. F. 1991. Effects of temperature, TSP, and percent non-exchangeable material in determining the gas-particle partitioning of organic compounds. *Atmospheric Environment* 25, 2241-2249.

Pankow, J. F., Bidleman, T. F. 1992. Interdependence of the slopes and intercepts from log-log correlations of measured gas-particle partitioning and vapor pressure: Part 1. Theory and analysis of available data. *Atmospheric Environment* 26A, 1071-1080.

Storey, J. M. *et al.* 1995. Gas/solid partitioning of semivolatile organic compounds to model atmospheric solid surfaces as a function of relative humidity: Part 1. Clean quartz. *Environmental Science and Technology* 29, 2420-2428.

Turpin, B. J., Huntzicker, J. J. 1994. Investigation of organic aerosol sampling artifacts in the Los Angeles Basin. *Atmospheric Environment* 28, 3061-3071.

Yamasaki, H. *et al.* 1984. Determination of vapor pressure of polycyclic aromatic hydrocarbons in the supercooled liquid phase and their adsorption on airborne particulate matter. *The Chemical Society of Japan* 8, 1324-1329.

$$K_{p,x} \ (m^3/cm^2) = \ K_p \ (m^3/\mu g) \ / \ [A_{filter} \ (cm^2) \ / \ M_{filter} \ (\mu g)] = \ K_p \ M_{filter} \ /A_{filter} \quad (4.2)$$

where M_{filter} (μg) is the mass of the filter, and A_{filter} (cm^2) is the face area of the filter. When gas/filter partitioning occurs by adsorption, normalizing gas/filter K_p values by the specific surface area of the filter a_f (m^2/g) yields

$$K_{p,s} \ (m^3/m^2) = \ K_p \ (m^3/\mu g) \ / \ [10^{-6} \ (g/\mu g) \cdot a_f \ (m^2/g)] = 10^6 \ K_p \ /a_f \quad (4.3)$$

The relationship between $K_{p,x}$ and $K_{p,s}$ is:

$$K_{p,x} \ (\ m^3/cm^2) = \ 10^{-6} \ a_f \ K_{p,s} M_{filter}/A_{filter} \quad (4.4)$$

Mader and Pankow (2000a; 2000b) have recently reported values of the gas/solid partition coefficient $K_{p,s}$ (m^3/m^2) for the adsorption of various PAH and PCDD/Fs to TMF and QFF. Further data is available from Storey, Luo et al. (1995) and Luo (1996) for the adsorption of PAHs and n-alkanes to QFFs. This paper compares the gas adsorptive affinity of TMF versus QFF for PAHs. Equations and diagrams are provided which enable estimation of the magnitude of the gas/filter adsorption artifact on measured values of c_g, c_p, and K_p, all as a function of filter type and compound class.

4.2 Discussion

4.2.1 Adsorptive affinity of ambient backup QFF *vs*. TMF for PAHs. A QFF placed behind a particle loaded QFF and exposed to ambient air is termed an ambient backup QFF. A clean QFF is free of particles and not placed behind a particle loaded QFF nor exposed to SOCs in ambient air. The adsorptive affinity of clean and ambient backup QFFs for PAHs is different Mader and Pankow (2000b). QFFs used to separate atmospheric gas- and particle-phase SOCs are exposed to ambient air; only ambient backup QFF data is relevant to study the gas adsorption artifact potential of QFFs. A comparison of the gas adsorptive affinity of ambient backup QFF versus TMF for PAHs was made based on the $K_{p,x}$ values of these compounds on each filter. These values were calculated using equation 4.4 and the $K_{p,s}$ values presented by Mader and Pankow (2000a; 2000b) and Luo (1996). The value of the term ($a_f \times M_{filter} \ / \ A_{filter}$) was 0.0126 and 0.0035 (m^2/cm^2) for QFF and TMF respectively, indicating that QFF have 3.4 times more surface area than TMFs. As shown in Figure 4.1, for the higher molecular weight PAHs studied the $K_{p,x}$ values on ambient backup QFF at relative humidity (RH) = 37% were on average five times greater than for TMF at RH = 21-52%. For the lower molecular weight
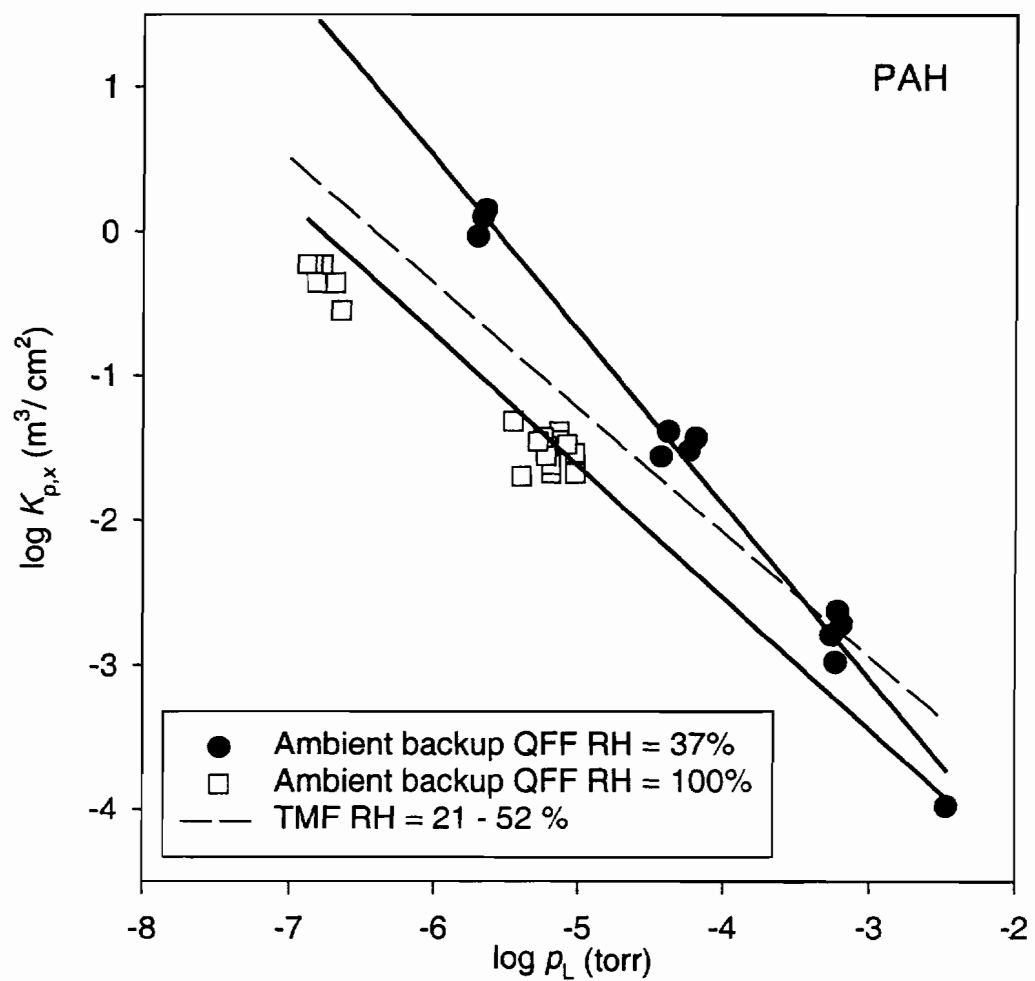
Figure 4.1 Log $K_{p,x}$ vs. log p_L^o plot for the partitioning of PAH and PCDD/Fs to TMF.

PAHs studied the $K_{p,x}$ values on ambient backup QFF at relative humidity (RH) = 37% were equal or slightly less than for TMF at RH = 21-52%. Also shown in Figure 4.1 is data from Luo (1996) for partitioning of PAH to ambient backup QFF at RH = 100%. For each of the PAHs studied the $K_{p,x}$ values on ambient backup QFF at RH = 100% was on average three times less than for TMF at RH= 21-52%. The difference in partitioning between ambient backup QFF and TMF is not explained by differences in filter surface area. RH does play an important role in the partitioning of PAH to ambient backup QFF; dlog $K_{p,x}$ / dRH was approximately –0.011. This value can be compared to the value of – 0.025 observed by Storey *et al.*, (1995) for the partitioning of PAHs to clean QFF at RHs between 30 to 70%. RH has little affect on the partitioning of PAH to TMFs (Mader and Pankow, 2000a). Using the $K_{p,x}$ values of the PAHs on ambient backup QFF at RH = 100% and the relationship; dlog $K_{p,x}$ / dRH = –0.011 for ambient backup QFF, it is estimated that at RH values below ≈ 54%, the $K_{p,x}$ values for PAHs are lower on TMFs than on ambient backup QFFs.

4.2.2 Air sample volume required to attain gas/filter equilibrium for selected compounds. At linear air velocities common to most ambient air sampling measurements, McDow (1990)(1999) has shown that QFF can adsorb gas-phase SOCs with greater than 90% efficiency. Until gas/filter equilibrium is achieved for a gaseous SOC, insignificant amounts of that compound will breakthrough the filter, leading to an underestimation of c_g. When a backup filter is used to correct for gas adsorption artifacts, the amounts of each SOC adsorbed on the front and backup filters are assumed equal. Since the front filter will tend to reach equilibrium with the incoming gaseous SOCs first, that equality might only be achieved after both filters have reached equilibrium with the gaseous SOCs in the sample air. If air sampling is ended prior to gas/backup filter sorption equilibrium, backup filter corrections will underestimate gas adsorption artifacts occurring on front filters.

For a given compound the minimum air sample volume required to reach gas/filter sorption equilibrium on a single filter is,

$$V_{t,filter} \ (m^3) = K_{p,x} \ A_{filter} \qquad (4.5)$$

where A_{filter} (cm^2) is the per-filter face area. The minimum air sample volume required to reach both gas/front filter *and* gas/backup filter equilibrium is:

$$V_{t,min} \, (m^3) = 2 \, V_{t,filter} \qquad (4.6)$$

The amounts of each SOC adsorbed on the front and backup filters can only be equal if the air sample volume (V_t) is greater than, or equal to $V_{t,min}$. The $V_{t,min}$ values of individual PAHs on TMF and ambient backup QFF at 20 °C are presented in Table 4.1 and $V_{t,min}$ values of individual PCDD/Fs on TMF at 20 °C are presented in Table 4.2. When sampling ambient atmospheric SOCs, V_t is typically in the range of 100 to 3000 m^3. A comparison of typical V_t values to the $V_{t,min}$ values presented in Tables 4.1 and 4.2 indicates that some of the backup-filter-based corrections described in the literature were carried out using sample volumes that were smaller than the $V_{t,min}$ values for some compounds of interest. Gas adsorption artifacts may have significantly influenced measurements of the c_g, c_p and K_p values of some compounds, even though backup filters were used to "correct" for gas adsorption artifacts.

4.2.2.2.1 log $V_{t,min}$ vs. log p_L^o plots. As shown by Mader and Pankow (2000a; 2000b) values of $K_{p,s}$ are a function of p_L^o and therefore temperature (T) dependent. Consequently $V_{t,min}$ will be T dependent. The vapor pressures of PAH and PCDD/Fs are known as a function of T, (Yamasaki et al., 1984; Mader and Pankow, 2000c); the effect of T on $V_{t,min}$ can be considered by plotting log $V_{t,min}$ vs. log p_L^o. Shown in Figure 4.2 are plots of log $V_{t,min}$ vs. log p_L^o for the partitioning of PAH and PCDD/Fs to TMF, and PAH to ambient backup QFF. The $V_{t,min}$ values in Figure 4.2 were calculated for 8×10 inch filters. Since partitioning to Teflon is non-specific in nature (Mader and Pankow, 2000a), the equation presented in Figure 4.2 for TMF can be used to determine the $V_{t,min}$ of any given compound on TMFs using the log p_L^o value of that compound at the T of interest. The equations given in Figure 4.2 for ambient backup QFF are valid only for PAHs at the given RH. The $V_{t,min}$ values of PAHs on ambient backup QFF at other RH can be approximated using the relationship, dlog $V_{t,min}$ / dRH = dlog $K_{p,x}$ / dRH = –0.011.

Figure 4.2 can be used to plan an air sampling study, it enables a V_t to be chosen such that $V_t \geq V_{t,min}$ for the most non-volatile compound of interest. Alternatively Figure 4.2 can be used to evaluate a past air sampling study; ensuring that $V_t \geq V_{t,min}$ for a particular compound.

4.2.3 Equations for the prediction of gas adsorption artifacts.

Table 4.1 Values of $V_{t,min}$ at 20 °C for PAHs on TMF and ambient backup QFF.

Filter	$V_{t,min}$ (m^3) @ 20 °C			
	fluorene	phenanthrene	pyrene	chrysene
TMF RH 21-52%	0.50	2.4	38	490
ambient backup QFF RH=37%	0.25	2.3	102	3700
ambient backup QFF RH=100%	0.15	0.79	14	220

Table 4.2 Values of $V_{t,min}$ at 20 °C for PCDD/Fs on TMF.

Compound	$V_{t,min}$ (m^3) @ 20 °C
2 F	2.3
28 F	10
238 F	52
2378 F	270
1 D	3.2
28 D	16
124 D	57
1234 D	390
12478 D	1500
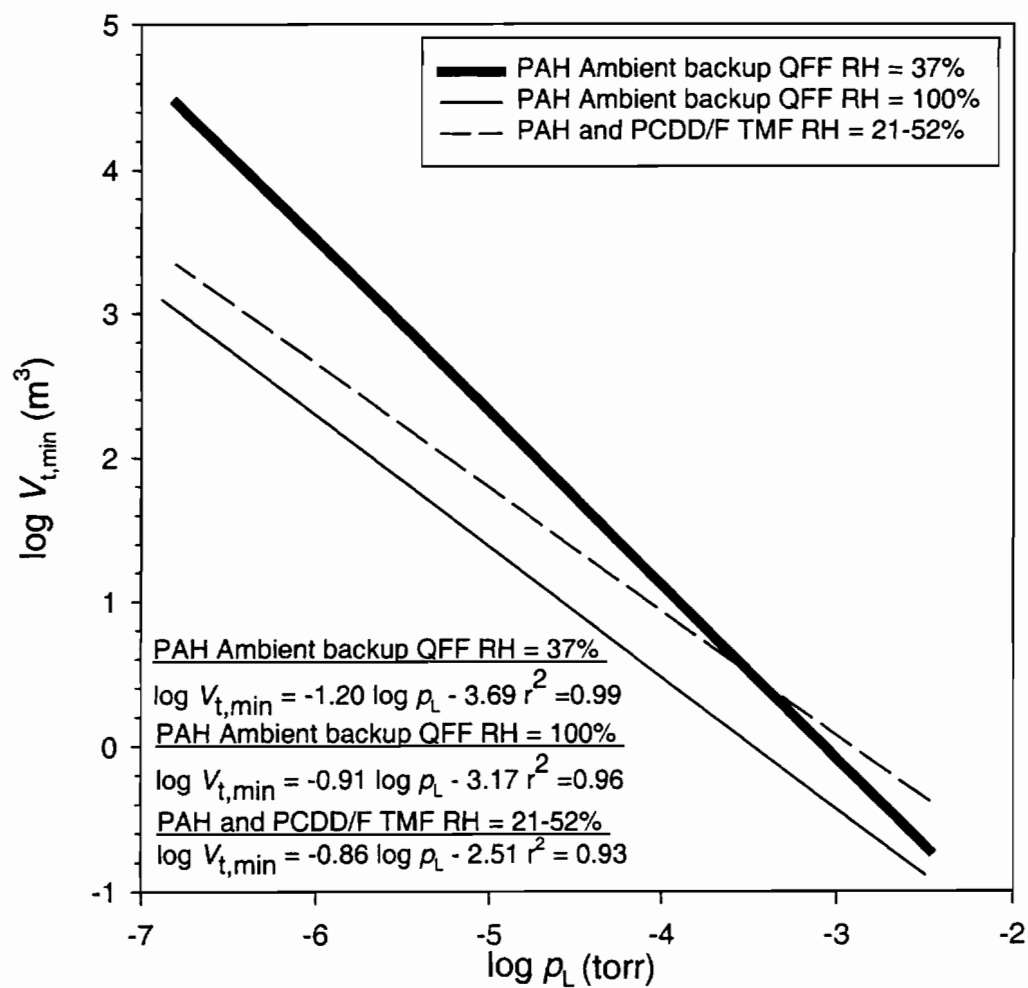
Figure 4.2 Log $V_{t,min}$ *vs.* log p_L^o plot for the partitioning of PAH and PCDD/Fs to TMF filters and PAH to ambient backup QFF. $V_{t,min}$ values were calculated for a pair of 8×10 inch filters.

4.2.3.1 The percent of the total mass of an SOC present on a front filter due to gas adsorption. Gas adsorption artifacts cause a positive bias in measured c_p and K_p values. Equation 4.7 is often used to quantify this bias. Where the percent of the total mass of an SOC present on a front filter due to gas adsorption is:

$$100 \times ((F_{filter} / (F_{particle} + F_{filter}))) \tag{4.7}$$

Where F_{filter} = the mass of an individual SOC adsorbed on the filter surface and $F_{particle}$ = the mass of an individual SOC present in/on the collected particles. Front and backup filters are used during field sampling of ambient gas and particle phase SOCs. The value of F_{filter} is the mass of an individual SOC extracted from the particle-free backup filter and $F_{particle}$ the mass of an individual SOC extracted from the particle laden front filter minus F_{filter}.

It would be useful to predict the bias in measured c_p and K_p values due to gas adsorption artifacts that would occur for a given sampling situation. Assuming gas/filter and G/P equilibrium, values of F_{filter} and $F_{particle}$ can be calculated from the $K_{p,x}$ and K_p values of the filters and particles, respectively.

$$F_{filter} = K_{p,x} \ (m^3/cm^2) \times c_g \ (ng/m^3) \times A_{filter} \ (cm^2) \tag{4.8}$$

$$F_{particle} = K_p \ (m^3/\mu g) \times c_g \ (ng/m^3) \times M_{particle} \ (\mu g) \tag{4.9}$$

Where $M_{particle}$ is the mass of particles collected on the front filter. Substituting equations 4.8 and 4.9 into equation 4.7 and simplifying leads to equation 4.10.

$$100 \times ((K_p \times M_{particle} / K_{p,xs} \times A_{filter}) + 1)^{-1} \tag{4.10}$$

For a given sampling situation, equation 4.10 can be used to predict the percent of the total mass of an SOC present on a front filter due to gas adsorption, and therefore the magnitude of the positive bias in measured c_p and K_p values due to gas adsorption artifacts. Equation 4.10 is valid for SOCs satisfying the criterion; $V_t \geq V_{t,filter}$. Values of K_p can be reasonably approximated for a given compound class at a given location, and compound specific $K_{p,x}$ values are available from this publication for adsorption of gaseous PAH and PCDD/Fs on commonly used filters. The value of $M_{particle} = V_t \ (m^3) \times TSP \ (\mu g/m^3)$. Where TSP is the total suspended particulate material. For a given sampling study V_t is known, the TSP measured or easily estimated within a factor 2, and for a given sampler A_{filter} is known.

The careful work of Ligocki (1986) and Luo (1996) can be used to test this predictive approach. Ligocki (1986) measured the K_p values of PAHs partitioning to Portland urban particulate material during rain events (RH = 100%). The author presented sampling parameters enabling calculation of the average $M_{particle}$, T and RH as well as disclosing the filter type and A_{filter}. Backup filters were used to correct for gas adsorption artifacts. An estimate of the percent of the total mass of an individual PAH present on the front filter due to gas adsorption was made (equation 4.7) using *measurements* of the mass of the individual PAHs present on the front and backup glass fiber filters (GFFs). The percent of the total mass of an individual PAH present on the front filter due to gas adsorption was predicted (equation 4.10) as follows: $K_{p,s}$ values measured for PAHs on ambient backup QFF at 100% RH were taken from Luo (1996) and converted to $K_{p,x}$ values using equation 4.3. It was assumed that at 100% RH, GFF and QFF have similar adsorptive properties. $K_{p,x}$ values were corrected for the difference in (M_{filter}/A_{filter}) between the two filter types. The values of K_p, $M_{particle}$, $K_{p,x}$ and A_{filter} were given by Ligocki (1986); using these data in equation 4.10; the average predicted value of the percent of the total mass of a given PAH present on a front filter due to gas adsorption was 14% which compares favorably to the 10% measured by Ligocki (1986). For a given SOC, if $V_t \geq V_{t,eq}$, equation 4.10 can be used with reasonable accuracy to predict the magnitude of the positive bias in the measured c_p and K_p values of that compound as caused by gas adsorption artifacts.

4.2.3.2 Equations describing the influence of gas adsorption on measurements of c_g, c_p and K_p. The gas-phase concentration of an SOC as measured using a typical filter/adsorbent air sampler is calculated using the relationship:

$$c_{g,measured} = F_{adsorbent} / V_t \qquad (4.11)$$

Where $F_{adsorbent}$ is the mass of an SOC collected on the adsorbent, often a polyurethane foam plug (PUF) or XAD cartridge. The adsorption of gaseous SOC to filters results in:

$$F_{adsorbent} = (c_g V_t - F_{filter}) \qquad (4.12)$$

Where c_g is the "true" gas-phase concentration of a given SOC. Substituting equation 4.12 into equation 4.11 and assuming gas/filter equilibrium is achieved allows the substitution of equation 4.8 for F_{Filter}, all of which results in equation 4.13.

$$(c_{g,measured} / c_g) = (1 - K_{p,x} A_{filter} / V_t) \qquad (4.13)$$

The particle-phase concentration of a given SOC as measured using a typical filter/adsorbent air sampler is calculated from:

$$c_{p,measured} = F_{front\ filter} / M_{particle} \tag{4.14}$$

Where $F_{front\ filter}$ is the mass of an SOC extracted from the front filter. As a result of the adsorption of gaseous SOC to filters:

$$F_{front\ filter} = c_p M_{particle} + F_{filter} \tag{4.15}$$

Where c_p is the "true" particle-phase concentration of a given SOC. Substitution of equation 4.15 into equation 4.14 and assuming gas/filter equilibrium is achieved allows the substitution of equation 4.8 for F_{Filter}; all of which results in equation 4.16:

$$(c_{p,measured} / c_p) = (1 + K_{p,xs} A_{filter} / TSP\ V_t\ K_p) \tag{4.16}$$

The relationship between the measured gas/particle partition coefficient ($K_{p,measured}$) and the "true" K_p value of a given SOC is derived from the ratio of 4.16 and 4.13.

$$K_{p,measured} / K_p = (c_{p,measured} / c_p) / (c_{g,measured} / c_g) =$$
$$(1 + K_{p,xs} A_{filter} / TSP\ V_t\ K_p) / (1 - K_{p,xs} A_{filter} / V_t) \tag{4.17}$$

Note that for a given class of SOCs, if the slope of a plot of log K_p vs. p_L^o is the same for partitioning to filters as to particles then the ratio ($K_{p,measured} / K_p$) will be independent of temperature. Therefore it would not be necessary to know $K_{p,xs}$ or $K_{p,s}$ as a function of temperature.

4.2.3.3 Equations to evaluate the magnitude of the positive bias in measured K_p values encountered when gas adsorption artifact corrections are made using backup filters which have not achieved equilibrium with the gas-phase SOCs of interest. Corrections for gas adsorption artifacts are typically made using backup filters; the corrected measured particle-phase concentration of an SOC is:

$$c_{p,corrected} = (F_{front\ filter} - F_{backup\ filter}) / M_{particle} \tag{4.18}$$

Where $F_{backup\ filter}$ is the mass of an SOC extracted from the backup filter. The corrected measured gas-phase concentration of an SOC is:

$$c_{g,corrected} = (F_{adsorbent} + 2\ F_{backup\ filter}) / V_t \tag{4.19}$$

and the corrected measured gas/particle partition coefficient:

$$K_{p,corrected} = c_{p,corrected} / c_{g,corrected} \approx K_p \tag{4.20}$$

This procedure assumes that the ng/cm^2 amounts of each SOC adsorbed on the front and backup filters are equal. Since the front filter will tend to reach equilibrium with the incoming gaseous SOCs first, that equality might only be achieved after both filters have reached equilibrium with the gaseous SOCs in the sample air. If a filter's collection efficiency for a gaseous SOCs is 100%, then at $V_t < (V_{t,min} / 2)$ none of the SOC will have passed through the front filter; a K_p or $K_{p,corrected}$ cannot be calculated for a given SOC since $F_{adsorbent}$ and $F_{backup\ filter} = 0$ and $c_{g,measured} = c_{g,corrected} = 0$. At $(V_{t,min} / 2) < V_t < V_{t,min}$, the front filter has reached gas/filter equilibrium with the SOC in the sample air but the backup filter has not, a $K_{p,corrected}$ value can be calculated but it will not equal K_p. At $(V_{t,min} / 2) < V_t < V_{t,min}$:

$$F_{backup\ filter} = (c_g V_t - c_g (V_{t,min} / 2)) \tag{4.21}$$

Substituting equation 4.21 into equations 4.18 and 4.19, and substituting these equations into equation 4.20 leads to:

$$(K_{p,corrected} / K_p) = (1 + (1/K_p TSP) ((V_{t,min}/V_t) - 1)) / 2 (1 - (V_{t,min} / 2 V_t)) \tag{4.22}$$

At $V_t > V_{t,min}$, if backup filter corrections are made using backup filters, equation 4.22 can be used to estimate the magnitude of the positive bias in the K_p value of a given SOC due to gas adsorption artifacts. Note that for a given class of SOCs, if the slope of a plot of log K_p vs. p_L^o is the same for partitioning to filters and particle then the ratio $(K_{p,corrected} / K_p)$ will be independent of temperature.

4.2.4 Diagnostic Plots

The equations derived in the previous section can be used to construct diagnostic plots to evaluate the magnitude of the influence of gas adsorption artifacts on measured values of c_g and K_p, as functions of the air sample volume (V_t), compound- and filter-dependent $K_{p,x}$ values and TSP (K_p values).

4.2.4.1 Influence of gas adsorption on measurements of c_g. Using the value of $K_{p,x}$ for a given compound and values of A_{filter} and V_t for a typical air sampling study, the influence of gas adsorption on $c_{g,measured}$ can be predicted using equation 4.13. The accuracy of these predictions can be evaluated by comparison to measured values of $(c_{g,measured} / c_g)$ at a given V_t. Mader and Pankow (2000a) equilibrated two, particle-free TMFs with gas-phase PAH and PCDD/Fs at $T = 25$ °C. The value of $c_{g,measured}$ was measured as a function of V_t; at gas/filter equilibrium $c_{g,measured} = c_{g,eq}$. Measured values

of the ratio ($c_{g,measured}$ / c_g) were determined by dividing $c_{g,measured}$ at a given V_t by $c_{g,eq}$. The $K_{p,x}$ values of the PAH and PCDD/Fs on TMF are available from Mader and Pankow (2000a); A_{filter} for the two TMFs was 77 cm². This data was used in equation 4.13 to predict ($c_{g,measured}$ / c_g) as a function of V_t. As shown in Figures 4.3a and b equation 4.13 did a good job of predicting the influence of gas adsorption artifacts on the $c_{g,measured}$ values of the low and mid molecular weight PAH and PCDD/Fs collected downstream of TMFs. For the higher molecular weight PCDD/Fs equation 4.13 underestimated $c_{g,measured}$; the collection efficiency of these compounds may be less than 100%.

Plots of ($c_{g,measured}$ / c_g) for PAHs as a function of V_t were constructed at 20 °C for three types of filters using equation 4.13, and assuming only a single filter is used during sampling (Figure 4.4). Similarly for the PCDD/Fs a plot of ($c_{g,measured}$ / c_g) as a function of V_t for a single TMF at 20 °C is presented in Figure 4.5. As illustrated in Figures 4.3-4.5, for a given compound $c_{g,measured}$ is zero until $V_t > V_{t,filter}$. At $V_t > V_{t,filter}$ the ratio ($c_{g,measured}$ / c_g) begins an asymptotic approach to 1. Figures 4.3-4.5 also indicate that the magnitude of the artifact in $c_{g,measured}$ is compound dependant; depending on the compounds p_L^o.

Typical ambient gas- and particle-phase PAH and PCDD/Fs measurements use high volume air samplers requiring $V_t \approx$ 100–1000 m³ and 1000-3000 m³, respectively. Figures 4.4 and 4.5 indicate that gas adsorption will cause a significant negative bias in the $c_{g,measured}$ values of chrysene, 2378 F and 1234 D. PAH having a $p_L^o \le$ chrysene and PCDD/Fs having $p_L^o \le$ 1234 D may also be negatively biased if the collection efficiency of filters for these gaseous compounds is near 100%.

4.2.4.2 Influence of gas adsorption on measurements of K_p. Figures 4.6 through 4.9 illustrate the influence of V_t, filter type and *TSP* on the magnitude of the positive bias in $K_{p,measured}$ due to gas adsorption artifacts. These plots were constructed using 4.17, assuming a single 8×10 inch filter was used during high volume air sampling. The K_p values used for the partitioning of PAHs to ambient particles were from Ligocki (1986) and K_p values for the PCDD/Fs from Eitzer and Hites (1989).

The accuracy of this approach can be evaluated by a comparison of predicted ($K_{p,measured}$ / K_p) values to the measured values of Hart and Pankow (1994). For $V_t \approx$ 500
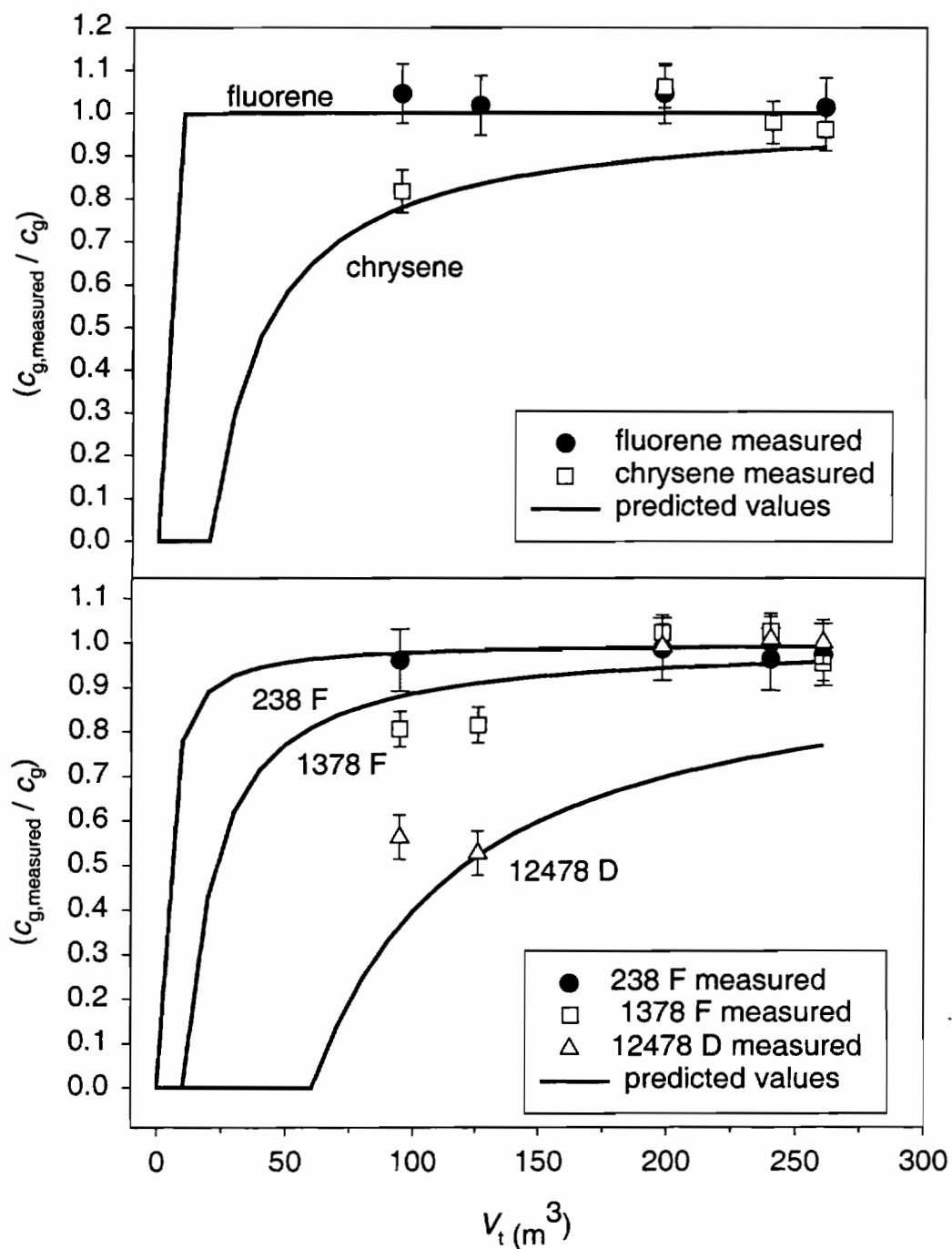
Figure 4.3 Plot of $(c_{g,measured} / c_g)$ *vs.* V_t comparing model predictions to measured values for the partitioning of selected PAH and PCDD/Fs to TMF at 25 °C.
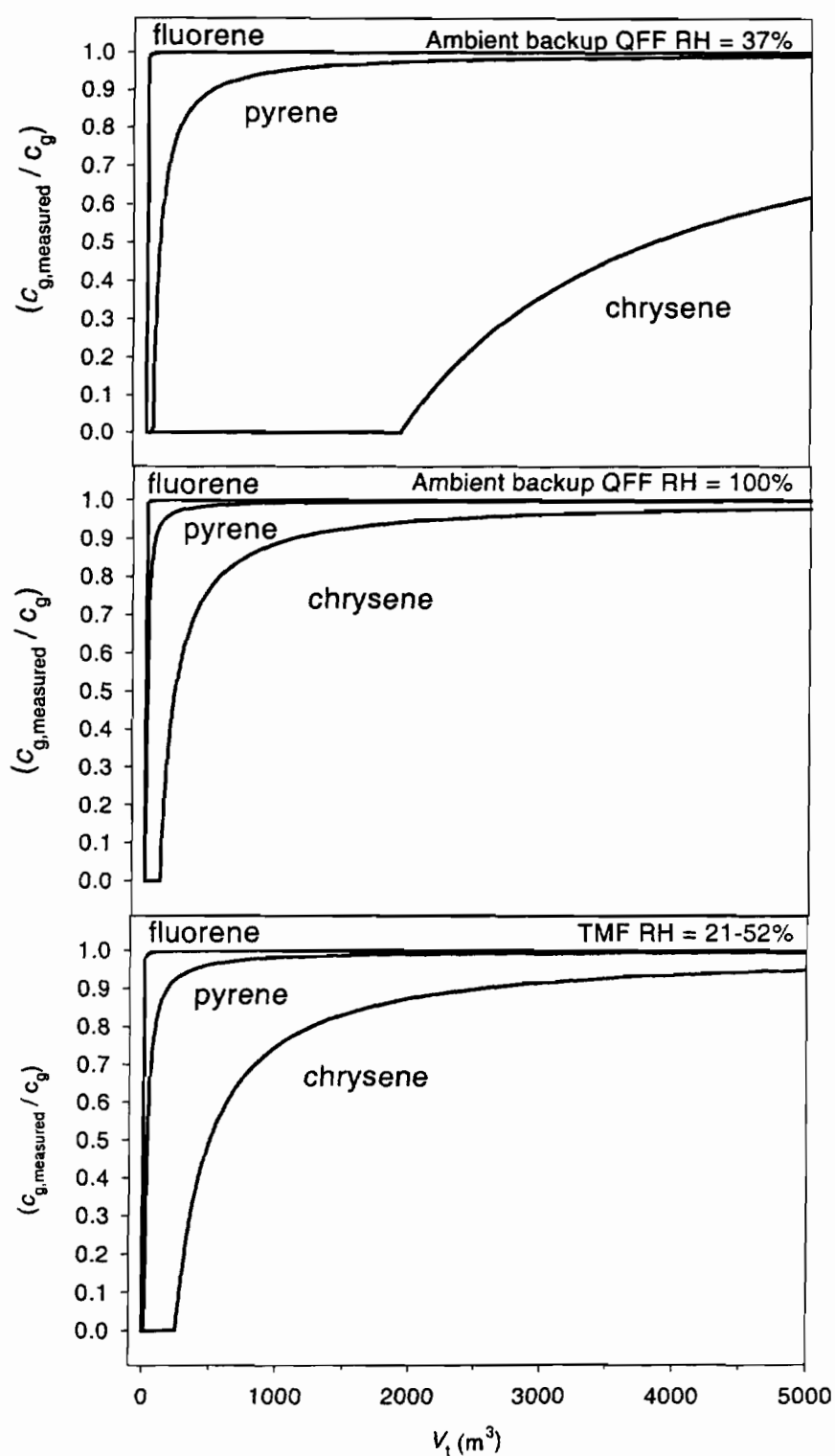
Figure 4.4 Plot of predicted ($c_{g,measured}$ / c_g) *vs.* V_t for the partitioning of selected PAHs to three types of filters at 20 °C. **a.** Ambient backup QFF at RH= 37% **b.** Ambient backup QFF at RH= 100% **c.** TMF at RH 21-52%
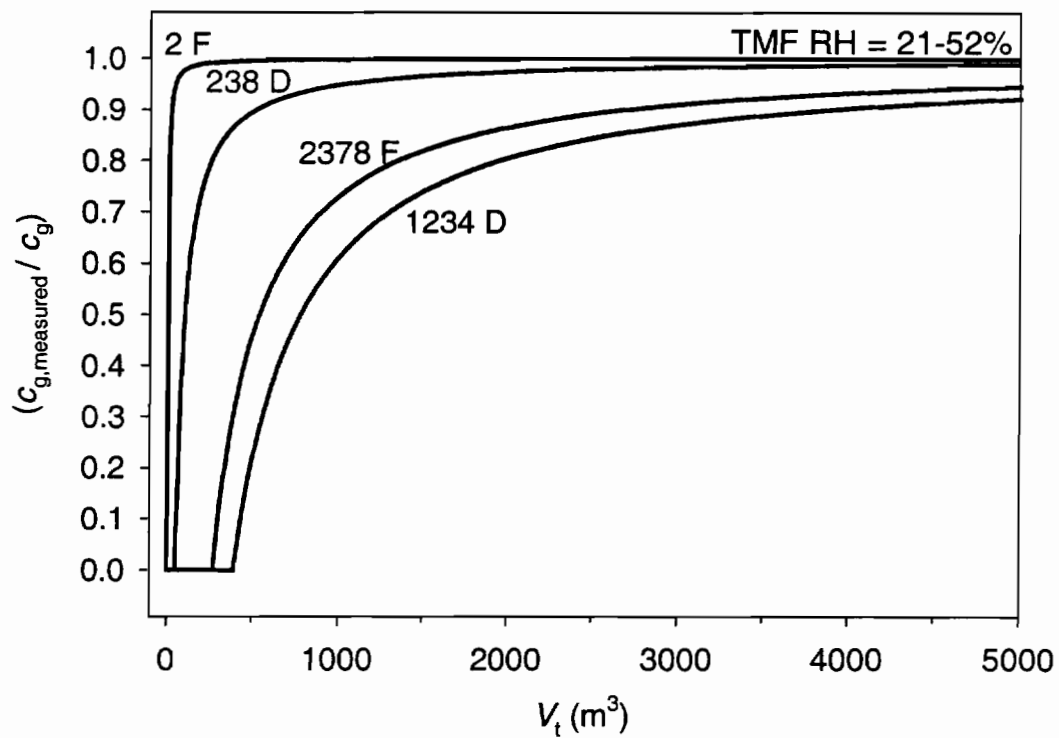
Figure 4.5 Plot of predicted ($c_{g,\text{measured}}$ / c_g) *vs.* V_t for the partitioning of selected PCDD/Fs to TMF at RH 21-52% at 20 °C.
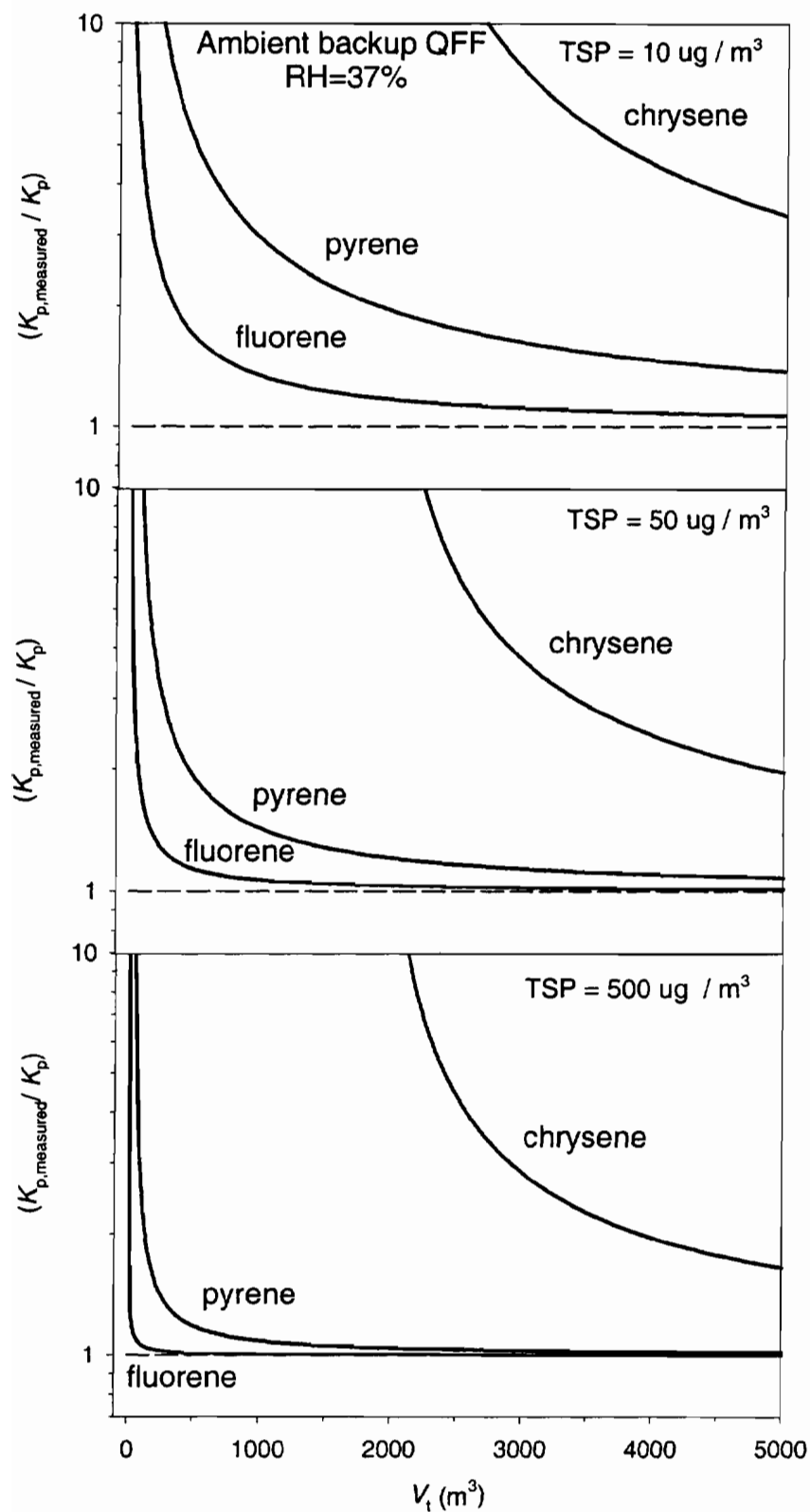
Figure 4.6 Plot of predicted ($K_{p,measured}$ / K_p) *vs.* V_t for the partitioning of selected PAH to ambient backup QFF at RH=37% at 20 °C
a. TSP =10 μg/m^3 **b.** TSP=50 μg/m^3 **c.** TSP=500 μg/m^3
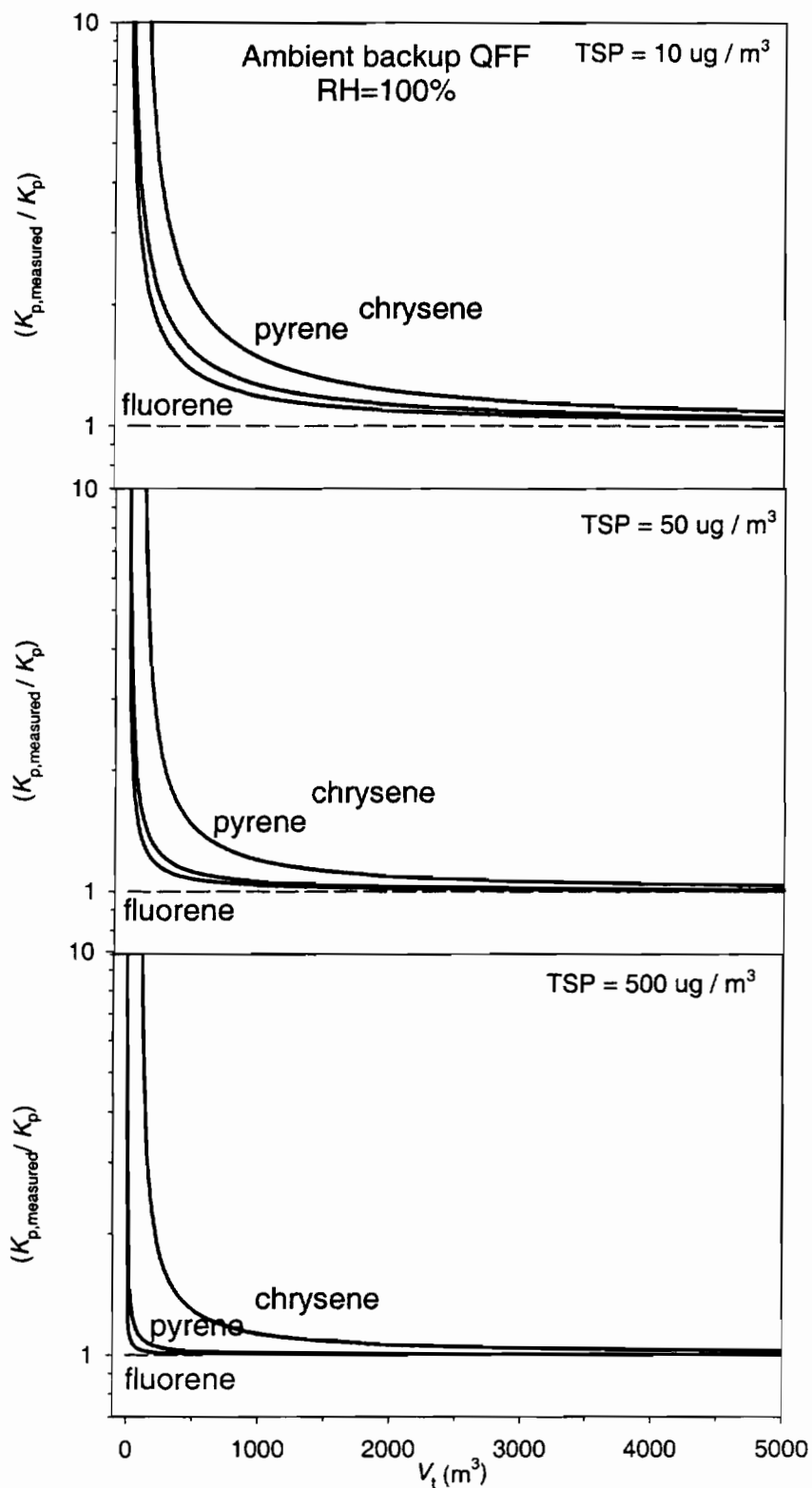
Figure 4.7 Plot of predicted ($K_{p,measured}$ / K_p) *vs.* V_t for the partitioning of selected PAH to ambient backup QFF at RH=100% **a**. TSP=10 μg/m³ **b**. TSP=50 μg/m³ **c**. TSP=500 μg/m³
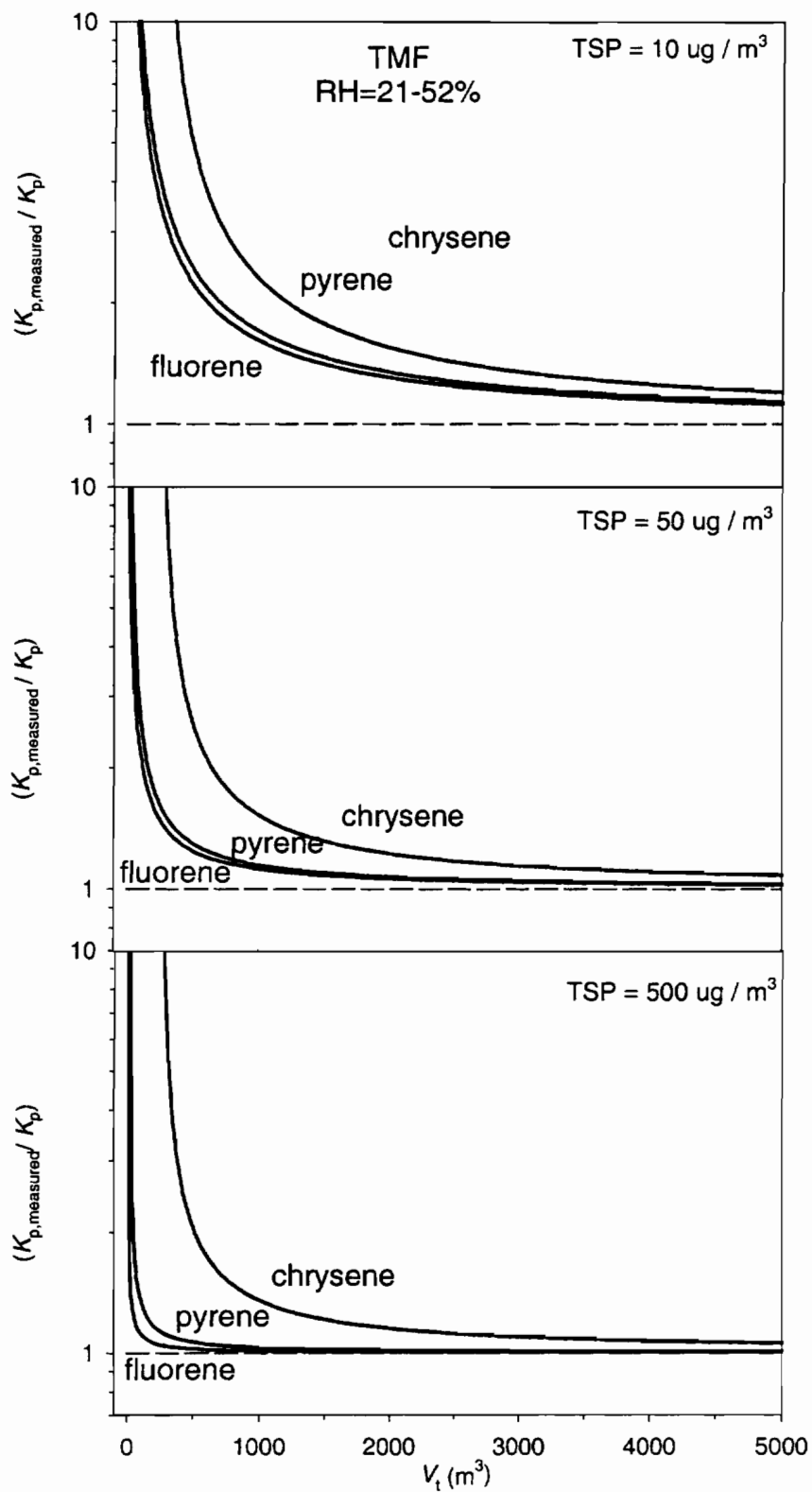
Figure 4.8 Plot of predicted ($K_{p,measured}$ / K_p) *vs.* V_t for the partitioning of selected PAH to TMF at RH=21-52% **a**. TSP=10 μg/m³ **b**. TSP=50 μg/m³ **c**. TSP=500 μg/m³
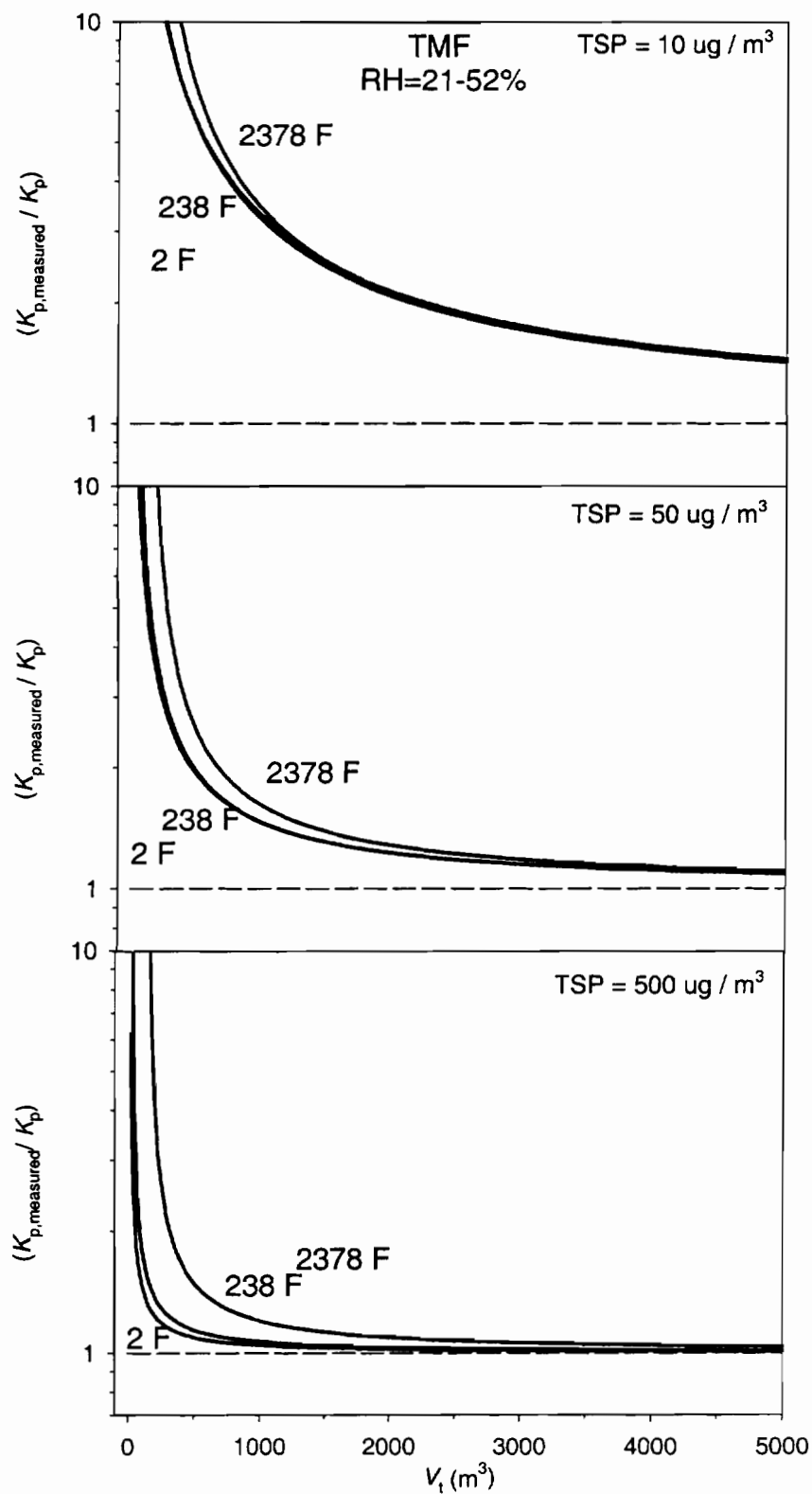
Figure 4.9. Plot of predicted ($K_{p,measured}$ / K_p) *vs*. V_t for the partitioning of selected PCDD/Fs to TMF at RH=21-52%. **a**. TSP=10 μg/m³ **b**. TSP=50 μg/m³ **c**. TSP=500 μg/m³

m^3, $TSP \approx 50$ µg m^{-3} and $RH \approx 90\text{-}100$ % Hart and Pankow (1994) observed that the adsorption of gaseous PAH to QFF filters will cause the ratio ($K_{p,measured}$ / K_p) of individual PAHs to be from 1.2 –1.6. As shown in Figure 4.7b, under similar conditions equation 4.17 predicts errors in the range of 1.1-1.4, which is very similar as those measured by Hart and Pankow (1994). For air sampling studies employing high volume air samplers to measure G- and P- phase PAHs and PCDD/Fs, Figures 4.6-4.9 provide accurate estimates of the magnitude of the positive bias in $K_{p,measured}$ caused by uncorrected gas adsorption artifacts.

As illustrated in Figures 4.6-4.9, for a given compound $K_{p,measured}$ is infinity until $V_t > V_{t,min}$. At $V_t > V_{t,min}$ the ratio ($K_{p,measured}$ / K_p) begins an asymptotic approach to 1. The magnitude of the positive bias in $K_{p,measured}$ due to the adsorption of gaseous SOCs to filters is: 1) compound dependent, the lower the compound's p_L^o the greater the artifact at a given V_t and 2) dependant on the ambient TSP, the lower the TSP the larger the artifact for a given compound.

Considering the typical V_t used to sample ambient PAH and PCDD/F sampling, at low RH gas adsorption artifacts on QFF can be very large for some PAHs and these artifacts will not be corrected properly by backup filters since, $V_t < V_{t,min}$. For studies concerned with the gas/particle partitioning of PCDD/Fs our results suggest that significant gas adsorption artifacts can occur, especially for samples in rural areas ($TSP \approx$ 10 µg/m^3).

4.2.4.3 Magnitude of the positive bias in measured K_p values encountered when gas adsorption artifact corrections are made using backup filters that have not achieved equilibrium with gas-phase SOCs. For a given SOC, when $V_t < V_{t,min}$, the ng/cm^2 amounts of each SOC adsorbed on the front and backup filters are not equal. Gas adsorption artifacts will not be eliminated despite corrections using backup filters. Figures 4.10 and 4.11 illustrate the error in $K_{p,corrected}$ as a function of V_t and were constructed as follows: At $V_t < (V_{t,min} / 2)$, $K_{p,corrected}$ and K_p are undefined since $c_{g,measured} = 0$. At $(V_{t,min} / 2) < V_t < V_{t,min}$ equation 4.22 was used to evaluate ($K_{p,corrected}$/ K_p) for a given SOC on a given filter at 20 °C. The K_p values used in equation 4.22 for the partitioning of chrysene and 2378 F to ambient particles were taken from Ligocki (1986) and Eitzer and Hites (1989), respectively. At $V_t > V_{t,min}$, $K_{p,corrected} \approx K_p$ assuming that the

ng/cm^2 amounts of gaseous SOC adsorbed on the front and backup filters are equal. Figures 4.10 and 4.11 indicate that at $V_t < V_{t,min}$ a significant positive bias in the measured K_p value of a compound will occur and this bias will *not* be eliminated by backup filter corrections.

4.2.5 Implications for the sampling of ambient gas- and particle-phase SOCs.

Our results indicate that gas adsorption artifacts can significantly affect the measured values of c_g, c_p and K_p. Such artifacts will be small when the amounts of the SOCs adsorbed on the filters are small compared to both: 1) the amounts in/on the collected particles (so that the errors in the c_p values are small); *and* 2) the amounts that entered the sampler in the gas phase (so that the errors in the c_g values are small). This will be achieved when the gas/filter K_p values for the compounds of interest are low, and/or the particle loading on the filter is high, and/or the sample volume is sufficiently large. If backup filter corrections are to properly eliminate gas adsorption artifacts, the ng/cm^2 amounts of each SOC adsorbed on the front and backup filters must be equal. This equality can only occur when V_t is large enough such that lowest volatility compounds of interest reach gas/filter equilibrium with backup filters.

Figures 4.2-4.11 enable one to accurately choose sampling parameters that minimize sampling artifacts and/or increase the likelihood that such artifacts can be properly corrected using backup filters. Interestingly the factor limiting the reduction in the V_t required for ambient gas- and particle-phase PAH and PCDD/F measurements using conventional high volume air samplers may be the adsorptivity of the filters rather than the detection limit of the GC/MS.
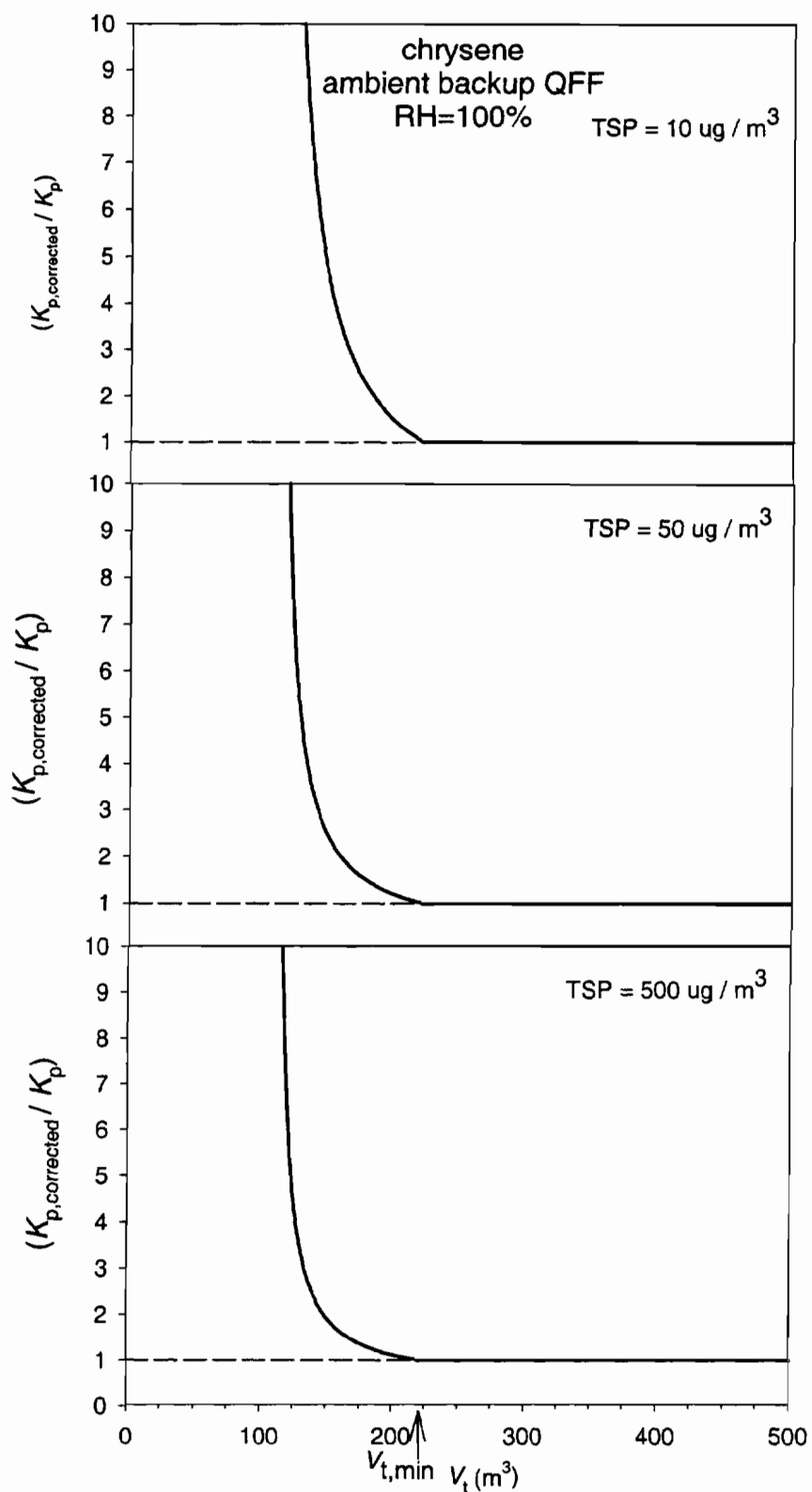
Figure 4.10 Plot of predicted ($K_{p,corrected}$ / K_p) *vs.* V_t for the partitioning of chrysene to QFF at RH=100%. **a**. TSP=10 μg/m^3 **b**. TSP=50 μg/m^3 **c**. TSP=500 μg/m^3
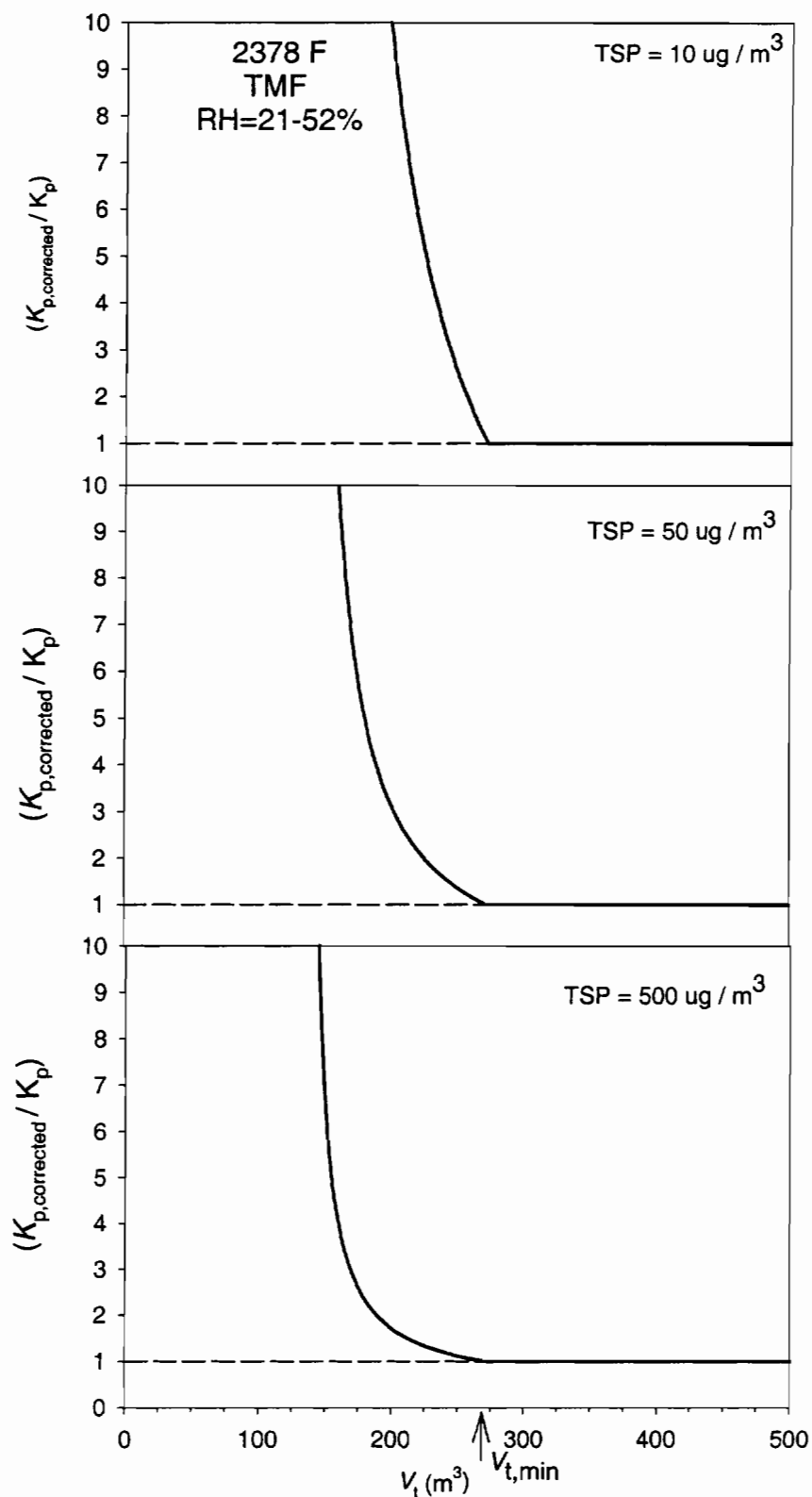
Figure 4.11 Plot of predicted ($K_{p,corrected}$ / K_p) *vs.* V_t for the partitioning of 2378 F to TMF at RH=21-52%. **a**. TSP=10 µg/m^3 **b**. TSP=50 µg/m^3 **c**. TSP=500 µg/m^3

4.3 References

Eitzer, B. D., Hites, R. A. 1989. Polychlorinated dibenzo-p-dioxins and dibenzofurans in the ambient atmosphere of Bloomington, Indiana. *Environmental Science and Technology* 23, 1389-1395.

Hart, K. M., Pankow, J. F. 1994. High volume air sampler for particle and gas sampling: Part 2. Use of backup filters to correct the adsorption of gas phase polycylic aromatic hydrocarbons to the front filter. *Environmental Science and Technology* 28, 655-661.

Ligocki, M. P. 1986. *The Scavenging of Atmospheric Trace Organic Compounds by Rain.* Ph.D. Thesis, Department of Environmental Science and Engineering, Oregon Graduate Institute.

Luo, W. 1996. *Gas/Particle partitioning of semi-volatile organic compounds to two model atmospheric particulate materials: quartz and graphitic carbon.* Ph.D. Thesis, Environmental Science and Engineering, Oregon Graduate Institute of Science and Technology.

Mader, B. T., Pankow, J. F. 2000a. Gas/solid partitioning of polychlorinated dibenzodioxins, polychlorinated dibenzofurans and polycyclic aromatic hydrocarbons to filter surfaces: Part 2. Quartz fiber filters. *Atmospheric Environment* submitted April 15, 2000.

Mader, B. T., Pankow, J. F. 2000b. Gas/solid partitioning of polychlorinated dibenzodioxins, polychlorinated dibenzofurans and polycyclic aromatic hydrocarbons to filter surfaces: Part 1. Teflon membrane filters. *Atmospheric Environment* in press April 15, 2000.

Mader, B. T., Pankow, J. F. 2000c. Vapor pressures of polychlorinated dibenzodioxins, polychlorinated dibenzofurans and polycylic aromatic hydrocarbons: measurements and evaluation of estimation techniques. *Environmental Science and Technology* submitted March 15, 2000.

McDow, S. R. 1999. Sampling Artifact Errors. In *Gas and Particle Phase Measurements of Atmospheric Organic Compounds.* Ed. D. A. Lane. Amsterdam, Gordon and Breach Science Publishers. pp. 105-126.

McDow, S. R., Huntzicker, J. J. 1990. Vapor adsorption artifact in the sampling of organic aerosol: face velocity effects. *Atmospheric Environment* 24, 2563-2571.

Odum, J. R. *et al.* 1996. Gas/particle partitioning and secondary organic aerosol yields. *Environmental Science and Technology* 30, 2580-2585.

Odum, J. R. *et al.* 1997. The atmospheric aerosol-forming potential of whole gasoline vapor. *Science* 276, 96-100.

Storey, J. M. *et al.* 1995. Gas/solid partitioning of semivolatile organic compounds to model atmospheric solid surfaces as a function of relative humidity. Part 1. Clean quartz. *Environmental Science and Technology* 29, 2420-2428.

Turpin, B. J., Huntzicker, J. J. 1994. Investigation of organic aerosol sampling artifacts in the Los Angeles Basin. *Atmospheric Environment* 28, 3061-3071.

Yamasaki, H. *et al.* 1984. Determination of vapor pressure of polycyclic aromatic hydrocarbons in the supercooled liquid phase and their adsorption on airborne particulate matter. *The Chemical Society of Japan* 8, 1324-1329.

CHAPTER 5

VAPOR PRESSURES OF POLYCHLORINATED DIBENZODIOXINS, POLYCHLORINATED DIBENZOFURANS AND POLYCYCLIC AROMATIC HYDROCARBONS: MEASUREMENTS AND EVALUATION OF PREDICTION TECHNIQUES

5.1 Introduction

Vapor pressure is an important parameter for modeling the fate of an organic compound in the environment (Mackay and Paterson, 1991). For this reason international commissions have selected vapor pressure as an important screening criteria for evaluating the environmental persistence of a chemical (Rodan *et al.*, 1999). Vapor pressure has also been used to parameterize the gas/particle and gas/solid distribution of semivolatile organic compounds (SOCs) (Pankow and Bidleman, 1992):

$$\log K_p = m_r \log p_L^o + b_r \quad \textit{adsorptive or absorptive partitioning} \quad (5.1)$$

where K_p is a compound's gas/particle or gas/solid partition coefficient and p_L^o the compounds pure subcooled liquid vapor pressure. Values of the slope (m_r) are frequently close to -1. Pankow (1987)(1994) and Pankow and Bidleman (1992) have shown the slope of a plot $\log K_p$ vs. $\log p_L^o$ can be affected by thermodynamic and kinetic effects. There has been much recent discussion regarding the mechanistic implications of slope of such plots (Goss and Schwarzenbach, 1998; Simcik *et al.* 1998). For a given class of SOCs the value of this slope depends directly on the accuracy of the vapor pressure data used in the correlation. For example if the measured p_L^o values of the higher molecular weight compounds of a homologues series SOCs are greater than their true values but the measured p_L^o of the lower molecular weight compounds are similar to their true values, the slope of the corresponding $\log K_p$ vs. $\log p_L^o$ plot will be steeper ($m_{r,measured} < m_{r,true}$) than the "true" slope calculated using accurate p_L^o values. Conclusions drawn from an

evaluation of the slope of a log K_p vs. log p_L^o plot that was constructed using biased p_L^o data would be incorrect. Therefore accurate vapor pressure data is necessary to enable thorough theoretical examination of the mechanisms of the gas/particle and gas/solid partitioning of SOCs.

The PCDD/Fs are a class of SOCs consisting of homologues series of 210 individual congeners. It is not feasible to measure the vapor pressure of each congener and correlation methods (Eitzer and Hites, 1988; Rordorf *et al.*, 1990; Eitzer and Hites, 1998) have been used to estimate the vapor pressure of these compounds. Some correlation methods can be quite precise, predicted vapor pressures measured using a gas-chromotography retention index (GC-RI) method can have relative standard deviations of 9%, but the accuracy of these predictions depend on the availability of directly measured vapor pressure data Bidleman (1984). The correlation method of Rordorf, *et al.* (1990) under-predicted the measured vapor pressures of penta and hexa-chlorinated PCDD/Fs by a factor two to three. Eitzer and Hites (1988)(1998) measured p_{gc} values using a GC-RI method. Where p_{gc} is an estimate of a compound's p_L^o. There was a systematic difference between the vapor pressures measured using the GC-RI method and predictions of Rordorf (1989)(1990). The GC-RI method underestimated the predicted vapor pressures of the lower chlorinated PCDD/Fs by up to a factor 8 and overestimated the predicted vapor pressures of the more highly chlorinated congeners by a factor of 5.

To help improve the accuracy of vapor pressure prediction methods more measured data is necessary. The most reliable vapor pressure measurement methods are direct methods such as gas saturation MacKay, Shui *et al.*, (1992). The goal of this study was to: 1) use a dynamic gas saturation technique to measure the vapor pressure of several PCDD/Fs and PAHs at 25 °C and 2) determine a correlation equation which enables the accurate estimation of the vapor pressure of PCDD/Fs for which direct measurements have not been made.

5.2 Materials/Methods

5.2.1 Methodology- General.
Vapor pressure measurements were conducted as part of a larger study of the gas/filter and gas/particle partitioning behavior of PCDD/Fs and PAHs. In separate experiments, Teflon filters, quartz fiber filters, and ambient

particulate material collected on Teflon filters, were equilibrated with gas-phase PCDD/Fs and PAHs. The specific details of these experiments are given elsewhere Mader and Pankow (2000a; 2000b; 2000c). Generator cartridges provided gas-phase PAHs and PCDD/Fs for these experiments. Vapor pressures of selected PAH and PCDD/Fs could be calculated from the equilibrium vapor densities achieved after gas/filter or gas/particle equilibrium.

5.2.2 Methodology- Specific.

5.2.2.1 Generator Cartridges. Generator cartridges were made of 3/8-inch OD × 0.30 inch ID stainless steel tubing and 3/8-inch Swagelock end fittings. Cartridges were packed with glass beads coated with PCDD/Fs and PAH. At each end of the cartridges a small plug of glass wool held the coated glass beads inside the stainless steel tubing. A 3/8-inch diameter punch of Quartz fiber filter was inserted between the end of the tubing and the inside of each Swagelock endfitting. The small Quartz filters prevented ambient particles from entering the cartridges and solid phase PAH or PCDD/F from the exiting the cartridges. The diameter of the glass beads was either 0.25 or 1 mm depending on the desired generator column flow rate. Glass beads were coated with a mixture of 2 to 4 compounds believed to be of similar vapor pressure and of the same compound class. Mixtures contained 2 to 20 mg and 10 to 30 mg of an individual PCDD/F and PAH, respectively. The mole fraction of each compound in the mixture was known and is presented in Table 5.1. Mixtures were prepared in 50 mL roundbottom flasks by dissolving a measured mass of each compound in 25 ml of methylene chloride. Once the compounds were dissolved, 20 gm of glass beads were added to the flask and the methylene chloride evaporated using ultra clean N_2. Once dried, the coated glass beads were transferred to the generator cartridges. For an individual compound the coated concentration ranged from 0.02 to 0.15% (w/w). These concentrations are higher than the 0.01% value suggested by Spencer and Cliath (1969) to ensure that vapor pressures measured over a coating of a compound is the same as measured over a pure compound. Prior to the first vapor pressure measurements generator cartridges were equilibrated by passing 6.75 to 8.78 m^3 and 0.03 to 14 m^3 and of air through the PCDD/F and PAH cartridges, respectively. The generator cartridges were then used to provide gas phase PCDD/F and PAH in 12 sets experiments. After all experiments were completed

Table 5.1 Generator cartridge specifications

Generator Cartridge	Flow rate range (ml/min)	Compounds	Mole fraction
PAH 1	9.70 – 27.4	phenanthrene	0.4332
		anthracene	0.5668
PAH 2	9.81 – 2900	fluoranthene	0.2522
		pyrene	0.2565
		benza(a)anthracene	0.1552
		chrysene	0.3205
PAH 3	177 – 3000	benza(a)anthracene	0.1875
		chrysene	0.7881
PCDD 3	50.3 – 774	28 D	0.4974
		28 F	0.5027
PCDD 4	32.2 – 424	124 D	0.5137
		246 F	0.4862
PCDD 5	659 – 3000	238 F	0.3104
	653 – 3000	1378 F	0.3480
		1234 D	0.3416
PCDD 6	1500 –3000	2378 D	0.4764
		2378 F	0.4374
		12378 F	0.0862
PCDD 7	1000 – 5500	23478 F	0.1409
		12478 D	0.5662
		12378 D	0.2929

the mole fraction of each individual PCDD/F and PAH in the generator cartridges was re-evaluated using GC/MS. There was less than a 10% difference in the mole fraction of the compounds before and after the 12 sets of experiments.

5.2.2.2 Experimental Apparatus. The generator cartridges were part of a filter equilibration apparatus previously described by Mader and Pankow (2000a). Briefly the apparatus consists of two major parts an air conditioning unit (ACU) which is responsible for adjusting and maintaining the air temperature and *RH* of the incoming air, and an Environmental Chamber (ECU). Air is first drawn into the system by a vacuum pump and the particulate matter removed using a Quartz fiber filter. In experiments using particle-free Teflon or Quartz filters gaseous SOCs were removed by absorption onto polyurethane foam (PUF) plugs. In experiments using particle-loaded Teflon filters gaseous SOC were not removed. In either experiment the cleaned or ambient air is passed through 45 cm long by 0.953 cm id stainless steel tubing placed in a thermostated water bath. The temperature within the ECU is adjusted to the same value as that within the ACU to ensure the entire sampling system is isothermal. Once inside the ECU a small portion of the incoming air flow is routed through generator cartridges and the flow controlled by needle valves. The flow through individual generator cartridges was monitored throughout each experiment. Depending on the generator cartridge, the flow ranged from 0.0097 to 5.5 L/min corresponding to linear velocities of 0.37 to 208 cm/s. The volumetric flow rate through each generator cartridge is presented in Table 5.1. The air flow from the generator cartridges was mixed back, at a point upstream of the filter holder, into the main air flow (60 L/min). The main air flow now containing PCDD/F and PAH was passed through a pair of filters held in a filter holder and then through front and backup polyurethane foam plugs (PUF) of density 0.022 g/mL. The gaseous PCDD/F and PAHs were collected with essentially 100% efficiency on the PUFs. The total air flow through the filter was constant within each experiment but ranged from 17 to 65 L/min among the different experiments. Experiments were run from approximately 1.5 to 21 days, using 55 to 920 m^3 of air. Front and backup PUFs were exchanged at regular intervals that ranged from 10 minutes to 20 hours. The sample volume for these intervals ranged from 0.6 to 70 m^3. To ensure that vapor pressures were measured accurately, the filters and internal surfaces of the filter head and tubing must have

attained sorptive equilibrium with gas-phase PCDDF and PAHs. The filter head and tubing were not cleaned between experiments, therefore after initial equilibration sorptive sites on these components should have remained saturated with PCDD/Fs and PAH. Since clean filters were used in each experiment, once gas/filter equilibrium was achieved it was likely that the entire apparatus was also at equilibrium with the gas-phase PCDD/F and PAHs. At the point that an experiment was ended, for each SOC of interest, it was considered likely that gas/filter equilibrium had been achieved if: 1) the gas phase concentration exiting the filter (as measured with the PUF plugs) had approached an asymptotic equilibrium value (designated as $c_{g,eq}$); and 2) V_t was at least twice the volume required to deliver the total mass that was found sorbed on the two filters, *i.e.*,

$$V_t \geq 2\, m_{eq} / c_{g,eq} \tag{5.2}$$

Where: m_{eq} is the sum of the mass found on the two filters at apparent equilibrium. Equation 5.2 assumes that the gas concentration entering the filter equaled $c_{g,eq}$ for the entire duration of the experiment

5.2.3 Extraction of Samples. The extraction of filters has been previously described by Mader and Pankow (2000a). PUFs were extracted using a flow through extraction method. Depending on the volume of the PUF, each PUF was loaded into a glass syringe with a volume of either 10 or 50 mLs. Once loaded each PUF was separately spiked with 4μL of a 250 ng/μl perduetrated fluorene solution; 4μL of a 250 ng/μL perduetrated pyrene solution; 16μL of a 50 ng/μL solution of fully carbon-13 labeled 1234 tetrachlorodibenzofuran; and 16μL of a 50 ng/μL L solution of fully carbon-13 labeled 2,7/2,8 dichlorodibenzodioxin. These solutions served as surrogate standards. Depending on the volume of the PUF, each PUF was extracted with either 40 or 200 mLs methylene chloride. Samples were evaporated to 4 mL using the roto-evaporator and stored until analyzed by GC/MS. Immediately before analysis by GC-MS, each extract was gently blown down to 200 μL using a stream of ultra-clean N_2, then spiked with 2000 ng of perdeutrated phenanthrene. No cleanup step was necessary. The extracts were analyzed on a Hewlett Packard 5890/5971 GC/MS and a 30m × 0.25mm DB-5 fused silica column (J&W Scientific Folsom, Ca). Each extract was injected "splitless" with the injector at 280 °C. The column temperature was held initially at 100 °C, ramped at 4 °/min to 200 °C, ramped at 5 °/min to 250 °C, and finally held isothermal

at 250 °C for 5 min. The linear velocity of the carrier gas was 25 cm/s at 100 °C corresponding to a flow rate of about 1 ml/min. The MS was operated in the electron impact mode with ionization at 70 eV and scanned from 50 to 400 amu. The multiplier voltage was 1900 eV and the detector temperature 170 °C. For the PAHs, a standard solution contained fluorene, fluorene-d_{10}, phenanthrene, phenanthrene-d_{10}, anthracene, fluoranthene, pyrene, pyrene-d_{10}, benz(a)anthracene and chrysene. For the PCDD/Fs, the standard solution contained 2 F, 28 F, 246 F, 238 F, 1378 F, 2378 F, 12378 F, 23478 F, 1 D, 2 D, 23 D, 28 D, 124 D, 1234 D, 2378 D, 12478 D, 12378 D (Cambridge Isotopes Labs) and the two fully carbon 13 labeled isotopic internal standard compounds (27+28 D and 1234 F). Response factors for the PCDD/Fs and PAHs were determined as a function of mass injected using serial dilutions of these primary standard solutions. The internal standard compound for the PAHs was phenanthrene-d_{10}. The internal standard compound for the PCDD/Fs were $^{13}C_{12}$ 27+28 D and $^{13}C_{12}$ 1234 F.

5.2.4 QA/QC. A blank filter and PUF was extracted for each experiment. With exception of chrysene, the PAH and PCDD/Fs blank levels were low, requiring corrections less than 5% of the total mass measured for compounds on both the filters and PUFs. For chrysene, if the blank corresponded to more than 10% of the mass measured on a sample a vapor pressure was not computed for that experiment. The average estimated recovery of the PCDD/F from the PUF plugs was 65% and the average recovery of the PAHs from the PUFs was 111%. Breakthrough of the most volatile compounds from the front to backup PUF averaged 5 and 7% for phenanthrene, anthracene, respectively, and 15 and 14% for 28-chlorodibenzofuran and 28-chlorodibenzodioxin, respectively. Breakthrough was negligible for the other compounds at 26 °C. Since the volume of the 178 mL backup PUF plug was over seven times that of the 24 mL front PUF plug, when combined, both plugs provided essentially quantitative recoveries for all compounds at all experimental temperatures.

The vapor densities attained in these experiments were approximately 1,000,000 to 30,000,000 and 10 to 1,000 times higher than ambient PCDD/Fs and PAHs vapor densities, respectively. Therefore during experiments using particle-loaded Teflon filters, gas-phase PCDD/F and PAH from ambient air was insignificant compared to the

concentrations generated from the cartridges. Furthermore desorption "stripping" of PCDD/F and PAH from previously collected particulate material could not occur.

5.3 Calculation of Vapor Pressures.

Each experiment consisted of at least four replicate stages during which gas-phase PCDD/F and PAH were generated and collected on PUFs. During each stage the flow rate of air through the generator cartridges, the pressure drop across the generator cartridges and the air temperature and relative humidity were measured. Using this data, the gas-phase partial pressure of a given PCDD/F and PAH was calculated for each stage as follows:

$$p_S^o = (n/V) \, (1/(p_{gen} - p_{water})) \, (RT) \tag{5.3}$$

Where: p_S^o is the partial pressure over the pure solid phase compound of interest (atm), n the moles of compound collected on the PUF, V the volume of air passed through the generator cartridge containing the compound of interest (L), p_{gen} the absolute pressure at the exit of the generator cartridge (atm), p_{water} the partial pressure of water vapor at the relative humidity and temperature of interest (atm), R the gas constant of 0.0821 (atm L/mole K) and T air temperature (K).

Generator cartridges were packed with a mixture of PCDD/F or PAHs. Depending on a compound's mole fraction, the mixtures in the generator cartridges were either separate crystals of pure solid phase compounds or crystals of a single solid solution of the compounds. For a mixture of solid phase anthracene and phenanthrene, Brady and Smith (1967) observed a miscibility gap at room temperature for mole fractions between 0.3 and 0.7. In the current study compounds having mole fractions between these values were considered to be a mixture pure crystals of each individual compound whereas compounds having mole fractions <0.3 and >0.7 were considered solid solutions. For compounds present as pure crystals, p_S^o was calculated by equation 5.3. If a compound formed a solid solution, p_S^o was calculated as follows:

$$p_S^o = p \, / \, (x \, \xi) \tag{5.4}$$

Where; x is the mole fraction of the compound in the mixture and ξ the compounds solid phase activity coefficient. As shown in Table 5.1, mixtures were made among

compounds from the same compound class and of similar structure; therefore the value of ξ was assumed one. Equation 5.4 was only used to calculate the vapor pressures of benz(a)anthracene and 12378 F.

The p_S^o values of the PCDD/Fs and PAHs measured in the current study were converted to experimentally inaccessible p_L^o values using equation 5.5 (Mackay, Bobra *et al.*, 1982).

$$\ln (p_L^o / p_S^o) = 6.8 \times (T_m - T) / T_m \qquad (5.5)$$

Where T_m (°K) is the melting point of the compound and T (°K) the temperature at which p_S^o was measured. Rordorf (1989) reports the T_m values of 25 PCDDs and 58 PCDFs.

5.4 Results

5.4.1 Solid/Vapor Equilibrium.
To ensure vapor pressures were measured accurately; the air passing though the generator cartridges must become saturated with the compounds of interest. As done in previous studies (Spencer and Cliath, 1969; Pella, 1976; Sonnefeld *et al.*, 1983), vapor pressures were measured as a function of the flow rate of air through the generator cartridges. This data is shown in Figures 5.1 and 5.2. The flow rate of air through the generator cartridges had no effect on measured vapor pressures.

To ensure that gas-phase PCDD/F and PAH had reached equilibrium with adsorptive sites in the system (i.e. stainless steel tubing, filter head and Teflon or quartz filters) it is necessary to show that the PCDD/F and PAHs vapor densities reach a nearly constant value during experiments. Vapor density is defined as the mass¯ of SOC collected on the PUF divided by the total air flow through the experimental apparatus. The adsorption of an SOC to a surface has been shown to be inversely proportional to the compound's vapor pressure (Pankow, 1987; Storey *et al.*, 1995). Therefore the equilibration volume necessary to saturate the system should be the greatest for the lowest volatility compounds measured. In Figure 5.3 the vapor densities of the lowest volatility compounds measured in this study are shown as a function of the total air volume passed through the system. During an initial equilibration period, the vapor densities rise, and attain a nearly constant value once equilibrium is achieved with the
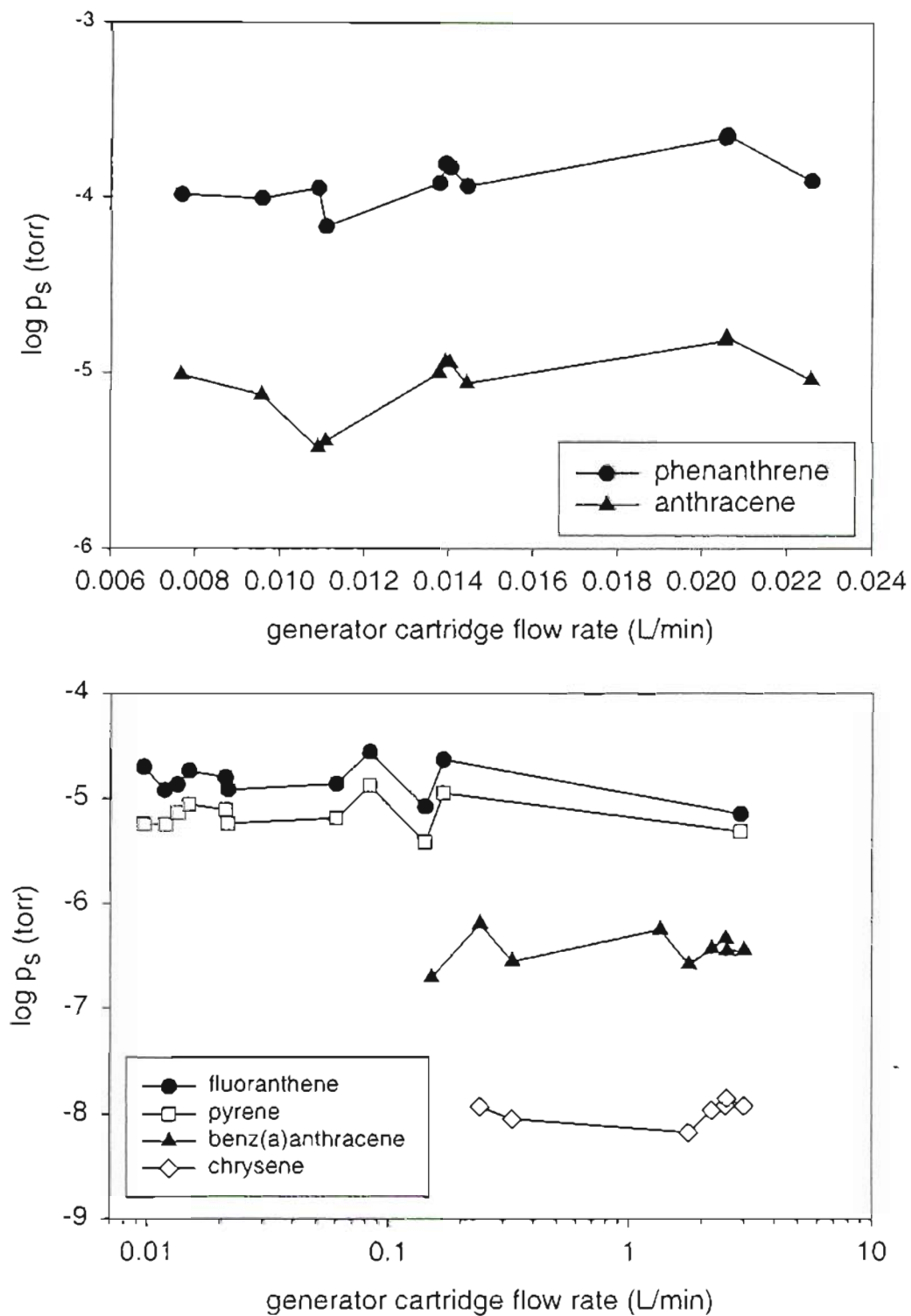
Figure 5.1 PAH Vapor pressures as a function of the flow rate of air through the generator cartridge.
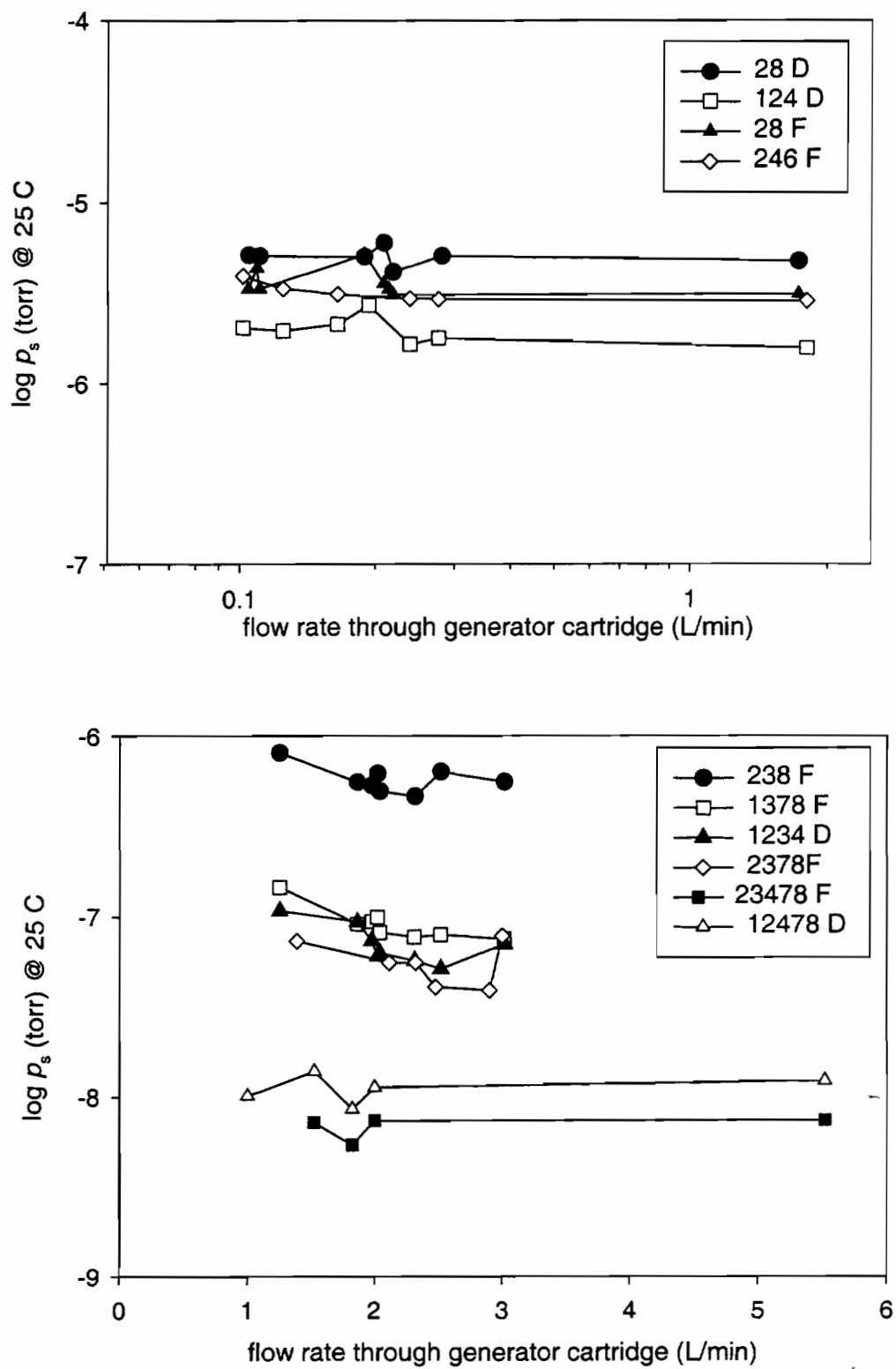
Figure 5.2 PCDD/F vapor pressures as a function of the flow rate of air through the generator column.
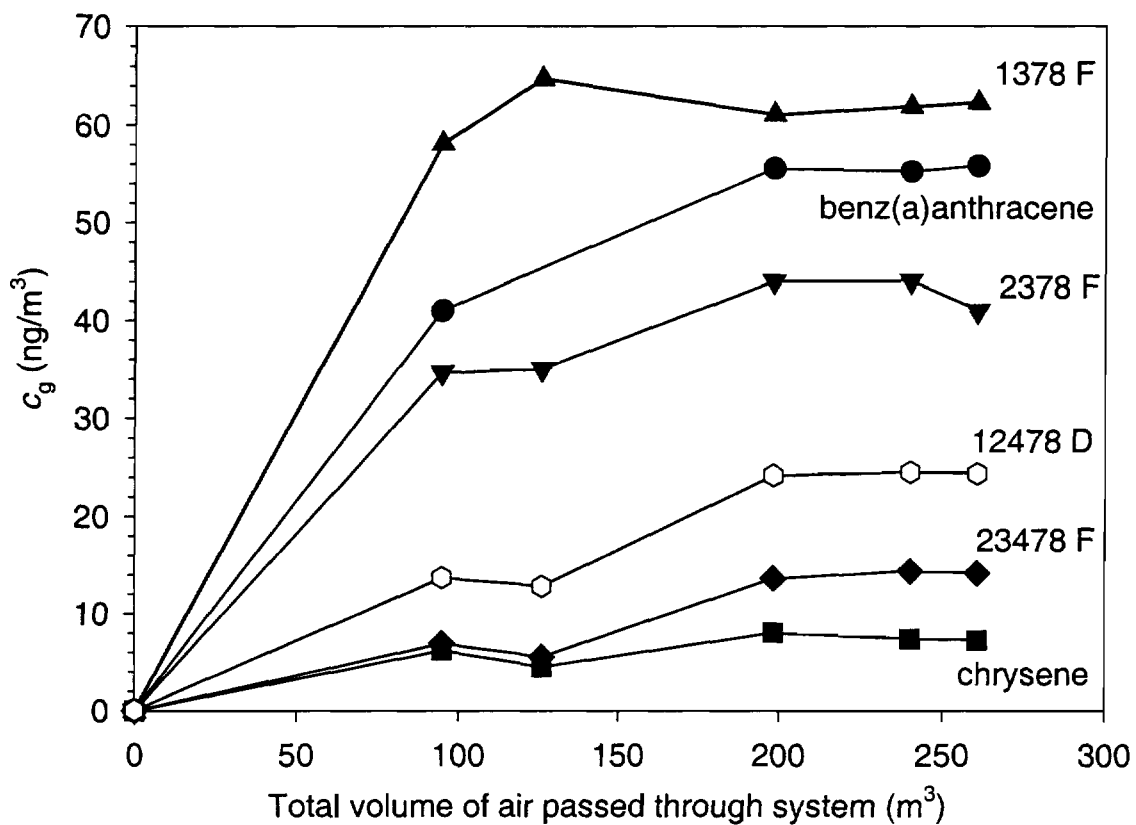
Figure 5.3 Vapor density of low volatility PAH and PCDD/Fs as a function of the total air flow through the filter head of experimental system.

Table 5.2 PAH vapor pressures at 25 °C.

Compound	log p_S^o (torr)	log p_L^o (torr)[a]
phenanthrene	-3.89 (±0.15)	-3.14
anthracene	-5.05 (±0.20)	-3.16
fluoranthene	-4.83 (±0.18)	-3.98
pyrene	-5.16 (±0.16)	-3.92
benz(a)anthracene	-6.44 (±0.16)	-5.03
chrysene	-7.97 (±0.11)	-5.69

[a] Calculated using equation 5.5.

internal surfaces of the system. Vapor pressures were calculated using only equilibrium vapor densities.

5.4.2 PAH Solid Phase Vapor Pressures. The p_s^o values of the PAHs measured in current study at 25 °C are presented in Table 5.2. In Figure 5.4a the accuracy of these values can be assessed by comparing these values to the measurements of Sonnefeld *et al.* (1983) who used a dynamic gas saturation technique at 25 °C with pure individual solid phase PAH. Sonnefeld *et al.*, (1983) did not measure the vapor pressure of chrysene, therefore a comparison is made to the literature average value at 25 °C as reported by MacKay *et al.*, (1992). The vapor pressures of the PAHs measured in the current study were within a factor 1.5 compared to those from the literature. Since the PCDD/F and PAHs were measured during the same experiments vapor pressures of the previously unmeasured PCDD/Fs should have been measured with similar accuracy.

If one does not consider the miscibility gap at mole fractions between 0.3 and 0.7, the vapor pressures of the PAHs measured in the current study were greater than literature values by up to a factor 4. This suggests that a miscibility gap must also occur for fluorene/pyrene and chrysene/benz(a)anthracene mixtures at room temperature and mole fractions between 0.3 and 0.7.

5.4.3 PCDD/F Vapor Pressures. The p_s^o values of the PCDD/Fs measured in this study at 25 °C are presented in Table 5.3. In Figure 5.4b these data are compared to extrapolated vapor pressures from the measurements of Rordorf *et al.* (1986; 1989; 1990). Rordorf (1985; 1985; 1986) used a dynamic gas saturation technique at elevated temperatures. Vapor pressures at 25 °C are made from extrapolations from these data. Rordorf *et al.*, (1986) observed order of magnitude differences between vapor pressures extrapolated to 20 °C as compared to those measured directly at 20 °C. Errors due to extrapolation are probably the reason why there is as much as a factor 5 difference between the vapor pressures measured in the current study and those of Rordorf *et al.*, (1986; 1989; 1990).

5.4.4 Evaluation of PCDD/F Vapor Pressure Prediction Techniques. Previous studies have used correlation methods to predict the vapor pressures of the PCDD/Fs, with new vapor pressure data it is possible to evaluate these predictions. As shown in

Figure 5.5a the correlation of Rordorf (1989) underestimates the measured vapor pressures of the di through penta-chlorinated PCDD/Fs by approximately a factor 3. Rordorf *et al.*, (1990) had previously observed that the correlation technique underestimated the vapor pressures of the penta and hexa-chlorinated PCDD/Fs by a factor two to three.

Eitzer and Hites (1988; 1998) used a GC-RI method to measure p_{gc} values and observed a precise correlation between p_{gc} and the RI of the PCDD/Fs. As shown in Figure 5.5b there is a systematic difference between the p_{gc} values of Eitzer and Hites (1988; 1998) and the p_L^o values from the current study. The slope of the regression line is 0.71 indicating that the GC-RI method overestimates the vapor pressure of the more chlorinated congeners and underestimates the vapor pressure of the less chlorinated congeners.

Equation 5.6 was derived from equations 1 and 2 from Hinckley *et al.*, (1990) and can be used to calculate p_L^o values from GC-RI data.

$$\ln p_{L,test}^o = (\Delta H_{vap,test} / \Delta H_{vap,reference}) \ln p_{L,reference}^o + \ln (\gamma_{reference} / \gamma_{test}) + c \quad (5.6)$$

Where for the test and reference compounds: ΔH_{vap} is the enthalpy of vaporization and γ the activity coefficient in the GC column stationary phase. In practice values of γ_{test} and γ_{ref} are unknown so a reference compound, structurally similar to the test compound is chosen and values of γ_{test} and γ_{ref} assumed equal. This assumption leads to equation 5.7; the equation most commonly used to calculate p_{gc} values from GC-RI data (Hamilton, 1980; Bidleman, 1984; Eitzer and Hites, 1988; Hinckley *et al.*, 1990; Eitzer and Hites, 1998).

$$\ln p_{gc, test} = (\Delta H_{vap,test\ compound} / \Delta H_{vap,reference\ compound}) \ln p_{L,reference}^o + c \quad (5.7)$$

For p_{gc} values determined using GC-RI method to be equal to p_L^o values three criteria must be met: 1) the ratio of the reference compound and test compounds enthalpies of vaporization must be constant with temperature or their temperature dependence known. 2) the reference compound's measured vapor pressure must be accurate, and 3) the reference and test compound's activity coefficients in the GC column stationary phase must be equal.

The systematic difference between Eitzer and Hites' (1988)(1998) p_{gc} values and

Table 5.3 PCDD/F vapor pressures 25 °C.

Compound	$\log p_S^o$ (torr)	$\log p_L^o$ (torr)[a]
28 D	-5.30 (±0.05)	-4.05
124 D	-5.71 (±0.08)	-4.68
1234 D	-7.15 (±0.11)	-5.52
2378 D	-8.71 (±0.16)	-5.92
12478 D	-7.95 (±0.08)	-6.16
12378 D	-8.69 (±0.38)	-6.55
28 F	-5.44 (±0.08)	-3.85
246 F	-5.50 (±0.05)	-4.58
238 F	-6.26 (±0.07)	-4.62
1378 F	-7.04 (±0.09)	NA
2378 F	-7.26 (±0.13)	-5.25
12378 F	-8.05 (±0.10)	-6.05
23478 F	-8.17 (±0.07)	-6.47

[a] Calculated using equation 5.5.
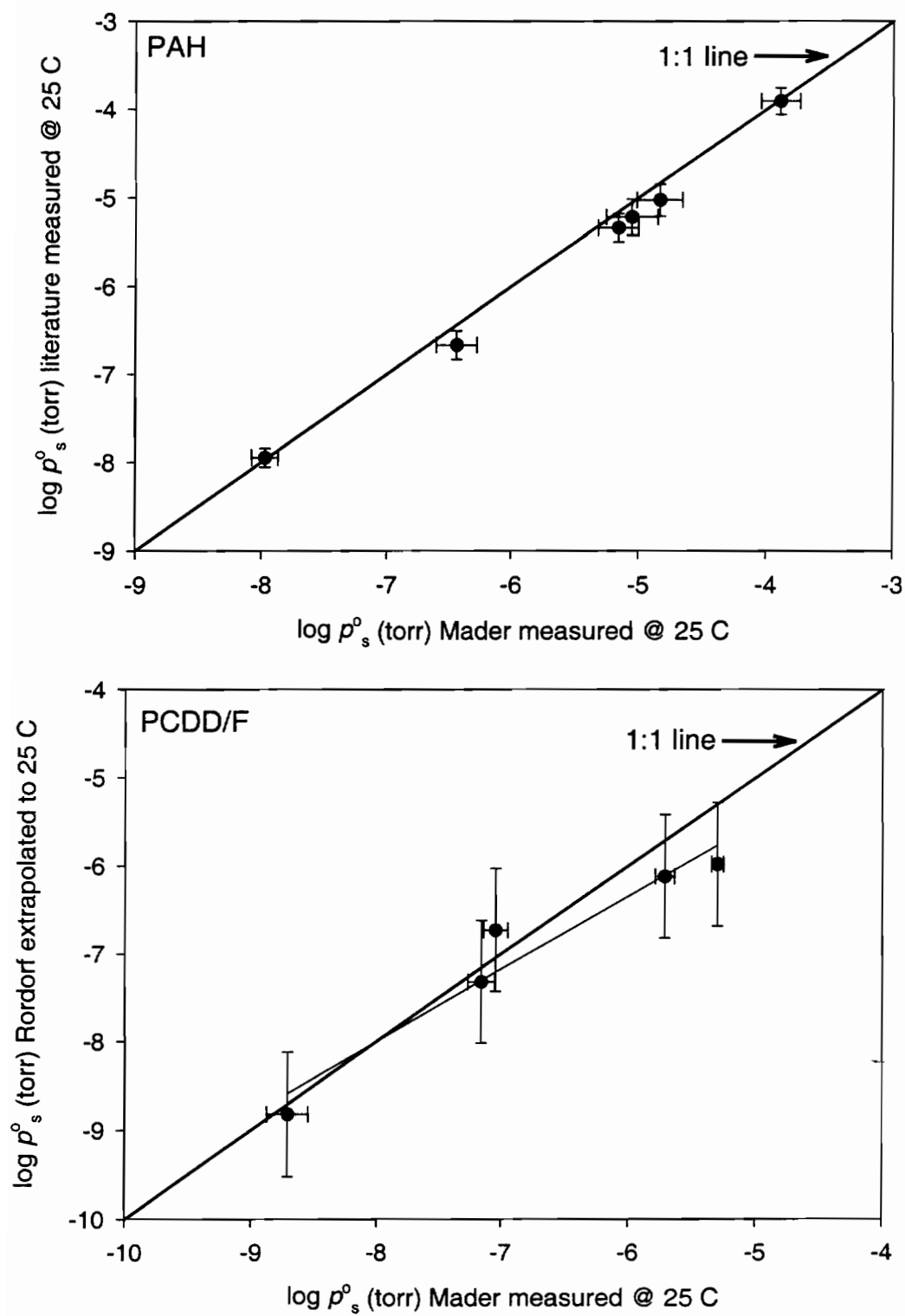
Figure 5.4 Comparison of directly measured vapor pressures to literature values **a**. PAHs **b.** PCDD/Fs
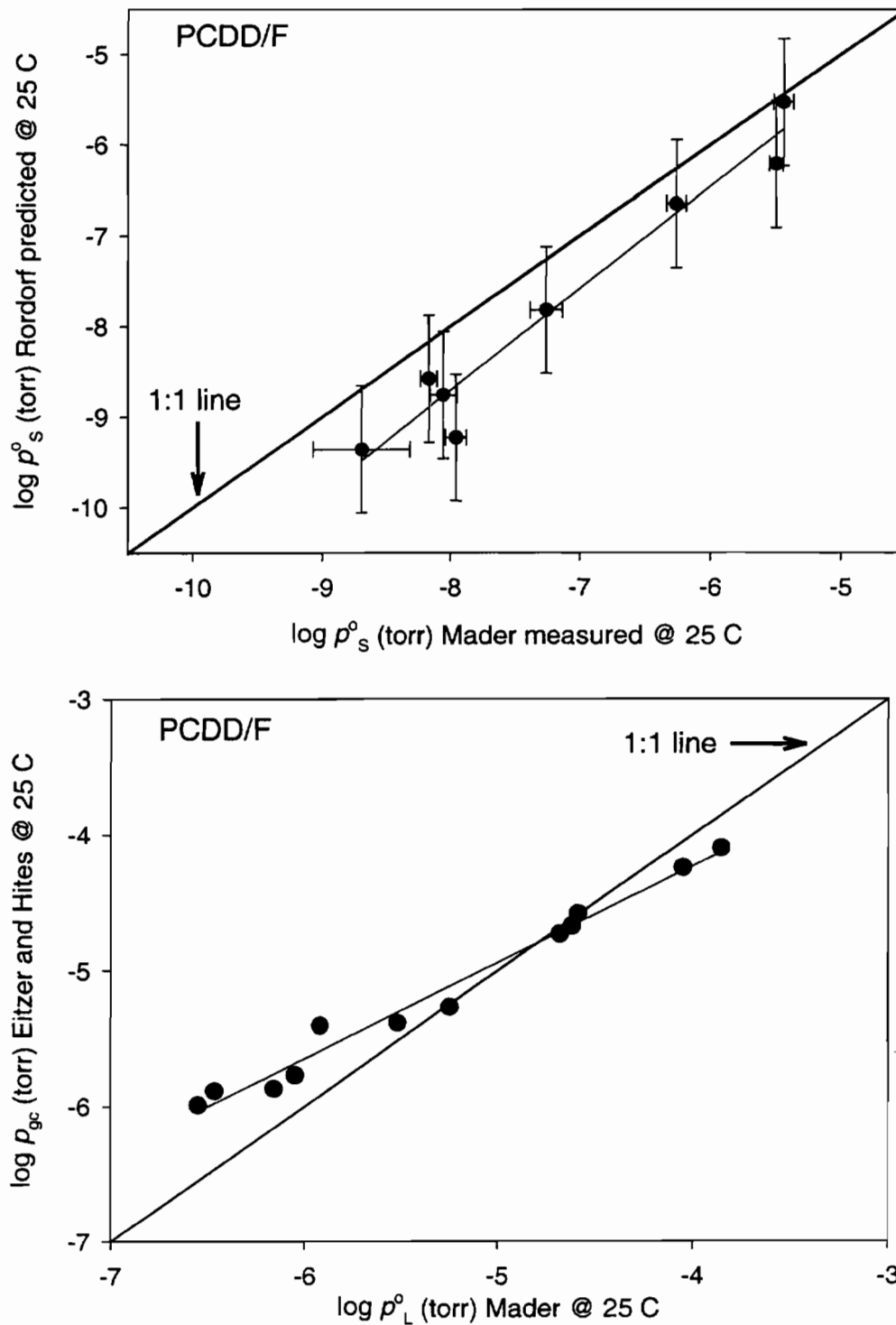
Figure 5.5 a. Comparison of directly measured PCDD/Fs vapor pressures to predictions from Rordorf, Sarna *et al.*, (1990). **b.** Comparison of P_L^o values to p_{gc} values of Eitzer and Hites, (1988)(1998).

the p_L^o values, measured in the current study could be due to either one or both of the following: A difference in the ratio of $\Delta H_{vap,test}$ / $\Delta H_{vap,reference}$ with temperature. In practice this ratio is measured at temperatures from 90 to 150 °C but p_{gc} is estimated at 25 °C. When this ratio is extrapolated down from experimental to room temperatures, the heat capacities (c_p^{g-l}) of the test and reference compounds are assumed to be equal. The c_p^{g-l} values of higher molecular weight PCDD/Fs are less than lower molecular weight PCDD/Fs (Rordorf *et al.*, 1990). Only a single reference compound was used, DDT (MW 352) which is significantly bigger than tetra-chlorinated-PCDF (MW 306) and significantly smaller than the hepta and octa-chlorinated PCDDs (MW 422 and 456). Therefore there must be a difference in the c_p^{g-l} values of the reference and test compounds. A difference in c_p^{g-l} values between test and reference compounds will cause the ratio of $\Delta H_{vap,test\ compound}$ / $\Delta H_{vap,reference\ compound}$ to be temperature dependant. Depending on the magnitude of the c_p^{g-l} value of the reference compound this could cause either an over or underestimation of the vapor pressures.

The second explanation for the difference between p_{gc} and p_L^o values could be due to the incorrect assumption that $\gamma_{test} = \gamma_{reference}$ in the GC-RI method. Combining equations 5.5 and 5.6 leads to an expression relating p_{gc} to p_L^o:

$$\ln p_{gc,\ test} = \ln\ p_{L,test}^o + \ln\ (\gamma_{test} / \gamma_{reference}) \qquad (5.8)$$

Schwarzenbach *et al.* (1993) mention that for the dissolution of highly hydrophobic compounds such as PAHs and PCBs into a nonpolar liquid phase such as octanol, the value of γ increases with increasing molecular size. In the GC-RI method compounds partition into a non-polar GC column stationary phase. For highly hydrophobic compounds such as PCDD/Fs it is likely that for test compounds having a higher molecular weight than the reference compound $\gamma_{test} > \gamma_{reference}$ and for test compounds having a lower molecular weight than the reference compound $\gamma_{test} < \gamma_{reference}$. According to equation 5.8 the vapor pressures of test compounds having a higher molecular weight than the reference compound will be overestimated and the vapor pressure of compounds having a lower molecular weight than the reference compound will be underestimated. These deviations would become greater as the difference between the molecular weight of the reference and test compounds becomes greater. At a given temperature this would

result in a plot of log p_{gc} versus log p_L^o having a slope less than 1 with values of log p_{gc} and log p_L^o being the most similar at a p_L^o closest to the p_L^o of the reference compound used in the GC-RI method. This is very similar to what is observed in Figure 5.5b where the reference compound for Eitzer and Hites (1988)(1998) had a log p_L^o equal to –5.68 torr at 25 °C. Eitzer and Hites (1988)(1998) never suggested that their p_{gc} values were equivalent to p_L^o values.

5.4.5 PCDD/F Vapor Pressure Prediction Equations. The new PCDD/Fs vapor pressure data was used to improve current PCDD/F vapor pressure prediction techniques; correlations were made between a compound's vapor pressure and molecular properties. Values of p_S^o were significantly correlated to melting point (T_m) (r^2=0.70), molecular weight (r^2=0.83), and number of chlorines (r^2=0.83), but a correlation between p_L^o and GC-RI (Figure 5.6) was the most precise and accurate. The retention of an SOC by a nonpolar GC column depends in part on the p_L^o of the compound (Hamilton, 1980; Hinckley *et al.*, 1990). The GC-RI for all 75 PCDD and 135 PCDFs on a DB-5 GC column are available from Donnelly, Munslow *et al.* (1987) and Hale, Hileman *et al.* (1985), respectively. The regression equation (equation 5.9) from Figure 5.6 was made using data that did not require physical chemical data from a reference compound and therefore is currently the most accurate method to predict the p_L^o value of the 210 PCDD/F at 25 °C.

$$\log p_L^o (\text{torr}) \text{ @ 25 °C} = (\text{-0.0040} (\pm 0.0002) \times \text{RI}) + 3.9 (\pm 0.4) \quad r^2 = 0.98 \quad (5.9)$$

Temperature (T) has a dramatic influence on a compound's p_L^o, consequently T affects the gas/particle and gas/solid partitioning of SOCs (Yamasaki *et al.*, 1982; Pankow, 1994). Since most field studies involving the gas/particle partitioning or gas/solid partitioning of SOCs involves measurements at T other than 25 °C it would be helpful to have an expression that relates the influence of T on p_L^o. The fundamental relationship between p_L^o and T is given by the Clausius-Clapeyron equation:

$$d \ln p_L^o / dT = \Delta H_{vap} / RT^2 \tag{5.10}$$
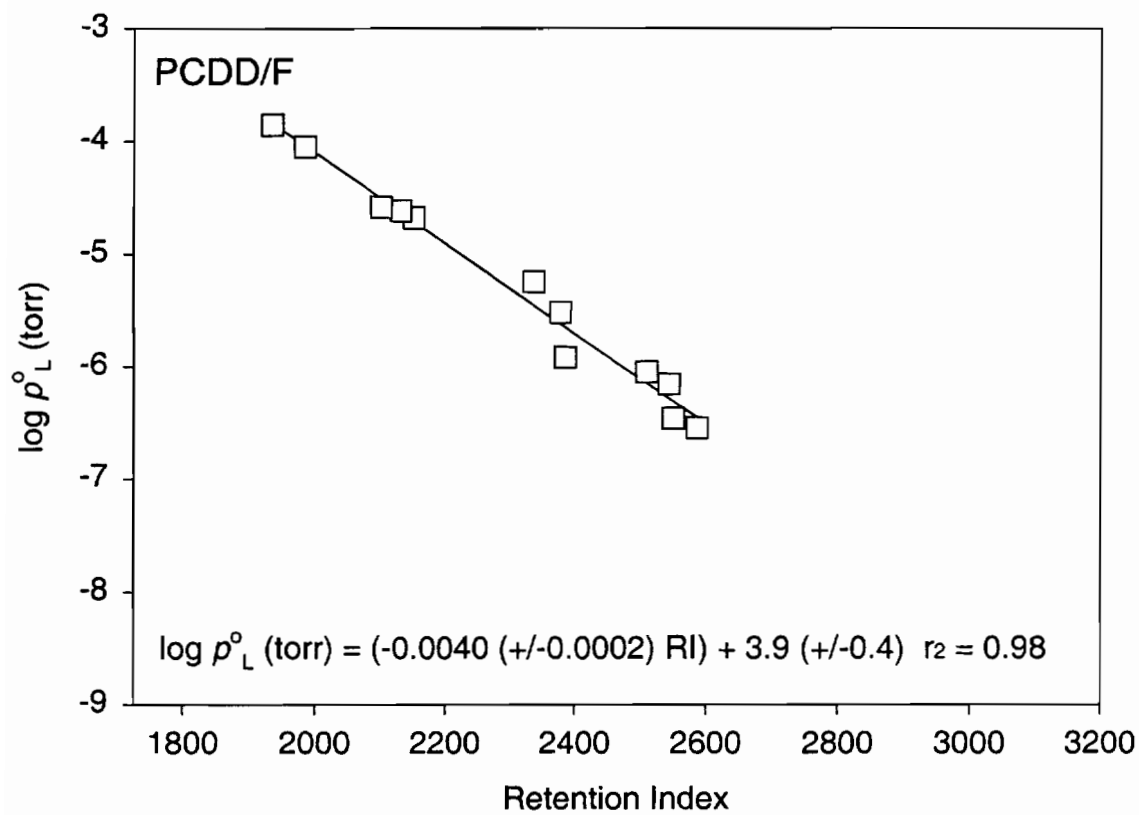
Figure 5.6 Correlation of PCDD/F log p_L^o values at 25 °C to their gas chromatograph retention index on a DB-5 column.

where $-\Delta H_{vap}$ is the enthalpy of vaporization at a given T and R is 8.314 J/ mol K. The dependence of ΔH_{vap} on T can be evaluated using the compound's liquid-gas heat capacity (c_p^{l-g}) where:

$$d\Delta H_{vap}/dT = c_p^{l-g}\ dT \tag{5.11}$$

Estimated values of the enthalpy of vaporization at the melting point ($\Delta H_{vap}(T_m)$), c_p^{l-g} and measured values of T_m were available for 25 PCDD and 58 PCDFs from Rordorf (1989). The integrated Clausius-Clapeyron equation:

$$\ln(\,p_{L,2}^o/\ p_{L,1}^o\,) = -\ \Delta H_{vap}/R\ (1/T_2 - 1/T_1) \tag{5.12}$$

was used to calculate the p_L^o of a given compound at a nine temperatures between -20 and 35 °C. ΔH_{vap} was evaluated at each T by extrapolating $\Delta H_{vap}(T_m)$ values down to the given temperature using equation 5.11. Equation 5.13 is a convenient means of parameterizing the influence of T on p_L^o (Yamasaki et al., 1984; Falconer and Bidleman, 1994).

$$\log\ p_L^o\ (\text{torr}) = m_L/T + b_L \tag{5.13}$$

Using the p_L^o values determined at nine temperatures between -20 and 35 °C, values of m_L and b_L were calculated from a regression of log p_L^o vs. 1/T for each compound. Values of m_L and b_L are presented in Tables 5.4 and 5.5 for the PCDD and PCDFs, respectively.

For the remaining PCDD/F congeners for which values of $\Delta H_{vap}(T_m)$ and T_m were unavailable, values of ΔH_{vap} at 25 °C ($\Delta H_{vap}(25°C)$) were predicted as follows: Rordorf (1989) predicted ΔH_{vap} at a compound's boiling point ($\Delta H_{vap}(T_b)$) using Fishtine's formula:

$$\Delta H_{vap}(T_b) = 1.01\ T_b\ (36.61 + R\ \ln\ T_b) \tag{5.14}$$

For compounds for which measured values of T_b were not available, Rordorf (1989) estimated T_b from a correlation between measured T_b values and the number of chlorines present on the PCDD/F (#Cl). Therefore a correlation between the ΔH_{vap} (25°C) values evaluated from the data of Rordorf (1989) and #Cl was expected. Using data for 25 PDDD and 58 PCDFs available from Rordorf (1989), a correlation between ΔH_{vap} (25°C)

and #Cl (Figure 5.8) was observed. Equations 5.15 and 5.16 are the regression equations for the PCDD and PCDFs, respectively and were used to predict values of $\Delta H_{vap}(25°C)$.

$$\Delta H_{vap}(25°C) = -0.59 \times \#Cl^2 + 9.0 \times \#Cl + 78 \qquad r^2 = 0.94 \qquad (5.15)$$

$$\Delta H_{vap}(25°C) = -0.41 \times \#Cl^2 + 6.3 \times \#Cl + 76 \qquad r^2 = 0.99 \qquad (5.16)$$

The predicted values of ΔH_{vap} (25°C) were within 12% of the values calculated from the GC-RI data of Eitzer and Hites (1988; 1998).

Predicted values of c_p^{l-g} for PCDD/Fs of a given level of chlorination were available from Rordorf (1989). Using values $\Delta H_{vap}(25°C)$, c_p^{l-g} and p_L^o values at 25 °C, values of m_L and b_L were calculated as described previously. Values of m_L and b_L are presented in Tables 5.4 and 5.5 for the PCDD and PCDFs, respectively.

5.5 Implications

The vapor pressures of all 210 PCDD/Fs at temperatures between -20 and 35 °C can be estimated using the data presented in Tables 5.4 and 5.5. Previous studies of the gas/particle partitioning behavior of PCDD/Fs (Eitzer and Hites, 1989; Lee and Jones, 1999) were limited by a lack of accurate vapor pressure data. These studies can be revisited and the slopes of plots of log K_p vs. log p_L^o recalculated using the new vapor pressure data for the PCDD/Fs. Such analysis will provide valuable insight into the mechanisms of the gas/particle partitioning of PCDD/Fs and will aid the modeling of their atmospheric behavior.

It was shown that if the ratio of $\Delta H_{vap,test}$ / $\Delta H_{vap,reference}$ is T dependant and/or the ratio of γ_{test} / $\gamma_{referece}$ variable throughout a class of compounds there will be a systematic error in the vapor pressures measured using the GC-RI method. Should the GC-RI method be used in future measurements of the p_L^o values of a homologues series of compounds (i.e. toxaphene, chlorinated naphthalenes, or chlorinated paraffins), at least one reference compound at each level of chlorination should be used to minimize systematic differences between p_{gc} and p_L^o. Furthermore the c_p^{l-g} values of test and reference compounds should be similar and/or experiments done at temperatures as close to ambient as possible.

Table 5.4 Parameters for the calculation of vapor pressure of PCDD congeners as a function of temperature.

chlorine position(s)	m_L	b_L	Chlorine position(s)	m_L	b_L
1	-4638	12.31	1236	-5467	12.71
2	-4643	12.32	1269	-5467	12.71
13	-5198	13.60	1234	-5467	12.83
14	-4897	12.52	1237	-5668	13.37
16	-5197	13.46	1238	-5467	12.70
17	-4897	12.44	2378	-5752	13.38
18	-4897	12.44	1239	-5467	12.66
27	-5192	13.38	1278	-5467	12.62
28	-5273	13.64	1267	-5467	12.59
19	-4897	12.40	1289	-5467	12.51
23	-5014	12.75	12479	-5659	12.86
12	-4897	12.35	12468	-5659	12.86
136	-5213	12.87	12469	-5659	12.73
137	-5344	13.29	12368	-5659	12.71
138	-5213	12.85	12478	-5827	13.38
139	-5213	12.81	12379	-5659	12.65
124	-5109	12.46	12369	-5659	12.59
148	-5213	12.79	12467	-5659	12.58
149	-5213	12.75	12489	-5659	12.58
178	-5213	12.67	12347	-5829	13.14
237	-5459	13.48	12346	-5659	12.52
123	-5213	12.64	12378	-5829	13.00
126	-5213	12.63	12367	-5659	12.45
127	-5213	12.61	12389	-5659	12.37
128	-5213	12.61	124689	-5790	12.45
129	-5213	12.57	124679	-5942	12.96
1368	-5667	13.74	123468	-5790	12.33
1379	-5467	13.01	123689	-5790	12.26
1369	-5467	12.97	123679	-5790	12.26
1378	-5666	13.54	123469	-5790	12.22
1247	-5467	12.87	123478	-5944	12.69
1248	-5467	12.87	123678	-5944	12.66
1469	-5467	12.86	123789	-5941	12.60
1268	-5467	12.83	123467	-5790	12.05
1246	-5467	12.84	1234679	-5859	11.73
1249	-5467	12.84	1234678	-6015	12.07
1478	-5467	12.81	12346789	-5919	10.93
1279	-5467	12.77			

Table 5.5 Parameters for the calculation of vapor pressure of PCDF congeners as a function of temperature.

chlorine position(s)	m_L	b_L	chlorine position(s)	m_L	b_L	chlorine position(s)	m_L	b_L
1	-4420	11.78	348	-4892	11.70	1239	-5064	11.40
3	-4415	11.72	236	-4892	11.74	1289	-5064	11.25
2	-4417	11.73	346	-4892	11.70	13468	-5193	11.63
4	-4420	11.69	149	-4892	11.70	12468	-5185	11.59
13	-4677	12.06	234	-4892	11.71	23479	-5193	11.44
14	-4677	11.94	129	-4892	11.54	13478	-5184	11.40
17	-4677	11.95	1368	-5063	11.97	13467	-5185	11.40
18	-4677	11.89	1468	-5064	11.91	12368	-5193	11.42
24	-4677	11.94	2468	-5063	11.86	12478	-5186	11.39
16	-4677	11.90	1347	-5064	11.85	12467	-5187	11.42
37	-4677	11.87	1378	-5064	11.83	13479	-5193	11.41
27	-4677	11.87	1247	-5064	11.82	23469	-5193	11.40
12	-4677	11.85	1348	-5064	11.77	12479	-5184	11.36
28	-4678	11.84	1346	-5064	11.83	23468	-5184	11.29
36	-4677	11.81	1248	-5059	11.76	13469	-5193	11.31
26	-4677	11.81	1246	-5064	11.82	12347	-5193	11.32
46	-4677	11.78	1367	-5060	11.78	12469	-5193	11.31
23	-4679	11.84	1379	-5061	11.78	12348	-5187	11.25
34	-4677	11.75	1268	-5064	11.75	12346	-5187	11.30
19	-4677	11.69	1478	-5064	11.72	12378	-5185	11.34
137	-4892	12.08	1467	-5058	11.71	12367	-5185	11.11
138	-4892	12.03	2368	-5060	11.68	12379	-5193	11.21
136	-4892	12.02	2467	-5062	11.65	23489	-5193	11.22
249	-4892	11.98	1369	-5064	11.69	13489	-5193	11.13
134	-4892	11.95	1237	-5059	11.68	23478	-5188	10.93
147	-4892	11.96	1238	-5063	11.65	23467	-5186	11.06
124	-4892	11.97	1234	-5063	11.63	12489	-5193	11.07
148	-4892	11.91	1236	-5064	11.65	12369	-5193	11.12
146	-4892	11.93	2349	-5064	11.64	12349	-5193	11.01
247	-4892	11.91	1469	-5064	11.62	12389	-5193	10.93
248	-4892	11.92	1278	-5063	11.59	123468	-5270	10.96
246	-4891	11.82	1349	-5064	11.58	134678	-5272	10.92
239	-4892	11.86	1267	-5060	11.55	124678	-5273	10.91
127	-4892	11.87	2347	-5062	11.52	134679	-5279	10.89
128	-4892	11.79	1279	-5063	11.51	124679	-5273	10.85
123	-4892	11.85	1249	-5064	11.54	124689	-5270	10.81
349	-4892	11.80	2348	-5060	11.50	123478	-5271	10.73
139	-4892	11.81	2346	-5059	11.50	123467	-5271	10.73
126	-4892	11.80	2378	-5063	11.73	123678	-5273	10.71
237	-4892	11.77	2367	-5061	11.45	123479	-5272	10.68
238	-4894	11.80	3467	-5064	11.43	123679	-5279	10.67
347	-4892	11.70	1269	-5064	11.42	123689	-5272	10.63

Table 5.5 continued.

Chlorine position(s)	m_L	b_L
123469	-5271	10.62
234678	-5273	10.57
123789	-5279	10.50
123489	-5279	10.46
1234678	-5315	10.11
1234679	-5323	10.07
1234689	-5315	10.01
1234789	-5314	9.75
12346789	-5434	9.51
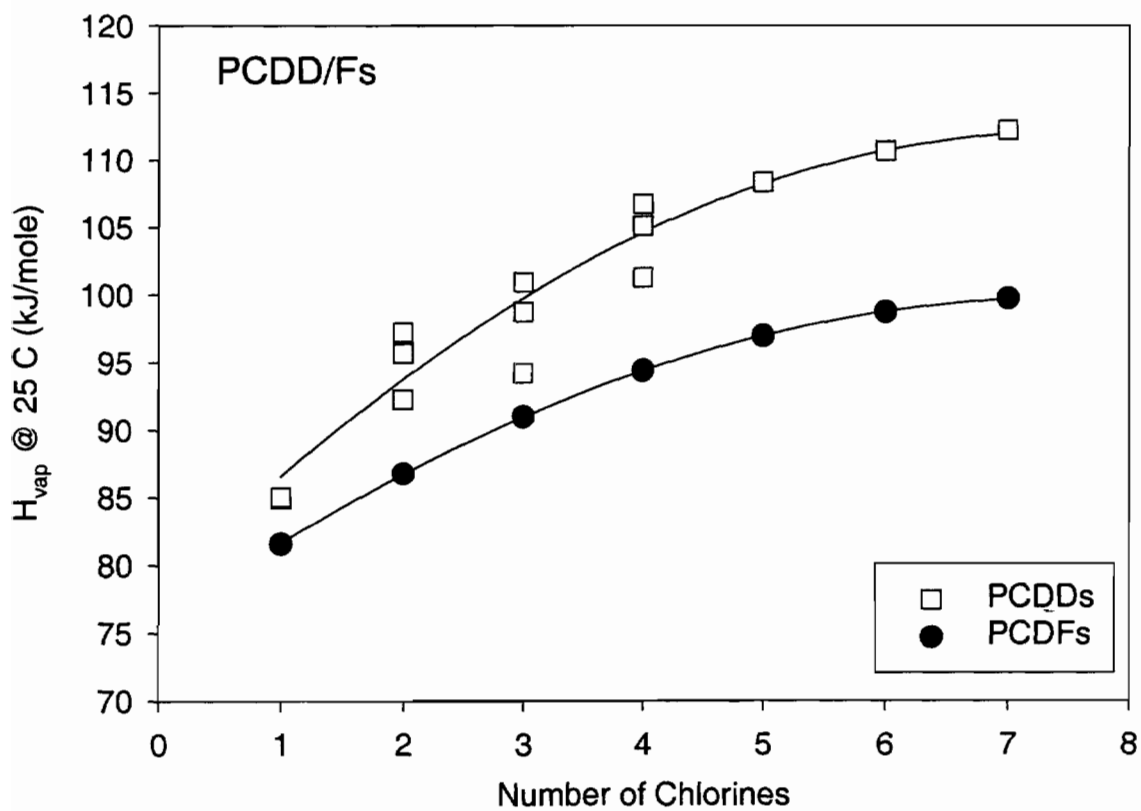
Figure 5.7 Correlation of PCDD/Fs ΔH_{vap} at 25 °C to the number of chlorines present on the molecule.

5.6 References

Bidleman, T. F. 1984. Estimation of vapor pressures for nonpolar organic compounds by capillary gas chromatography. *Analytical Chemistry* 56, 2490-2496.

Brady, M., Smith, N. O. 1967. Pressure-temperature-composition relations in the system anthracene-phenanthrene. *Canadian Journal of Chemistry* 45, 1125-1134.

Donnelly, J. R. *et al.* 1987. Correlation of structure with retention index for chlorinated dibenzo-p-dioxins. *Journal of Chromatography* 392, 51-63.

Eitzer, B. D., Hites, R. A. 1988. Vapor pressures of chlorinated dioxins and dibenzofurans. *Environmental Science and Technology* 22, 1362-1364.

Eitzer, B. D., Hites, R. A. 1989. Polychlorinated dibenzo-p-dioxins and dibenzofurans in the ambient atmosphere of Bloomington, Indiana. *Environmental Science and Technology* 23, 1389-1395.

Eitzer, B. D., Hites, R. A. 1998. Correction: vapor pressures of chlorinated dioxins and dibenzofurans. *Environmental Science and Technology* 32, 2804.

Falconer, R. L., Bidleman, T. F. 1994. Vapor pressures and predicted particle/gas distributions of polychlorinated biphenyl congeners as functions of temperature and ortho-chlorine substitution. *Atmospheric Environment* 28, 547-554.

Goss, K. U., Schwarzenbach, R. P. 1998. Gas/solid and gas/liquid partitioning of organic compounds: critical evaluation of the interpretation of equilibrium constants. *Environmental Science and Technology* 32, 2025-2032.

Hale, M. D. *et al.* 1985. Mathematical modeling of temperature programmed capillary gas chromatographic retention indexes for polychlorinated dibenzofurans. *Analytical Chemistry* 57, 640-648.

Hamilton, D. J. 1980. Gas chromatographic measurement of volatlity of herbicide esters. *Journal of Chromatography* 195, 75-83.

Hinckley, D. A. *et al.* 1990. Determination of vapor pressures for nonpolar and semipolar organic compounds from gas chromatographic retention data. *Journal of Chemical and Engineering Data* 35, 232-237.

Lee, R. G. M., Jones, K. C. 1999. Gas-particle partitioning of atmospheric PCDD/Fs: Measurements and observations on modeling. *Environmental Science and Technology* 33, 3596-3604.

Mackay, D. *et al.* 1982. Vapor pressure correlation for low-volatility environmental chemicals. *Environmental Science and Technology* 16, 645-649.

Mackay, D., Paterson, S. 1991. Evaluating the multimedia fate of organic chemicals: A level III Fugacity model. *Environmental Science and Technology* 25, 427-436.

MacKay, D. *et al.* 1992. *Illustrated Handbook of Physical-Chemical Properties and Environmental Fate for Organic Chemicals: Polynuclear Aromatic Hydrocarbons, Polychlorinated Dioxins and Polychlorinated Dibenzofurans.* Boca Raton, Lewis Publishers.

Mader, B. T. 2000a. *Gas/solid and gas/particle partitioning of polychlorinated dibenzodioxins, polychlorinated dibenzofurans and polynuclear aromatic hydrocarbons to filter surfaces and ambient atmospheric particles.* Ph.D. Thesis, Environmental Science and Engineering, Oregon Graduate Institute of Science and Technology.

Mader, B. T., Pankow, J. F. 2000b. Controlled field experiments to study the gas/particle partitioning of polychlorinated dibenzodioxins, polychlorinated dibenzofurans and polycyclic aromatic hydrocarbons to urban, suburban, and rural particles. *Environmental Science and Technology* submitted March 15, 2000.

Mader, B. T., Pankow, J. F. 2000c. Gas/solid partitioning of polychlorinated dibenzodioxins, polychlorinated dibenzofurans and polycyclic aromatic hydrocarbons to filter surfaces: Part 1. Teflon membrane filters. *Atmospheric Environment* in press April 15, 2000.

Mader, B. T., Pankow, J. F. 2000d. Gas/solid partitioning of polychlorinated dibenzodioxins, polychlorinated dibenzofurans and polycyclic aromatic hydrocarbons to filter surfaces: Part 2. Quartz fiber filters. *Atmospheric Environment* submitted April 15, 2000.

Pankow, J. F. 1987. Review and comparative analysis of the theories on partitioning between the gas and aerosol particulate phases in the atmosphere. *Atmospheric Environment* 21, 2275-2283.

Pankow, J. F. 1994. An absorption model of gas/particle partitioning of organic compounds in the atmosphere. *Atmospheric Environment* 28, 185-188.

Pankow, J. F., Bidleman, T. F. 1992. Interdependence of the slopes and intercepts from log-log correlations of measured gas-particle partitioning and vapor pressure-I. Theory and analysis of available data. *Atmospheric Environment* 26A, 1071-1080.

Pella, P. A. 1976. Generator for producing trace vapor concentrations of 2,4,6-trinitrotoluene, 2,4-dinitrotoluene, and ethylene glycol dinitrate for calibrating explosives vapor detectors. *Analytical Chemistry* 48, 1632-1637.

Rodan, B. D. *et al.* 1999. Screening for persistant organic pollutants: Techniques to provide a scientific basis for POPs criteria in international negotiations. *Environmental Science and Technology* 33, 3482-3488.

Rordorf, B. F. 1985. Thermodynamic and thermal properties of polychlorinated compounds: The vapor pressures and flow tube kinetics of ten dibenzo-para-dioxins. *Chemosphere* 14, 885-892.

Rordorf, B. F. 1985. Thermodynamic properties of polychlorinated compounds: The vapor pressures and enthalpies of sublimation of ten dibenzo-para-dioxins. *Thermochimica Acta* 85, 435-438.

Rordorf, B. F. 1989. Prediction of vapor pressures boiling points and enthalpies of fusion for twenty-nine halogenated dibenzo-p-dioxins and fifty-five dibenzofurans by a vapor pressure correlation method. *Chemosphere* 18, 783-788.

Rordorf, B. F. *et al.* 1986. Vapor pressure for several polychlorinated dioxins by two gas saturation methods. *Chemosphere* 15, 2073-2076.

Rordorf, B. F. *et al.* 1990. Vapor pressure measurements on halogenated dibenzo-p-dioxins and dibenzofurans an extended data set for a correlation method. *Chemosphere* 20, 1603-1609.

Schwarzenbach, R. P. *et al.* 1993. Organic Solvent-Water Partitioning: The Octanol-Water Partition Constant. In *Environmental Organic Chemistry*. Eds. R. P. Schwarzenbach, P. M. Gschwend and D. Imboden. New York, John Wiley & Sons. pp. 76-156.

Simcik, M. F. *et al.* 1998. Gas particle partitioning of PCBs and PAHs in the Chicago urban area and adjacent coastal atmosphere states of equilibrium. *Environmental Science and Technology* 32, 251-257.

Sonnefeld, W. J. *et al.* 1983. Dynamic coupled-column liquid chromatographic determination of ambinet temperature vapor pressures of polynuclear aromatic hydrocarbons. *Analytical Chemistry* 55, 275-280.

Spencer, W. F., Cliath, M. M. 1969. Vapor density of dieldrin. *Environmental Science and Technology* 3, 670-674.

Storey, J. M. *et al.* 1995. Gas/solid partitioning of semivolatile organic compounds to model atmospheric solid surfaces as a function of relative humidity: Part 1. Clean quartz. *Environmental Science and Technology* 29, 2420-2428.

Yamasaki, H. *et al.* 1982. Effects of ambient temperature on aspects of airborne polycyclic aromatic hydrocarbons. *Environmental Science and Technology* 16, 189-194.

Yamasaki, H. *et al.* 1984. Determination of vapor pressure of polycyclic aromatic hydrocarbons in the supercooled liquid phase and their adsorption on airborne particulate matter. *The Chemical Society of Japan* 8, 1324-1329.

CHAPTER 6

MEASUREMENTS OF AMBIENT GAS AND PARTICLE-PHASE POLYCYCLIC AROMATIC HYDROCARBONS (PAHS) AND PARTICLE-PHASE ORGANIC (OC) AND ELEMENTAL CARBON (EC): NORMALIZATION OF THE GAS PARTICLE PARTITION COEFFICENTS OF PAHS BY THE WEIGHT FRACTION OF OC AND EC

6.1 Introduction

The term semi-volatile organic compounds (SOCs) refer to organic compounds having vapor pressures between 10^{-11} and 10^{-4} atm (Bidleman, 1988). In the presence of suspended particulate material, atmospheric SOCs will be distributed between the gas and particle-phases. Many organic contaminants of interest are considered semi-volatile, examples are; polycyclic aromatic hydrocarbons (PAHs), the polychlorinated dibenzodioxins and dibenzofurans (PCDD/Fs), polychlorinated biphenyls (PCBs), components of tobacco smoke such as nicotine and finally many aromatic organic compounds comprising secondary organic aerosols present in urban smog (Odum et al., 1996). In order to understand the environmental behavior of these contaminants, it is important to quantify the extent to which an SOC is distributed between the gas and particle-phases: the processes affecting the fate and transport of these phases differ significantly.

At a given temperature the distribution of a compound between the gas and particle-phases has been well parameterized using the gas/particle partition coefficient, K_p (m³/µg) (Yamasaki et al., 1982; Bidleman et al., 1986; Bidleman and Foreman, 1987; Pankow, 1991; Pankow and Bidleman, 1992):

$$K_p = (F/TSP) / A \qquad (6.1)$$

Where: F = concentration of compound associated with the particle phase (ng/m³);

TSP = the total suspended particle concentration ($\mu g/m^3$); and *A* = the gas phase concentration of the compound (ng/m^3). When based on sampling results, the gas and particle-phase concentrations are operationally defined. Thus, *F* gives the portion of the compound that is retained on a filter, and *A* gives the portion which passes through the filter and is collected on a sorbent material.

Urban air contains significant amounts of particle-phase organic carbon (OC) and elemental carbon (EC). OC can be divided into two types: primary OC which is emitted directly from sources, and secondary OC (SOA) which is produced by the condensation and partitioning of products of hydrocarbon oxidation to existing particulate material (Seinfeld, 1986; Pandis *et al.*, 1992; Pankow, 1994; Odum *et al.*, 1996). Several authors have suggested that UPM is actually coated with a thin, liquid organic phase and it is likely that the *G/P* partitioning of SOCs could be dominated by absorption into this phase (McDow *et al.*, 1994; Liang and Pankow, 1996; Jang *et al.*, 1997; Liang *et al.*, 1997; Jang and Kamens, 1998). Indeed, recent field and laboratory work by Liang and Pankow (1996) and Liang *et al.* (1997) have suggested that the *G/P* partitioning of PAHs and *n*-alkanes to UPM is indeed *ab*sorptive in nature. Such behavior is analogous to the paradigm describing soil water partitioning, whereby the hydrophobic organic compounds are believed to partition into soil organic matter and partitioning is independent of the specific soil type (Chiou *et al.*, 1979; Kile *et al.*, 1995).

The organic matter phase present on ambient particles consists of organic carbon but also absorbed water and dissolved ionic species. In Los Angeles, it has been estimated that the concentration of the organic matter phase (OM) present on urban particulate material (UPM) is approximately 1.4 times the measured OC concentration (Gray, 1986). Using the data of Larson and Cass (1989) and Gray, Cass *et al.* (1986) it is possible to calculate that Los Angeles UPM contains approximately 18-31% OM, a range which encompasses the 26% measured by Liang, Pankow et al. (1997) for Los Angeles ambient smog.

When a compound *absorptively* partitions from the gas phase *into* a particle's OM, Pankow (1994) has derived:

$$K_p = f_{om} \, 760 \, RT \, / \, \zeta_{om} \, MW_{om} \, p_L^{\circ} \, 10^6 \tag{6.2}$$

Where f_{om} is the weight fraction that is absorbing organic material phase (OM), ζ_{om} is the activity coefficient of the compound of interest in the OM on a mole fraction scale and MW_{om} is the mean molecular weight of the absorbing OM (g/mol). If partitioning is dominated by *ab*sorption, K_p will be proportional to f_{om} (equation 6.2). Particles from different sources and/or locations may have different amounts of OM. For example, environmental tobacco smoke (ETS) particles have an $f_{om} \approx 1$ but an airborne soil particle may have an $f_{om} \approx 0.02$. If the value of $\zeta_{om} MW_{om}$ is similar among particles from different sources and/or locations, the K_p value of a given compound at a given p_L^o could vary by a factor 50 due to differences in f_{om} among the different types of particles. Some authors have suggested normalizing K_p by f_{om} where:

$$K_{p,om} = K_p / f_{om} \tag{6.3}$$

(Pankow, 1994; Odum *et al.*, 1996). In practice, OC concentrations can be directly measured. The conversion factor (CF) relating OM to OC and consequently f_{om} to f_{oc} requires an assumption regarding the chemical composition of the given OM, for which few data exists. It is currently more practical to normalize K_p by f_{oc};

$$K_{p,oc} = K_p / f_{oc} \tag{6.4}$$

Where f_{oc} is the weight fraction of OC present on particulate material. Since f_{oc} values do not consider the chemical composition of the absorbing OM, $K_{p,oc}$ values may be less universal than $K_{p,om}$ values.

In this study conventional high volume air sampling was used to measure the ambient gas and particle-phase concentration of several individual PAHs as well as ambient OC and EC. Sampling was conducted at three locations thought to have ambient particulate material with different levels of OC. The goal of this study was to determine if differences in the K_p value of a given PAH at a given p_L^o among samples taken at different times and/or at different locations could be normalized by f_{oc}.

6.2 Materials and Methods

6.2.1 Sampling Locations. The sampling locations were as follows. University of Colorado at Denver, Denver, CO (urban), Oregon Graduate Institute (OGI), Beaverton, OR (suburban), and Hills Observatory, Hills, IA (rural/farm).

6.2.2 Sampling Protocol. Ambient sampling was carried out using a standard high volume air sampler (Graseby Manufacturing, Village of Cleves OH). Particle-phase PAHs were collected on 20.3×25.4 cm quartz fiber filters (Pallflex, CT); gas adsorption to the QFF was estimated using backup QFF. Prior to sampling, each QFF was prepared by baking at 450 °C for 4 hours and equilibrated overnight in a constant 70% RH chamber. Gas-phase PAHs were collected on pre-cleaned 8.5 cm diameter, 8.0 cm thick PUF plugs. PUF plugs were precleaned by soxhlet extraction in methylene chloride for 24 hours. Breakthrough of the PAHs was determined using backup PUF plugs. Sampling times were from 6 to 12 hours depending on the sampling site. Most sampling events were conducted at times of the day where temperature fluctuations were minimized. The sampler flow rate was $1 m^3$/min resulting in sample volumes of 360 to 720 m^3.

6.2.3 Extraction of Samples. Each filter was separately spiked with 4μL of a 250 ng/μl perduetrated fluorene solution and 4μL of a 250 ng/μL perduetrated pyrene solution (Cambridge Isotope Labs, Andover Ma). These solutions served as surrogate standards. Each filter was then extracted for 24 hours using soxhlet extraction with 100 mL of methylene chloride. After extraction samples were concentrated to 2 mL using a Bucci Roto-evaporator (Buchi Instruments, Switzerland). The sample was cleaned up and dried on a mini-column made from a disposable pipette and filled with 0.2 g SiO_2, and topped off with 1 g of Na_2SO_4. Each extract was then transferred to a precleaned 4 mL mini vial and stored at -20 °C. Immediately before analysis by GC-MS, each extract was gently blown down to 200 μL using a stream of ultra-clean N_2, then spiked with 2000 ng of perdeutrated phenanthrene. The extracts were analyzed on a Hewlett Packard 5890/5971 GC/MS and a 30m $\times$ 0.25mm DB-5 fused silica column (J&W Scientific Folsom, Ca). Each extract was injected "splitless" with the injector at 280 °C. The column temperature was held initially at 100 °C, ramped at 4 °C /min to 200 °C, ramped at 5 °C /min to 250°C, and finally held isothermal at 250°C for 5 min. The linear velocity of the carrier gas was 25 cm/s at 100 °C corresponding to a flow rate of about 1 ml/min. The MS was operated in the electron impact mode with ionization at 70 eV and scanned from 50 to 400 amu. The multiplier voltage was 1900 eV and the detector

temperature 170 °C. For the PAHs, a standard solution contained fluorene, fluorene-d_{10}, phenanthrene, phenanthrene-d_{10}, anthracene, fluoranthene, pyrene, pyrene-d_{10}, benz(a)anthracene and chrysene (Supelco, Bellefonte PA). Response factors for the PAHs were determined as a function of mass injected using serial dilutions of these primary standard solutions. The internal standard compound for the PAHs was phenanthrene-d_{10}.

Each PUF was extracted using a flow through extraction (FTE) method. Each PUF was loaded into a glass syringe with a volume of 100 mLs, i.e. approximately one quarter the volume of the non-deformed PUF. Each PUF was then spiked with an aliquot of each surrogate standard solution and extracted with 300 mLs methylene chloride, i.e. approximately 1.5 times of the volume of the non-deformed PUF. The samples were evaporated to 4 mL using the Roto-evaporator (Buchi Instruments, Switzerland) and stored until analyzed by GC/MS. No cleanup step was necessary. Immediately before analysis by GC-MS, each extract was gently blown down to 200 µL using a stream of ultra-clean N_2, then spiked with 2000 ng of perdeutrated phenanthrene.

6.2.4 Organic and Elemental Carbon Measurements. A punch from each front and backup QFF was sent to Sunset Labs (Forest Grove, OR) for carbon analysis. The inorganic, organic and elemental carbon contents of the particle-loaded, backup and blank filters was determined using a thermal optical carbon analyzer (Birch and Cary, 1996).

6.2.5 QA/QC. A blank filter and PUF was extracted for each experiment. With exception of chrysene, the blank levels were low, requiring corrections less than 5 % of the total mass measured for compounds on both the filters and PUF plugs. For chrysene, if the blank corresponded to more than 10% of the mass measured on a sample a K_p value was not computed for that experiment. The average recoveries of the PAHs from filters were 80 and 91% for fluorene d^{10} and pyrene d^{10}, respectively. Recoveries from PUF were 82 and 86% for fluorene d^{10} and pyrene d^{10}, respectively. Breakthrough of the most volatile compounds from the front to backup PUF averaged 31, 10 and 6 % for fluorene, phenanthrene, and anthracene respectively. If breakthrough was greater than 10% the gas phase concentration was not reported. Gas adsorption, as quantified by the percent mass of an individual PAH on backup QFF compared to the mass on front QFF, averaged 3,

12, 4, 17, 22, 4 and 1% for fluorene, phenanthrene, anthracene, fluoranthene, pyrene, benz(a)anthracene and chrysene, respectively.

Backup filters were used to correct for gas adsorption artifacts. To correct the particle-phase PAH concentrations, the mass of each individual PAH measured on the backup filter was subtracted from the individual mass measured on the front filter. To correct the gas-phase PAH concentration, two times the mass of the individual PAH measured on the backup filter was added to the mass of the individual PAH measured on the front PUF. With the exception of the samples taken in Denver corrections for PAH were small and had little influence of the measured K_p values. Similarly OC measurements were corrected for gas adsorption artifacts by subtracting the mass of organic carbon measured on the backup filter from the mass measured on the front filter. The percent of organic carbon mass on backup filters as compared to front filters averaged 22%. There was no significant EC on backup filters.

The G/P partitioning behavior of PAHs at the Denver location could not be evaluated using our data. High levels of individual PAHs were observed on backup QFF; the K_p data were rejected since it was thought that gas adsorption artifacts could have influenced these data. The percent of the mass extracted from the backup QFF compared to the mass found on front QFF was 78, 69 and 14% for phenanthrene, fluoranthene and benz(a)anthracene, respectively. The amounts of PAH on backup QFF could not be reconciled by travel blanks and are not the result of contamination. The relative humidities (RH) measured during the two sampling events at the Denver location were 25 and 34.7%. Using data from a separate study, Mader and Pankow (2000) have predicted that substantial gas adsorption artifacts can occur at these RHs due to the adsorption of gaseous PAHs to QFF.

6.3 Results and Discussion
6.3.1 Ambient OC and EC Characterization.
6.3.1.1 Ambient OC and EC concentrations. The OC and EC concentrations are presented in Table 6.1. At the 95% confidence level there was a statistically significant difference between the OC concentrations measured during stable conditions and those measured during rain events in Beaverton. The average OC concentration

during stable conditions was 5.64 (±2.2) µg /m^3 and the average value during rain events was 2.1 (±1.01) µg /m^3. The value for stable conditions is lower than the 12.5 (±5.48) µg /m^3 value measured in downtown Denver and slightly greater than the 4.27 (±1.14) µg /m^3 measured in rural Iowa during stable conditions.

A two tailed t-test revealed that there is only a 22% percent probability that the EC concentrations measured during stable conditions and rain events in Beaverton were the same. The average EC concentration for stable conditions was 1.25 (±0.343) µg /m^3 and the average value during rain events was 1.98 (±1.31) µg /m^3. These values are lower than the 2.75 (±0.235) µg /m^3 value measured in Denver and greater than the 0.16 (±0.16) µg /m^3 measured in Iowa during stable conditions. These data are consistent with the fact that Denver, Beaverton and Iowa were urban, suburban and rural locations, respectively and suggests that the human activities are an important source of organic and elemental carbon to the Beaverton and Denver airsheds.

6.3.1.2 Estimation of the Percent of OC that is Secondary in Origin. At the Beaverton location there was a statistically significant difference between the value of the OC/EC ratio of particulate material sampled under stable meteorological conditions as compared to that sampled during rain events. Stable atmospheric conditions are defined as high atmospheric pressure, no rain events, few clouds, low winds and daytime temperatures near 25 °C. The average OC/EC ratio was 4.61 during stable conditions and 1.34 during rain events. Secondary OC, also called secondary organic aerosol (SOA), is formed when gas-phase organic compounds are photochemically oxidized and transformed into lower vapor pressure compounds which condense or partition onto/into existing primary particles. That the OC:EC ratio was higher for samples taken under stable conditions than during rain events is consistent with the view that photochemical processes increase the OC content of ambient particulate material. During rain events the atmospheric lifetime of particles is short and SOA formation minimal, OC collected during these events was considered primary. Air sampling was conducted on 5/19/98 during a rain event and few weeks later on 6/29/98 under stable conditions. It is reasonable to assume that the source(s) of primary particles to the Beaverton airshed was/were similar on 5/19/98 and 6/29/98. Therefore the OC:EC ratio measured on 5/19/98 was used as an estimate of the OC:EC ratio for primary particles emitted to

Table 6.1 Sampling conditions and atmospheric particle-phase carbon characterization.

Location	Date	Met.[b]	T (°C)	ΔT^a	% RH	f_{oc}	f_{ec}	OC/EC	TSP (μg/m^3)
Beaverton	5/1/98	Stable	19.2	-14	30	0.099	0.016	6.19	96
Beaverton	5/19/98	Rain	12.8	0	100	0.187	0.164	1.14	12
Beaverton	6/29/98	Stable	12.5	NA	NA	0.200	0.055	3.64	15
Beaverton	6/29/98	Stable	12.5	0	86	0.200	0.055	3.64	27
Beaverton	7/21/98	Stable	16.6	-6	81	0.138	0.019	7.26	43
Beaverton	10/01/98	Stable	11.7	-1	95	0.147	0.046	3.20	32
Beaverton	12/1/98	Rain	9.4	-2	89	0.153	0.262	0.58	15
Beaverton	1/20/99	Rain	7.22	NA	96	0.089	0.097	0.92	10
Beaverton	3/5/99	Rain	3.95	0	89	0.142	0.052	2.73	22
Denver	5/18/99	Stable	21.1	-8.8	35	0.200	0.072	2.78	36
Denver	5/23/99	Stable	25.2	6.2	25	0.162	0.027	6.00	110
Hills	8/23/99	Stable	16.2	4.4	96	0.157	0.016	9.81	20
Hills	8/26/99	Stable	25.8	-5.3	86	0.018	0.000	NA	300

[a] Change in ambient temperature during sampling period. [b] Meteorological conditions

Table 6.2 Estimates of atmospheric primary and secondary OC observed at Beaverton, OR under stable meteorological conditions.

Location	Date	Time	Estimated Primary OC (μg/μg particle)	Estimated Secondary OC (μg/μg particle)	Estimated % of OC that is SOA
Beaverton	6/29/98	1000-1545	0.063	0.14	69
Beaverton	7/21/98	2307-0808	0.022	0.12	84
Beaverton	10/01/98	0030-0833	0.053	0.095	64

Beaverton during stable conditions. Using this ratio and the procedure of Turpin and Huntzicker (1991; 1995) the percent of OC that is secondary in origin was estimated. As shown in Table 6.2, for stable meteorological conditions in Beaverton, 64-84 % of the OC was estimated to be SOA. For comparison, during stable meteorological conditions in Los Angeles, Turpin and Huntzicker (1991; 1995) observed 40 to 80% of the OC was SOA.

6.3.2 Gas/Particle Partitioning of Ambient Atmospheric PAHs.

6.3.2.1 Normalization of K_p by f_{oc}. As shown in Figure 6.1a there was a two order of magnitude difference in the K_p values of PAHs with similar p_L^o values among the nine sampling events. After normalization by f_{oc} the range of $K_{p,oc}$ values was reduced to about one and a half orders of magnitude (Figure 6.1b). The individual m_p, $m_{p,oc}$, b_p, $b_{p,oc}$ values for each sampling event are given in Table 6.3.

For samples obtained at the Beaverton location during rain events, there was an order of magnitude variation in the K_p values of PAHs with a similar p_L^o values among the different sampling events. Differences in f_{oc} could not account for this variation.

The K_p and $K_{p,oc}$ values of PAHs measured in Beaverton during stable atmospheric conditions are compared in Figures 6.2a and b, respectively. For the sample obtained on 5/1/98, the K_p value of a given PAH at a given p_L^o was significantly lower than for the other sampling events. The 5/1/98 sample was obtained at a time when particles from a Chinese dust storm were present in the Beaverton airshed; over a four-day period ambient TSP ranged from 96 to 128 $\mu g/m^3$. These TSP values are much higher than the average value of 30 $\mu g/m^3$ measured at the same site during the 1998-1999 sampling period. The f_{oc} of particulate material collected during this event was 0.08 as compared to the average value of 0.16 measured at this site for all sampling events. After normalizing K_p by f_{oc} there was no significant difference (95% confidence level) in the $K_{p,oc}$ value of a given PAH at a given p_L^o on 5/1/98 as compared to the other four samples obtained in Beaverton under stable atmospheric conditions.

The K_p and $K_{p,oc}$ values of PAHs measured in Beaverton during stable atmospheric conditions are compared in Figures 6.2a and b, respectively. For the sample obtained on 5/1/98, the K_p value of a given PAH at a given p_L^o was significantly lower
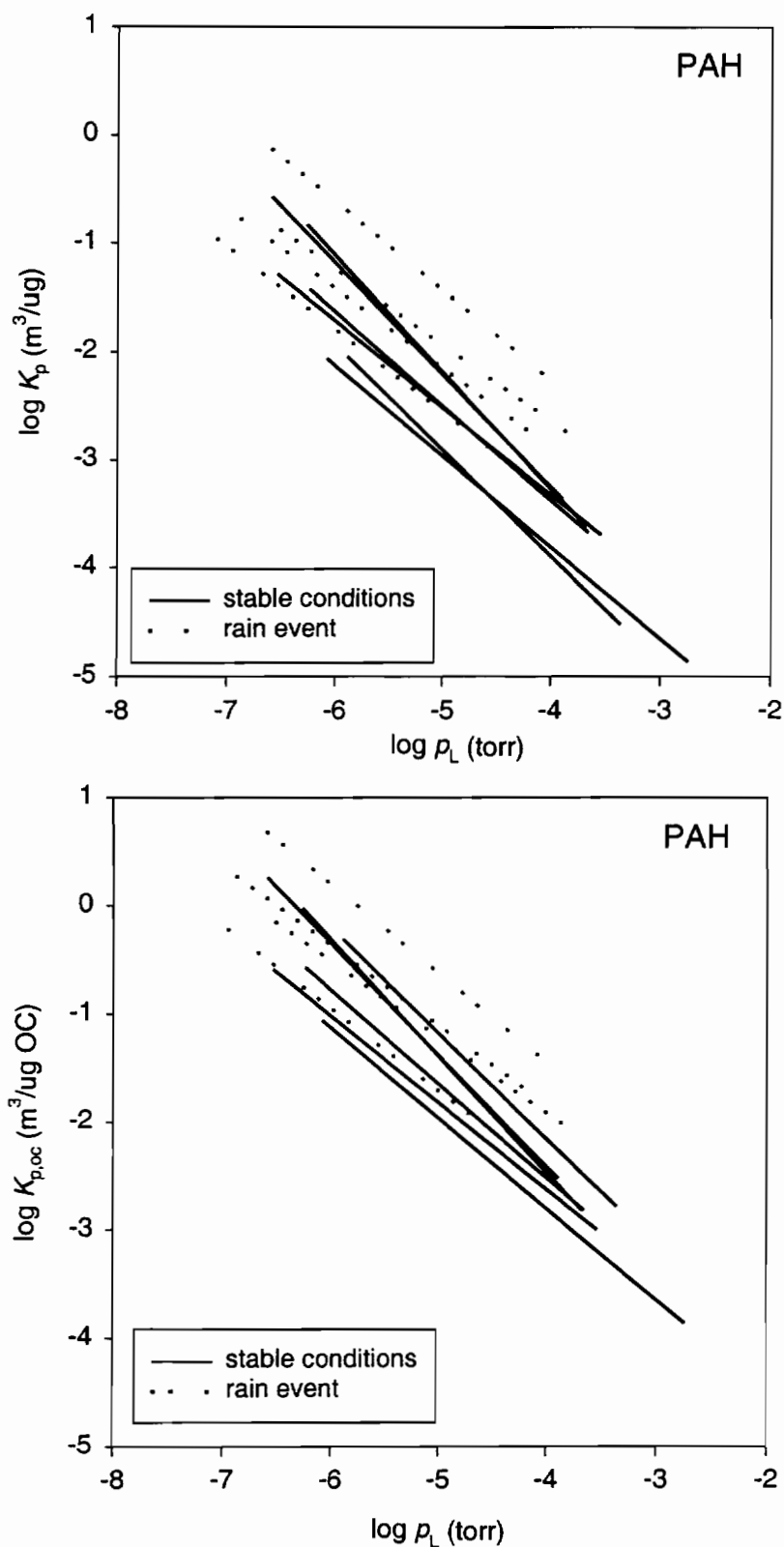
Figure 6.1 *G/P* partitioning of PAHs as measured at the Beaverton, OR and Hills, IA locations. **a**. Regression lines for plots of log K_p *vs.* log p_L^o. **b**. Regression lines for plots of log $K_{p,oc}$ *vs.* log p_L^o.

Table 6.3 Regression coefficients for log K_p vs. log p_L^o and log $K_{p,oc}$ vs. log p_L^o plots.

location	date	m_p	b_p	r^2	$m_{p,oc}$	$b_{p,oc}$	r^2
Beaverton	5/1/98	-0.84	-7.17	0.98	-0.84	-6.17	0.98
Beaverton	5/19/98	-0.70	-5.45	0.95	-0.70	-4.72	0.95
Beaverton	6/29/98	-0.80	-6.55	0.91	-0.80	-5.84	0.91
Beaverton	7/21/98	-0.87	-6.87	0.96	-0.87	-6.00	0.96
Beaverton	10/01/98	-1.03	-7.39	0.97	-1.03	-6.55	0.97
Beaverton	12/1/98	-0.82	-5.55	0.99	-0.82	-4.74	0.99
Beaverton	1/20/99	-0.73	-5.82	0.99	-0.73	-4.77	0.99
Beaverton	3/5/99	-0.76	-6.38	0.97	-0.76	-5.54	0.97
Hills	8/23/99	-1.08	-7.58	0.99	-1.08	-6.78	0.99
Hills	8/26/99	-0.98	-7.82	0.95	-0.98	-6.08	0.95

Figure 6.2 *G/P* partitioning of PAHs as measured at the Beaverton, OR location under stable meteorological conditions **a.** log K_p *vs.* log p_L^o plots. **b.** log $K_{p,oc}$ *vs.* log p_L^o plots.

than for the other sampling events. The 5/1/98 sample was obtained at a time when particles from a Chinese dust storm were present in the Beaverton airshed; over a four-day period ambient *TSP* ranged from 96 to 128 μg/m^3. These *TSP* values are much higher than the average value of 30 μg/m^3 measured at the same site during the 1998-1999 sampling period. The f_{oc} of particulate material collected during this event was 0.08 as compared to the average value of 0.16 measured at this site for all sampling events. After normalizing K_p by f_{oc} there was no significant difference (95% confidence level) in the $K_{p,oc}$ value of a given PAH at a given p_L^o on 5/1/98 as compared to the other four samples obtained in Beaverton under stable atmospheric conditions.

The K_p value of a given PAH at a given p_L^o as measured on 8/26/99 in Hills, Iowa was nearly a factor of 7 smaller than the value observed on 8/23/99 at the same site (Figure 6.3a). Both days were sunny with high RH (90-100%) and daytime temperatures around 25 °C. During the 8/26/99 sampling event agricultural activities caused high levels of *TSP*. The OC content of the collected *TSP* was low. After normalizing K_p values by f_{oc}, the resulting $K_{p,oc}$ values of PAHs with similar p_L^o values were the same (95% confidence level) for the two days (Figure 6.3b).

At a given location and under stable meteorological conditions the $K_{p,oc}$ values of PAHs with similar p_L^o values are the same among the different sampling events but differ by over an order of magnitude among the two locations. These observations suggest the chemical composition of OM may be quite different among locations. The conversion factor (CF) relating OC to OM, the product ζ_{om} MW_{om}, or the ratio CF / ζ_{om} MW_{om} may vary by an order of magnitude among particles from different sources and/or locations.

6.3.2.2 Normalization of K_p by f_{ec}. Luo (1996) has shown that at RH <40%, the adsorption of PAH to graphitic carbon may play a role in the sorption of PAHs to UPM. For this reason the EC content of UPM may be important. The fraction of the particle surface area consisting of EC was not determined, but the EC content on a mass basis was measured. The K_p values of individual PAHs were normalized by f_{ec} where, $K_{p,ec}$ = K_p / f_{ec}. Among the four samples taken in Beaverton during rain events there was a factor one and a half variation in the K_p values of a given PAH at a given p_L^o but the $K_{p,ec}$
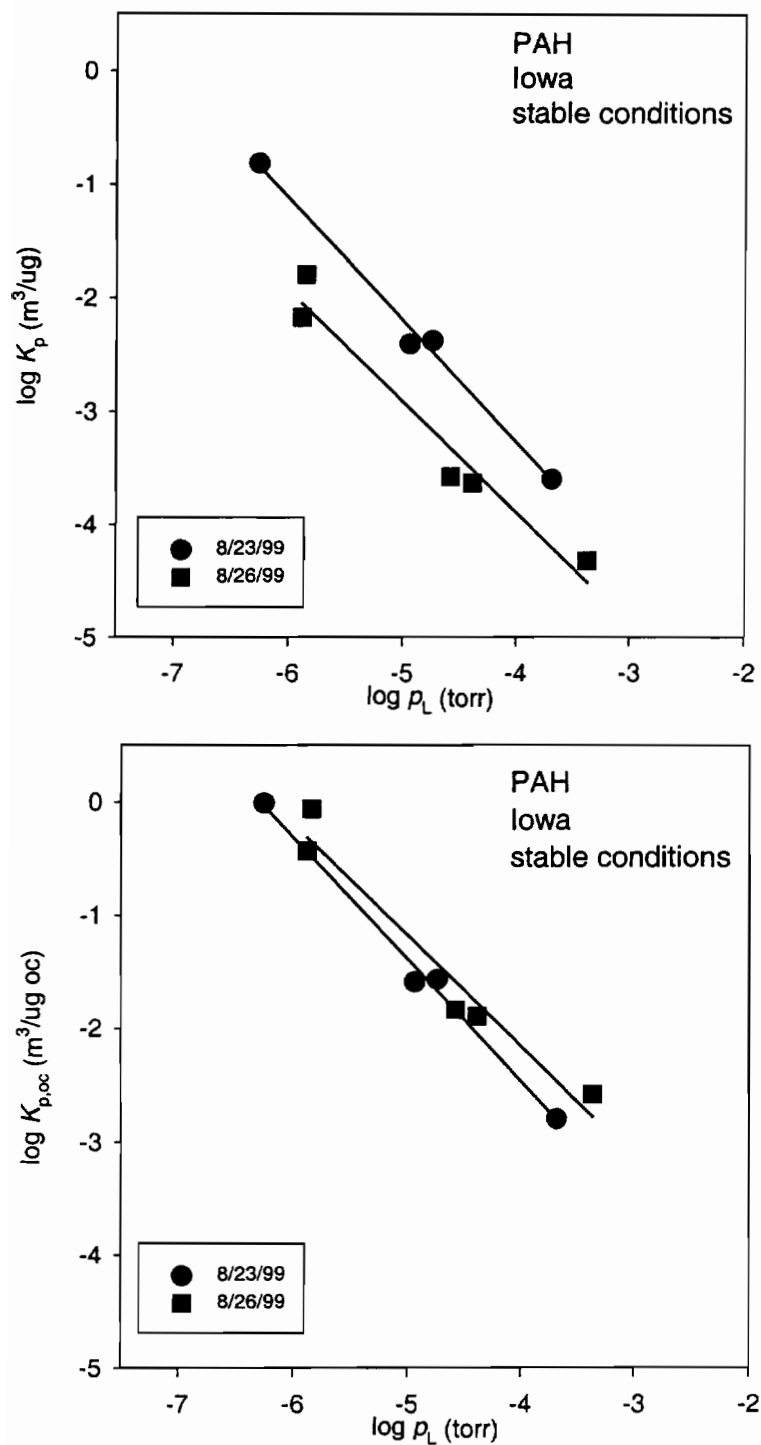
Figure 6.3 *G/P* partitioning of PAHs as measured at the Hills, IA location under stable meteorological conditions. **a.** Log K_p vs. log p_L^o plots. **b.** Log $K_{p,oc}$ vs. log p_L^o plots.

values were the same (95% confidence level) for three of four of the events (Figures 6.4 a and b). For samples taken in Beaverton under stable conditions there was no difference in the variation in K_p values and $K_{p,ec}$ values of a given PAH at a given p_L^o among sample events.

6.3.3 Relationship between EC and ΣPAH particle-phase concentrations.

The sum of the particle-phase concentration of fluorene, phenanthrene, anthracene, fluoranthene, pyrene, benz(a)anthracene and chrysene was defined as ΣPAH c_p (ng/µg). For samples collected at the Beaverton location during rain events, a significant correlation (r^2=0.96) between EC and ΣPAH c_p was observed (Figure 6.5a) but no relationship was observed for data collected on days with stable atmospheric conditions (Figure 6.5b). EC is formed only by combustion of organic material and thus solely primary (Seinfeld, 1986). Based on the similarity of EC and PAH particle size distributions in automobile exhaust, Venkataraman and Friedlander (1994) and Venkataraman et al. (1994) have suggested that PAHs and EC are formed simultaneously during combustion. Our data suggests the following: During rain events particle removal by wet scavenging is rapid and SOA formation minimal. It is likely that particles collected during rain events were freshly emitted primary particles from a combustion source(s).

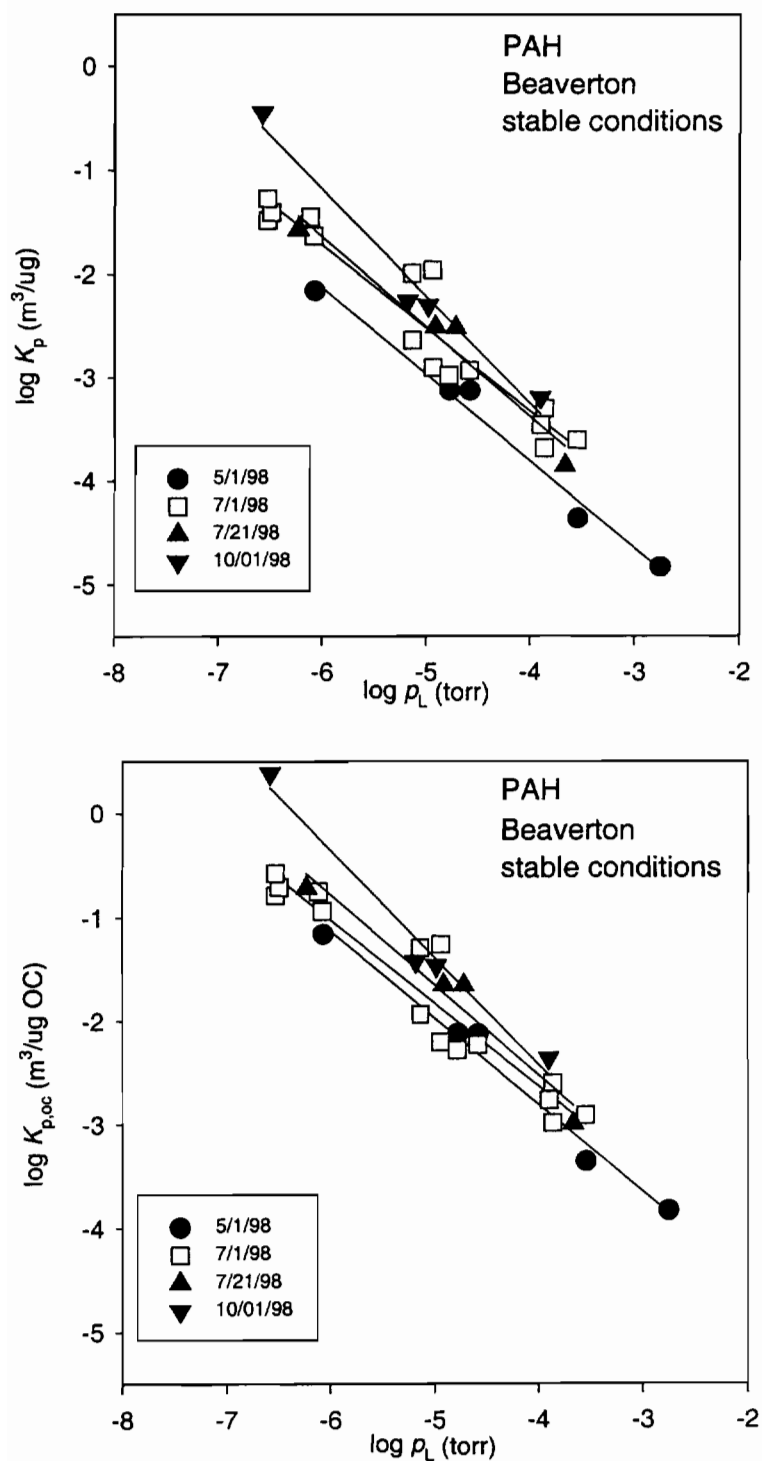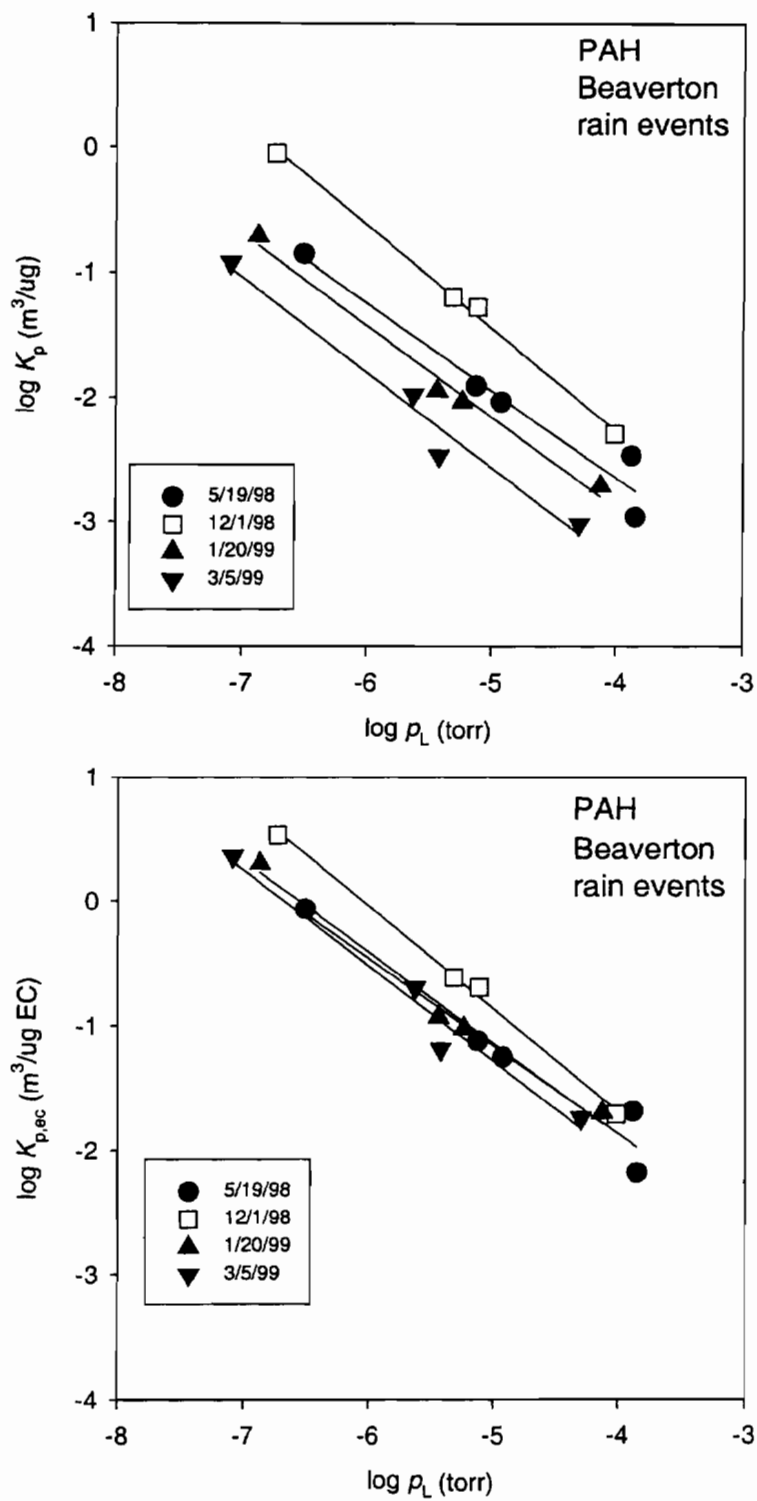**Figure 6.4** *G/P* partitioning of PAHs as measured at the Beaverton, OR location during rain events **a.** Log K_p *vs.* log P_L^o plots. **b.** Log $K_{p,ec}$ *vs.* log P_L^o plots.
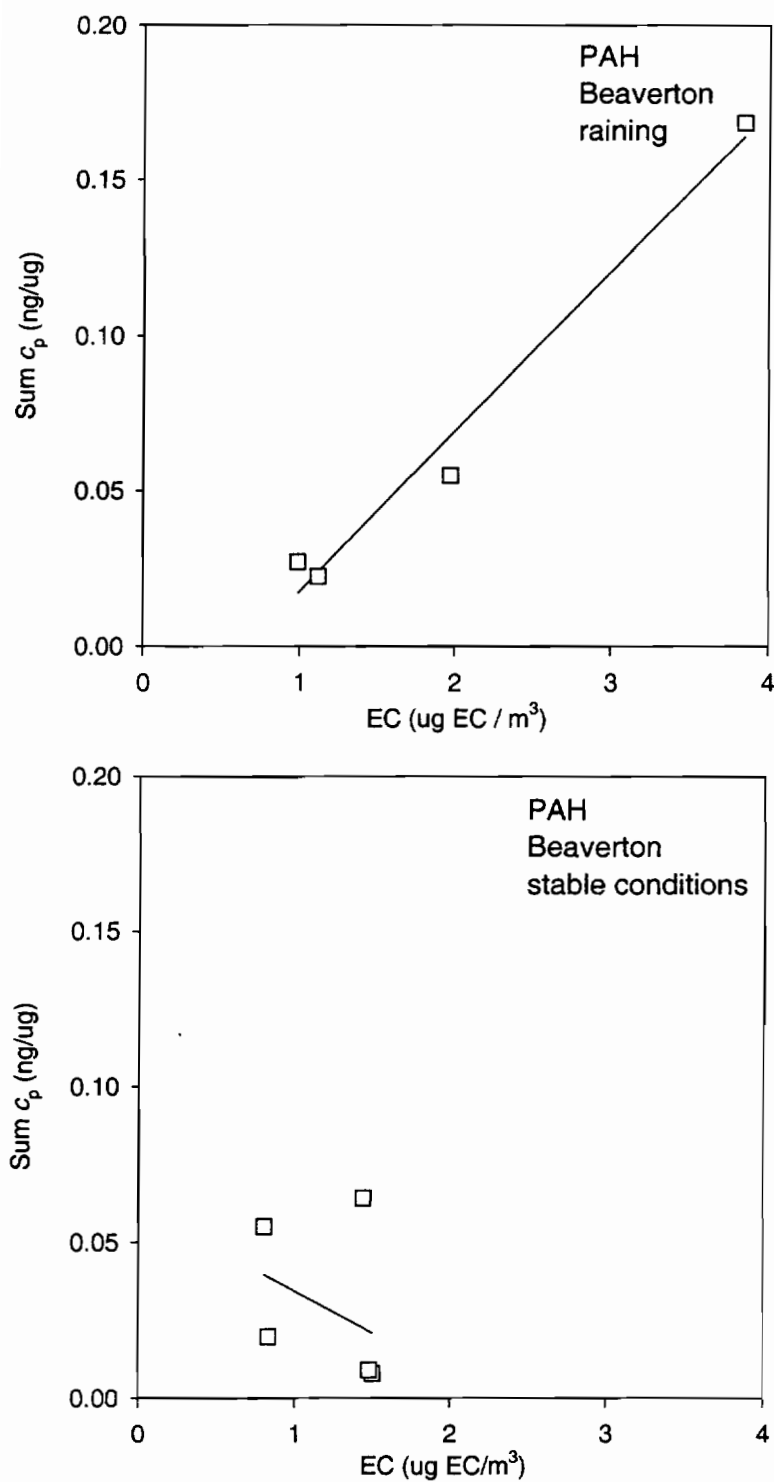
Figure 6.5 Plots of ΣPAH c_p *vs*. EC concentration constructed using data collected at the Beaverton, OR location. **a.** samples collected during rain events. **b.** samples collected under stable meteorological conditions.

6.4 References

Bidleman, T. F. 1988. Atmospheric processes- wet and dry deposition of organic compounds are controlled by their water vapor partitioning. *Environmental Science and Technology* 22, 361-367.

Bidleman, T. F. *et al.* 1986. Vapor-particle partitioning of semivolatile organic compounds: estimates from field collections. *Environmental Science and Technology* 20, 1038-1043.

Bidleman, T. F., Foreman, W. T. 1987. Vapor-particle partitioning of semivolatile organic compounds. In *Sources and Fates of Aquatic Pollutants*. Eds. R. A. Hites and S. J. Eisenreich. New York, ACS. pp. 27-56.

Birch, M. E., Cary, R. A. 1996. Elemental carbon-based method for monitoring occupational exposures to particulate diesel exhaust. *Aerosol Science and Technology* 25, 221-241.

Chiou, C. T. *et al.* 1979. Physical concept of soil-water equilibria for nonionic organic compounds. *Science* 206, 831-832.

Gray, H. A. 1986. *Control of atmospheric fine primary carbon particulate concentrations*. Ph.D. Thesis, Environmental Engineering Science, California Institute of Technology.

Gray, H. A. *et al.* 1986. Characteristics of atmospheric organic and elemental carbon particle concentration in Los Angeles. *Environmental Science and Technology* 20, 580-589.

Jang, M., Kamens, R. 1998. A thermodynamic approach for modeling partitioning of semivolatile organic compounds on atmospheric particulate matter: humidity effects. *Environmental Science and Technology* 32, 1237-1243.

Jang, M. *et al.* 1997. A thermodynamic approach using group contribution methods to model the partitioning of semivolatile compounds on atmospheric particulate matter. *Environmental Science and Technology* 31, 2805-2811.

Kile, D. E. *et al.* 1995. Partitioning of nonpolar organic pollutants from water to soil and sediment organic matters. *Environmental Science and Technology* 29, 1401-1406.

Larson, S. M., Cass, G. R. 1989. Characteristics of summer midday low-visibility events in the Los Angeles Area. *Environmental Science and Technology* 23, 281-289.

Liang, C., Pankow, J. F. 1996. Gas/particle partitioning of organic compounds to environmental tobacco smoke: partition coefficient measurements by desorption and comparision to urban particlate material. *Environmental Science and Technology* 30, 2800-2805.

Liang, C. *et al.* 1997. Gas/particle partitioning of semi-volatile organic compounds to model inorganic, model organic and ambient smog aerosols. *Environmental Science and Technology* 31, 3086-3092.

Luo, W. 1996. *Gas/Particle partitioning of semi-volatile organic compounds to two model atmospheric particulate materials: quartz and graphitic carbon.* Ph.D. Thesis, Environmental Science and Engineering, Oregon Graduate Institute of Science and Technology.

Mader, B. T., Pankow, J. F. 2000. Gas/solid partitioning of polychlorinated dibenzodioxins (PCDDs), polychlorinated dibenzofurans (PCDFs) and polycyclic aromatic hydrocarbons (PAHs) to filter surfaces: Part 3. Comparison of the gas adsorption artifact potential of Teflon membrane vs. quartz fiber filters and prediction of the magnitude of gas adsorption artifacts. *Environmental Science and Technology* submitted March 15, 2000.

McDow, S. R. *et al.* 1994. Effect of composition and state of components on polycyclic aromatic hydrocarbon decay in atmospheric aerosols. *Environmental Science and Technology* 28, 2147-2153.

Odum, J. R. *et al.* 1996. Gas/particle partitioning and secondary organic aerosol yields. *Environmental Science and Technology* 30, 2580-2585.

Pandis, S. N. *et al.* 1992. Secondary organic aerosol formation and transport. *Atmospheric Environment* 26, 2269-2282.

Pankow, J. F. 1991. Common y-intercept and single compound regressions of gas-particle partitioning data vs. 1/T. *Atmospheric Environment* 25A, 2229-2239.

Pankow, J. F. 1994. An absorption model of gas/particle partitioning of organic compounds in the atmosphere. *Atmospheric Environment* 28, 185-188.

Pankow, J. F., Bidleman, T. F. 1992. Interdependence of the slopes and intercepts from log-log correlations of measured gas-particle partitioning and vapor pressure-I. Theory and analysis of available data. *Atmospheric Environment* 26A, 1071-1080.

Seinfeld, J. H. 1986. *Air Pollution.* New York, John Wiley & Sons.

Turpin, B. J., Huntzicker, J. J. 1991. Secondary formation of organic aerosol in the Los Angeles Basin: A descriptive analysis of organic and element carbon concentrations. *Atmospheric Environment* 25a, 207-215.

Turpin, B. J., Huntzicker, J. J. 1995. Identification of Secondary Organic Aerosol Episodes and Quantitation of Primary and Secondary Organic Aerosol Concentrations during SCAQS. *Atmospheric Environment* 29, 3527-3544.

Venkataraman, C., Friedlander, S. K. 1994. Size distributions of polycyclic aromatic hydrocarbon and elemental carbon. Part 2. Ambient measurements and effects of atmospheric processes. *Environmental Science and Technology* 28, 563-572.

Venkataraman, C. *et al.* 1994. Size distributions of polycyclic aromatic hydrocarbons and elemental carbon. Part 1. Sampling, measurement methods and source characterization. *Environmental Science and Technology* 28, 555-562.

Yamasaki, H. *et al.* 1982. Effects of ambient temperature on aspects of airborne polycyclic aromatic hydrocarbons. *Environmental Science and Technology* 16, 189-194.

CHAPTER 7

CONTROLLED FIELD EXPERIMENTS TO STUDY THE GAS/PARTICLE PARTITIONING OF POLYCHLORINATED DIBENZODIOXINS, POLYCHLORINATED DIBENZOFURANS AND POLYCYCLIC AROMATIC HYDROCARBONS TO URBAN, SUBURBAN AND RURAL PARTICULATE MATERIALS.

7.1 Introduction

Polychlorinated dibenzodioxins and dibenzofurans (PCDD/Fs) are primarily released to the environment via air emissions from combustion processes (Brzuzy and Hites, 1996; Duarte-Davidson, Sewart et al.,1996). Consequently, atmospheric transport has been considered to be the dominant process responsible for the movement of these compounds from combustion sources to relatively remote receptors such as lake sediments, soils, and grasses (Czuczwa and Hites, 1984; Czuczwa, McVeety et al., 1984; Czuczwa and Hites, 1986; Brzuzy and Hites, 1995; Brzuzy and Hites, 1996); Eitzer and Hites, 1989; Duarte-Davidson, Sewart et al., 1996);Welsch-Paulsch, McLachlan et al., 1995). Thus understanding the gas/particle (G/P) partitioning of PCDD/Fs has important implications. For example, it appears that degradation via reaction with OH radical is more rapid for a compound in the gas phase than a compound in the particle phase, Brubaker and Hites (1997) and that dry gaseous deposition is the primary mechanism of uptake of PCDD/Fs by farm grasses (Welsch-Paulsch, McLachlan et al., 1995). Furthermore, optimizing the removal of PCD/Fs from municipal waste incinerator flue gas requires knowledge of how the compounds are distributed between the gas and particle phases as a function of temperature, particle concentration and particle type Smolka and Schmidt (1997).

G/P partitioning can be parameterized using the coefficient K_p (m^3/μg):

$$K_p = c_p / c_g \tag{7.1}$$

117

Where c_g (ng/µg) and c_p (ng/m³) are the gas and particle-phase concentrations, respectively. Compound-dependent values of log K_p can usually be correlated using the corresponding values of the sub-cooled liquid vapor pressure p_L^o torr) (Pankow (1987); Pankow,1994a; Pankow, 1994b). In the general case, we have:

$$\log K_p = m_r \log p_L^o + b_r \qquad \text{adsorptive or absorptive partitioning} \qquad (7.2)$$

Values of the slope m_r are frequently close to -1. When a compound *ab*sorptively partitions from the gas phase *into* a particle's OM, Pankow (1994a) has derived:

$$K_p = f_{om} \, 760 \, RT \, / \, \zeta_{om} \, MW_{om} \, p_L^o \, 10^6 \qquad (7.3)$$

Where f_{om} is the weight fraction that is absorbing organic material phase (OM), ζ_{om} is the activity coefficient of the compound of interest in the OM on a mole fraction scale and MW_{om} is the mean molecular weight of the absorbing OM (g/mol). If partitioning is dominated by *ab*sorption, K_p will be proportional to f_{om} (equation 7.3). Particles from different sources and/or locations may have different amounts of OM. For example, environmental tobacco smoke (ETS) particles have an $f_{om} \approx 1$ but an airborne soil particle may have an $f_{om} \approx 0.02$. If the value of $\zeta_{om} \, MW_{om}$ is similar among particles from different sources and/or locations, the K_p value of a given compound at a given p_L^o could vary by a factor 50 due to differences in f_{om} among the different types of particles. Some authors (Pankow, 1994a; Odum, Hoffman *et al.*, 1996) have suggested normalizing K_p by f_{om} where:

$$K_{p,om} = K_p / f_{om} \qquad (7.4)$$

Previous measurements of ambient atmospheric gas and particle-phase PCDD/Fs were made using conventional high volume air sampling. Air sampling during all these studies was carried out over several days with no T or RH control. Variations in T of up to 20 °C were observed in some of these studies; the results of such studies were certainly subject to sampling artifacts. Examples would be "blow off" of filter bound compounds during higher daytime temperatures, and "blow on" during colder nighttime temperatures. Diurnal changes in RH may also have affected the measured G/P partitioning. Finally, it is not possible to compare whether the partitioning was dominated by *ad*sorption or *ab*sorption since the particulate material sampled was not characterized for the fraction organic carbon.

Controlled field experiments (CFEs) represent a new air sampling approach, which minimizes sampling artifacts. CFEs are conducted by equilibrating previously collected ambient particulate materials with SOCs generated in the gas phase using particle free ambient air maintained at a constant T and RH to prevent their diurnal cycling. Backup filters are used to correct for gas adsorption to filter surfaces. CFEs were used to study the G/P partitioning behavior of PCDD/Fs and Polycyclic Aromatic Hydrocarbons (PAHs). Data collected from CFEs will lead to a better understanding of the G/P partitioning process; CFEs provide information regarding the possibility that differences in the K_p value of a given compound at a given p_L^o among samples taken at different times and/or at different locations could be normalized by f_{om}.

7.2 Material/Methods

7.2.1 General experimental. The three sampling sites used were located as follows: University of Colorado at Denver, Denver, CO (urban), Oregon Graduate Institute, Beaverton, OR (suburban), and Hills Observatory, Hills, IA (rural/farm). The CFEs consisted of two stages; in the first stage ambient particles were collected on a TMF. At some point during the first stage, ambient gas and particle phase PAHs were collected using conventional high volume air sampling (HVOL) with a second sampler. Once an adequate amount of particulate material had been collected to allow G/P K_p values to be measured using the CFE method, particle collection on the TMF was halted. In the second stage of the CFEs, particles collected on TMFs were equilibrated with SOCs using the apparatus shown in Figure 7.1.

7.2.2 Conventional High Volume Air Sampling (HVOL) specifics. Ambient gas and particle-phase PAHs were collected using a standard high volume air sampler (Graseby Manufacturing, Village of Cleves OH). Particle-bound PAHs were collected on a 20.3 × 25.4 cm quartz fiber filter (QFF) (Pall/Gelman, Ann Arbor MI); gas adsorption to the QFF was estimated using backup QFF. Prior to sampling, each QFF was prepared by baking at 450 °C for 4 hours and equilibrated overnight in a constant 65% RH chamber. Gas-phase PAHs were collected on pre-cleaned 8.5 cm diameter, 8.0 cm thick PUF plugs. PUF plugs were precleaned by soxhlet extraction in methylene chloride for 24 hours. Breakthrough of the PAHs was determined using backup PUF plugs.

Sampling times were from 6 to 12 hours depending on the sampling site. Most sampling events were conducted at times of the day where temperature fluctuations were minimized. The sampler flow rate was $1 m^3$/min resulting in sample volumes of 360 to $720 m^3$.

7.2.3 CFE specifics. Ambient particles were collected on a 20.32 cm × 25.4 cm Teflon membrane filter (TMF) located in the filter holder of a high-volume air sampler for a period of 11-430 hours. The ambient gas phase was not collected. The TMFs were obtained from Pall-Gelman Sciences (Ann Arbor, MI). Each TMF was precleaned by washing three times with 50 mL of methylene chloride. For each experiment, TMF were held overnight at RH = 65%, then weighed and loaded into a filter holder. TMFs sent to Micrometrics (Norcross, GA) yielded a specific surface area value of 0.21 m^2/g. A 100 mm diameter punch of the particle loaded TMF and a particle free backup TMF filter were loaded into the filter holder of the environmental chamber unit (ECU) (Figure 7.1). A glass fiber filter (GFF) was placed in front of the filter holder and T and RH regulation of the air was begun using the air conditioning unit (ACU). Ambient, outdoor air was cleaned of particles by passage through the GFF. The gaseous organic compounds passing through the GFF were allowed to continue on to the particle loaded TMF thereby minimizing the de-sorption "stripping" of organic compounds from the particles. The cleaned air was then drawn into the ACU in which the air passed through a 45 cm long, 0.95 cm i.d. stainless steel tube in a water bath; the temperature sensor governing the heating/cooling of the water bath was located in the stainless steel filter holder containing the TMFs. The expected maximum outdoor T for the experimental period was selected as the set-point T for the experiment, *i.e.* for the water bath. The air produced by the ACU was characterized by that T, and by a nearly-constant RH. (During stable meteorological conditions, air parcels do not tend to mix vertically, and the water content expressed in ppmV will generally stay constant. Under these conditions, adjusting the air temperature to a constant value will maintain a near-constant RH.) The RH was measured using an Omega CTH89 temperature/humidity recorder (Omega Engineering, Stamford, CT).

The air produced by the ACU was drawn into the ECU in which SOCs were added; the air was then equilibrated with the TMFs. The ECU was set at the same
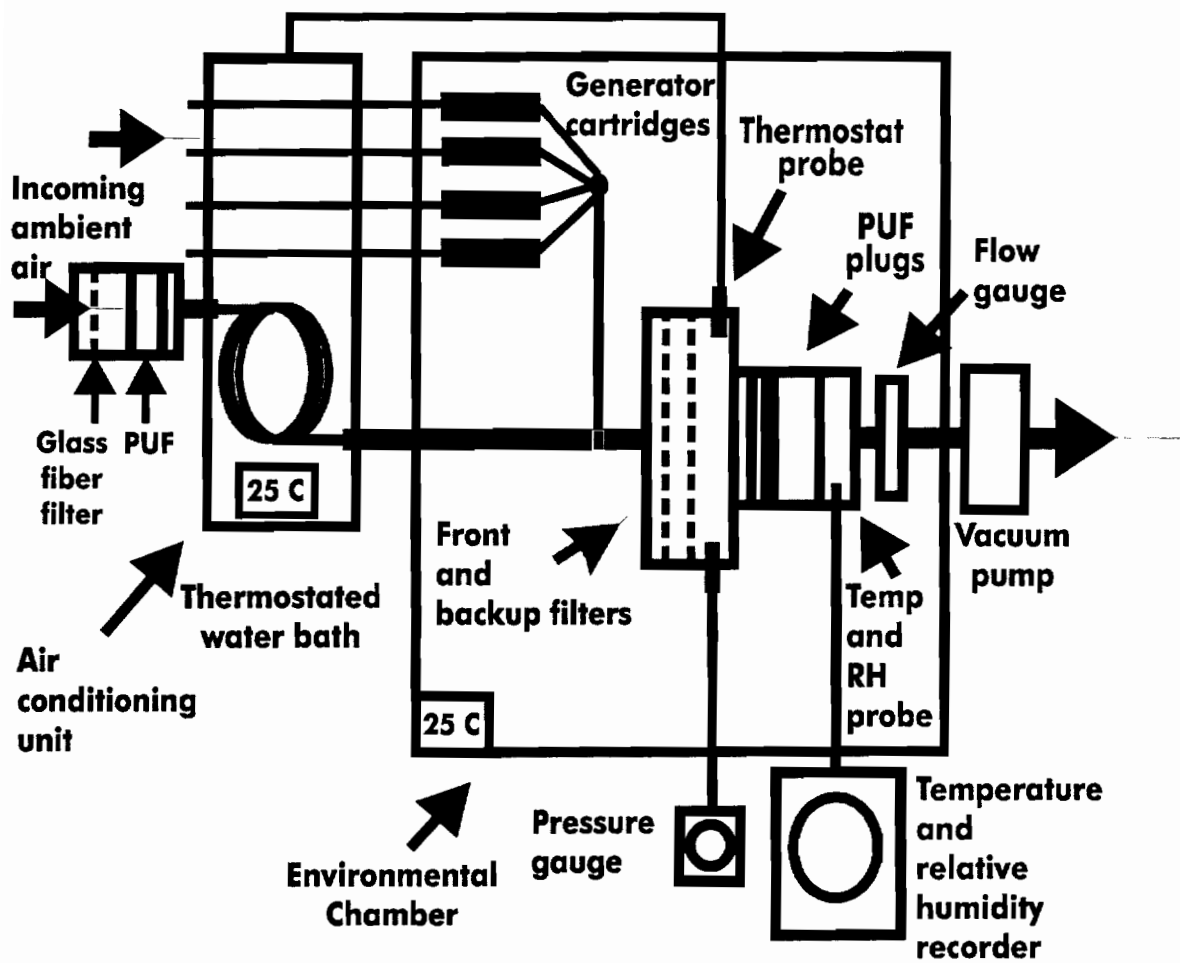
Figure 7.1 The apparauts used to conduct CFEs.

temperature as the ACU. SOCs were added to the air flow in the ECU by routing a small portion (5 L/min) of the incoming air through SOC "generator cartridges". Specific details of the design and operation of the generator cartridges is provided by Mader Mader and Pankow (2000). The flow from the generator cartridges was then mixed back into the main flow at a point upstream of the filter holder. After the filter holder, the air was directed through a 24 mL front PUF plug, followed by a 178 mL backup PUF plug (PUF density = 0.022 g/mL). The purpose of the PUF plugs was to determine the c_g values to which the collected particles and TMFs were exposed. PUF plugs behind the TMFs were changed at intervals that ranged from 10 minutes to 20 hours; the sample volumes for those intervals ranged from 0.6 to 70 m^3.

The total air flow rate through the TMFs was constant within every experiment, but ranged from 11 to 72 L/min among the different experiments depending on the particle loading of the front filter. A flow rate was chosen such that the pressure drop across the filters was less than 0.1 atm (40 inches of H_2O). The duration of each experiment depended on the air temperature, and ranged from 1.5 days to 21 days, using a total air volume V_t between 55 and 920 m^3. Colder temperatures required longer experimental times because the *G/P* and G/TMF partition coefficients were correspondingly larger.

At the point that an experiment was ended, for each SOC of interest, it was considered likely that *G/P* and G/TMF equilibrium had been achieved if: 1) the gas phase concentration exiting the filter (as measured with the PUF plugs) had approached an asymptotic equilibrium value (designated as $c_{g,eq}$); and 2) V_t was at least twice the volume required to deliver the total mass that was found sorbed on the front and backup TMFs, *i.e.*,

$$V_t \geq 2 \, m_{eq} / c_{g,eq} \qquad (7.5)$$

Where: m_{eq} is the sum of the mass found on the two filters at apparent equilibrium. Equation 7.5 assumes that the gas concentration entering the filter equaled $c_{g,eq}$ for the entire duration of the experiment

7.2.4 Extraction of Samples- Filters. Immediately after an experiment, each TMF was spiked with four surrogate standard solutions: 4 µL of 250 ng µl^{-1}

perdeuterated fluorene in hexane; 4 µL of 250 ng µL^{-1} perdeuterated pyrene in hexane; 16 µL of 50 ng µL^{-1} fully-^{13}C labeled 1234 F in toluene; and 16 µL of 50 ng µL^{-1} fully-^{13}C labeled 2,7+2,8 D in toluene. Each particle loaded filter was then extracted for 24 hours using soxhlet extraction with 100 mL of methylene chloride. Backup filters were then extracted four times; 25 mL of methylene chloride and 10 minutes of sonication was used each time. After extraction samples were concentrated to 2 mL using a Bucci Roto-evaporator (Buchi Instruments, Switzerland). The samples from particle-laden filters were cleaned up and dried on a mini-column made from a disposable pipette and filled with 0.2 g SiO$_2$, and topped off with 1 g of Na$_2$SO$_4$. For particle-free backup filters no cleanup step was necessary. Each extract was then transferred to a precleaned 4 mL mini vial and stored at -20 °C. Immediately before analysis by GC/MS, each extract was gently blown down to 200 µL using a stream of ultra-clean N$_2$, then spiked with 2000 ng of perdeuterated phenanthrene. All deuterated and ^{13}C-labeled compounds were obtained from Cambridge Isotope Labs (Andover, MA).

The extracts were analyzed on a Hewlett Packard 5890/5971 GC/MS using a 30 m × 0.25 mm DB-5 fused silica capillary column (J&W Scientific Folsom, Ca). Each extract was injected "splitless" with the injector at 280 °C. The GC temperature program was: 100 to 200 °C at 4 °C / min; 200 to 250°C at 5 °C / min; hold isothermal at 250°C for 5 min. The linear velocity of the carrier gas was 25 cm/s at 100 °C corresponding to a flow rate of about 1 ml/min. The MS was operated in the electron impact mode with ionization at 70 eV and scanned from 50 to 400 amu. The multiplier voltage was 1900 eV and the detector temperature 170 °C. The PAH standard solution contained fluorene, fluorene-d$_{10}$, phenanthrene, phenanthrene-d$_{10}$, anthracene, fluoranthene, pyrene, pyrene-d$_{10}$, benz(a)anthracene, and chrysene. The PCDD/F standard solution contained the compounds 2 F, 28 F, 246 F, 238 F, 1378 F, 2378 F, 12378 F, 23478 F, 1 D, 2 D, 23 D, 28 D, 124 D, 1234 D, 2378 D, 12478 D, 12378 D, and the two fully-^{13}C-labeled internal standard compounds (all from Cambridge Isotopes Labs). Response factors for the PAHs and PCDD/Fs were determined as a function of mass injected. The internal standard compound for the PAHs was phenanthrene-d$_{10}$. The internal standard compounds for the PCDD/Fs were the ^{13}C-labeled PCCD/Fs.

7.2.5 Extraction of Samples- PUF. Each PUF was extracted using the flow through extraction (FTE) method of Maddalena, McKone et al. (1998). Each PUF was loaded into a glass syringe with a volume of 100 mLs, i.e. approximately one quarter the volume of the non-deformed PUF. Each PUF was then spiked with an aliquot of each surrogate standard solution and extracted with 300 mLs methylene chloride, i.e. approximately 1.5 times of the volume of the non-deformed PUF. The samples were evaporated to 4 mL using the Roto-evaporator (Buchi Instruments, Switzerland) and stored until analyzed by GC/MS. No cleanup step was necessary. Immediately before analysis by GC-MS, each extract was gently blown down to 200 μL using a stream of ultra-clean N_2, then spiked with 2000 ng of perdeutrated phenanthrene.

7.2.6 QA/QC. Blank filters and PUF plugs were extracted regularly. Except for chrysene, the blank levels were always less than 5% of the total mass measured for each compound on the filters and PUF plugs. For chrysene, when the blank amount corresponded to more than 10% of the sample amount, a $K_{p,s}$ value was not computed for that experiment. For the PAHs, absolute recoveries from the PUF plugs and TMFs averaged 111% and 107% respectively. For the PCDD/Fs, they averaged approximately 65% and 92% respectively. For the PUF plugs behind the TMF filter holder, at the warmest experimental temperature used (26 °C), breakthrough from the front to backup plug averaged 60, 5, and 7% for fluorene, phenanthrene, and anthracene, respectively, and 15, 8, and 9% for 1 F, 1 D and 2 D, respectively. Breakthrough was negligible for the other compounds at 26 °C. Since the volume of the 178 mL backup PUF plug was over seven times that of the 24 mL front PUF plug, when combined, both plugs provided essentially quantitative recoveries for all compounds at all experimental temperatures.

7.3 Results/Discussion

7.3.1 Conservation of particle organic carbon (OC) during CFEs. Cotham and Bidleman (1992) observed that OC could be stripped from particles collected on GFF when clean air was passed through the filter. During CFEs ambient gaseous organic compounds were allowed to pass through the system and on through the particle loaded TMF thereby minimizing the desorption "stripping" of organic compounds from the particles. To ensure that OC was conserved during a CFE the following experiment was

done: ambient particulate material was collected on a 8 × 10 inch QFF. When enough particulate material had been collected to allow G/P K_p values to be measured using the CFE method, particle collection on the QFF was halted. Immediately after collection was completed two-1 cm^2 punches were removed from the particle-loaded filter and their OC and EC content measured. A 78.5 cm^2 punch from the same particle-loaded filter was used as a front filter in a CFE and a 78.5 cm^2 punch of a clean particle-free QFF used as the backup filter. Upon completion of the CFE the OC and EC content of the front and backup QFF was measured. These data are presented in Table 7.1. There *appears* to be a 4% decrease in the OC content of the front filter after a CFE, however there was also an 8% decrease in the EC content as well. EC is essentially non-volatile and cannot be stripped off during a CFE. It is likely that the particle loading on the QFF may not be completely homogeneous; the OC and EC loading may be slightly different (*i.e.* 10%) depending on where the punch was taken on the filter. It is likely that there was no significant difference in OC before and after particulate material was used in a CFE.

7.3.2 Gas/particle partitioning equilibrium. As equilibrium between the gaseous SOCs, collected particles, and backup TMF was approached, the gas-phase concentration of each SOC in the air exiting the filter approached a constant value of $c_{g,eq}$ (*e.g.*, see Figure 7.2). For the PAHs, $c_{g,eq}$ was computed as the average of the measured c_g values once c_g varied by no more than ±10%. For the PCDD/Fs, the criterion was variation by no more than ±20%. Values of K_p are reported here only for those cases when the Equation 7.5 criterion was satisfied.

7.3.3 Comparison of PAH and PCDD/F G/P partitioning behavior among locations. Plots of log K_p *vs.* log p_L^o were made using G/P partitioning data for PAH and PCDD/Fs obtained using CFEs at a number of locations (Figures 7.3a and b). The slope (m_p) and intercept (b_p) values for the regression lines of these data are presented in Tables 7.2 and 7.3. Also shown in Figure 7.3a are the K_p values of PAHs for partitioning to environmental tobacco smoke (ETS) (Pankow, Isabelle *et al.*,1994), diesel exhaust (Kamens, Odum *et al.*, 1995), and Los Angeles secondary organic aerosol (LA-SOA) (Liang, Pankow *et al.*, 1997). These data were measured using conventional air sampling methods but sampling artifacts were minimized; the variation in *T* and *RH* during sampling was small and backup filters were used to correct gas adsorption artifacts. In

Table 7.1 Organic carbon (OC) and elemental (EC) carbon before and after CFEs.

	OC (ug/cm^2) (±6%)	EC (ug/cm^2) (±6%)
front filter before CFE	46.8	12.8
front filter after CFE	45.1	11.8
backup filter after CFE	4.16$^\phi$	0

$^\phi$Relative error 15%
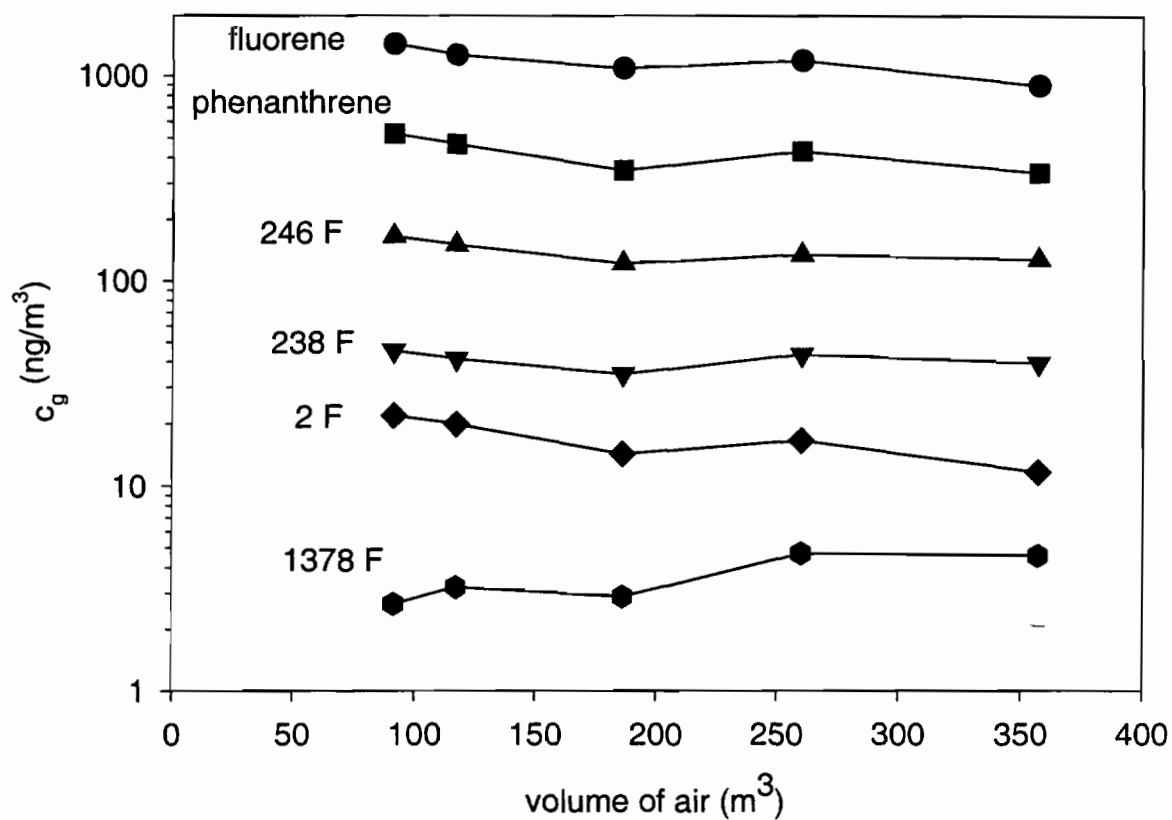
Figure 7.2 Gas phase concentration of selected PAH and PCDD/Fs as a function of the total air flow through the filter head of experimental system.
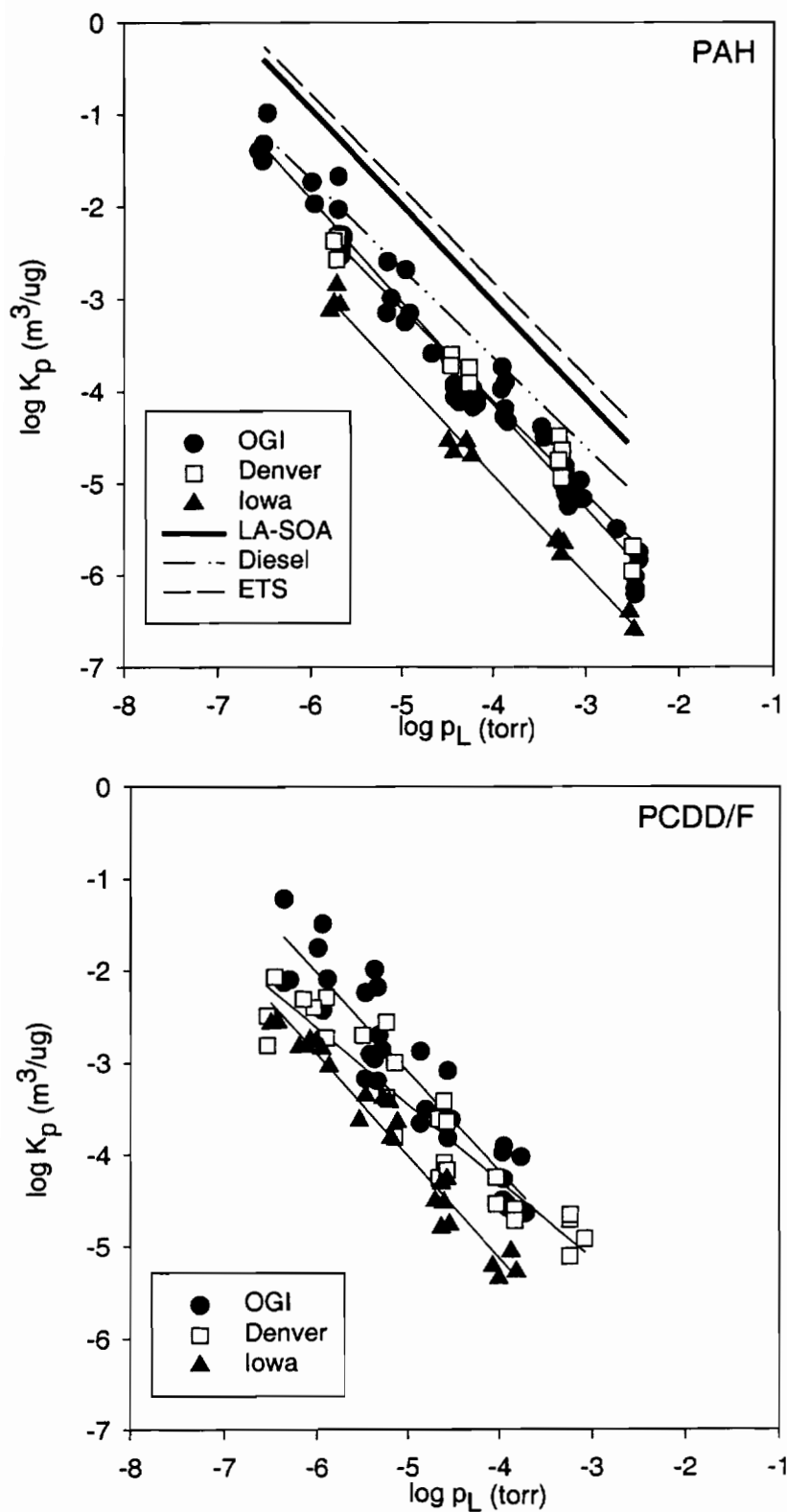
Figure 7.3 Log K_p vs. log p_L^o plots for the *G/P* partitioning of selected compounds at a number of locations. **a.** PAHs **b.** PCDD/Fs.

Table 7.2 Regression coefficients for the general equation ($\log K_p = m \log p_L^o + b$) for PAHs measured at a number of locations.

Location	m_p	b_p	r^2	$m_{p,om}$	$b_{p,om}$	r^2	$m_{p,oc}$	$b_{p,oc}$	r^2
Beaverton	-1.12	-8.62	0.97	-1.13	-8.00	0.96	-1.12	-7.75	0.97
Denver	-1.00	-8.13	0.98	-1.01	-7.61	0.98	-1.00	-7.40	0.98
Iowa	-1.07	-9.21	0.99	-1.07	-7.73	0.99	-1.07	-7.47	0.99

Table 7.3 Regression coefficients for the general equation ($\log K = m \log p_L^o + b$) for PCDD/Fs measured using CFEs at a number of locations.

Location	m_p	b_p	r^2	$m_{p,om}$	$b_{p,om}$	r^2	$m_{p,oc}$	$b_{p,oc}$	r^2
Beaverton	-1.13	-8.81	0.89	-1.18	-8.28	0.88	-1.14	-7.99	0.90
Denver	-0.91	-7.95	0.90	-0.92	-7.47	0.92	-0.92	-7.26	0.92
Iowa	-1.11	-9.59	0.96	-1.11	-8.11	0.96	-1.11	-7.85	0.96

addition the organic carbon content of the collected particles had been measured. As shown in Figure 7.3a, for PAHs with similar p_L^o values, there was a two order of magnitude range in K_p values among the different locations (*e.g.* ETS vs. Iowa). Only at the Denver and Beaverton locations were K_p values of PAHs with similar p_L^o values the same at the 95% confidence level.

As shown in Figure 7.3b, for PCDD/Fs with similar p_L^o values, there was variation in K_p values among locations. At the 95% confidence level, the K_p value of PCDD/Fs with similar p_L^o values was significantly the same for partitioning to Denver or Beaverton particulate but less for partitioning to Iowa particulate material.

7.3.4 Comparison of *G/P* partitioning behavior of PAHs vs. PCDD/Fs Ambient particles were equilibrated with PAH and PCDD/Fs in CFEs conducted at the Denver, Beaverton and Iowa locations. Despite their structural differences, PAHs and PCDD/Fs with similar p_L^o values exhibited similar K_p values (95% confidence interval) at *each* location (Figure 7.4).

7.3.5 Comparison of K_p values measured using CFE and HVOL. At some point during the particle collection stage of a CFE, conventional high volume air sampling (HVOL) was used to collect ambient gas and particle-phase PAHs. For each experiment K_p values of PAHs were measured using both CFE and HVOL methods. To compare the two sampling methods the log K_p values measured by each method were plotted versus log p_L^o in a single plot for a given experiment. Since variation in T during sampling can affect the slope of plots of log K_p *vs.* log p_L^o Pankow and Bidleman (1991), comparisons were made using HVOL data where the variation in T was less than 2 °C. Data from five experiments satisfy this criterion. In all five experiments the K_p values of PAHs having relatively high vapor pressures (*e.g.* phenanthrene, anthracene) were significantly lower as measured by CFEs than the K_p values measured using HVOL, but the K_p values of PAHs having relatively lower vapor pressures (*e.g.* benz(a)anthracene and chrysene) were similar as measured by the two methods (Figure 7.5). A possible explanation for this difference could be the presence of non-exchangeable or slowly exchangeable material in the native particles. Pankow (1988) and Pankow and Bidleman (1991; 1992) have theorized that non-exchangeable material could significantly affect the
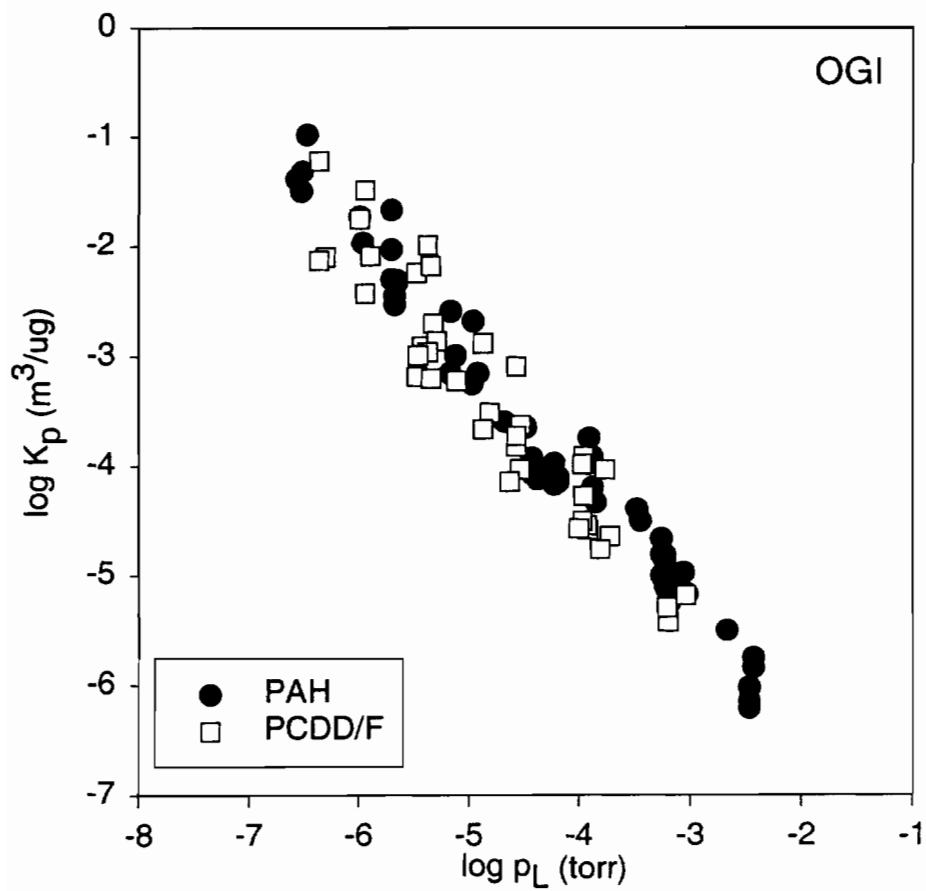
Figure 7.4 Log K_p *vs.* log p_L^o plots for the *G/P* partitioning of PAH and PCDD/Fs at Beaverton, OR.

G/P partitioning behavior of the PAHs. If some fraction of the particle is non-exchangeable, the PAH in this fraction will not reach equilibrium with the gas phase. The measured c_p value ($c_{p,measured}$) and consequently the measured K_p value for that compound ($c_{p,measured}$) and consequently the measured K_p value for that compound will be larger than if the entire particle were exchangeable.

$$c_{p,measured} = (M_{PAH,exchangeable} + M_{PAH,non-exchageable})/M_{particle} \qquad (7.6)$$

Where: $M_{PAH,exchangeable}$ is the mass of an SOC present in the particle that is exchangeable, $M_{PAH,non-exchageable}$ the mass present on the particle that is non-exchangeable and $M_{particle}$ the particle mass. Non-exchangeable material has a small effect on the $c_{p,measured}$ value of low volatility compounds since the majority of the mass of these compounds is distributed on the particle phase hence $M_{PAH,exchangeable}$ is large for these compounds; however the more volatile compounds are strongly affected since $M_{PAH,exchangeable}$ is small. The following *G/P* partition coefficients can be defined: $K_{p,non-exchangeable}$ is the partition coefficient for a particle having a non-exchangeable fraction and $K_{p,exchangeable}$ is the partition coefficient for a completely exchangeable particle. We have that $K_{p,non-exchangeable}$ ≈ $K_{p,exchangeable}$ for the relatively low volatility compounds but $K_{p,non-exchangeable}$ > $K_{p,exchangeable}$ for the relatively high volatility compounds. The presence of non-exchangeable material results in the slope of a plot of log K_p *vs.* log p_L^o being shallower than the slope observed for completely exchangeable particles Pankow and Bidleman (1992). Note that the non-exchangeable fraction of the particle could also be thought of as "slowly exchangeable". For particles formed via combustion and condensation, compounds present within the particles must diffuse out of the particle to attain *G/P* equilibrium. If the time for intra-particle diffusion is longer than the atmospheric residence time of the particle then some fraction of the mass of an SOC present on the particle could be considered essentially non-exchangeable. The slope of a plot of log K_p *vs.* log p_L^o for slowly exchangeable particles would be shallower than the slope observed for freely exchangeable particles.

7.3.6 Estimation of the percent of non-exhangeable material present in native particles. The $c_{g,eq}$ values of PAHs generated during the CFEs were 10 to 1,000 times higher than ambient levels. Upon *G/P* equilibrium the mass of PAH delivered to the particles during a CFE is orders of magnitude greater than that present initially. If a
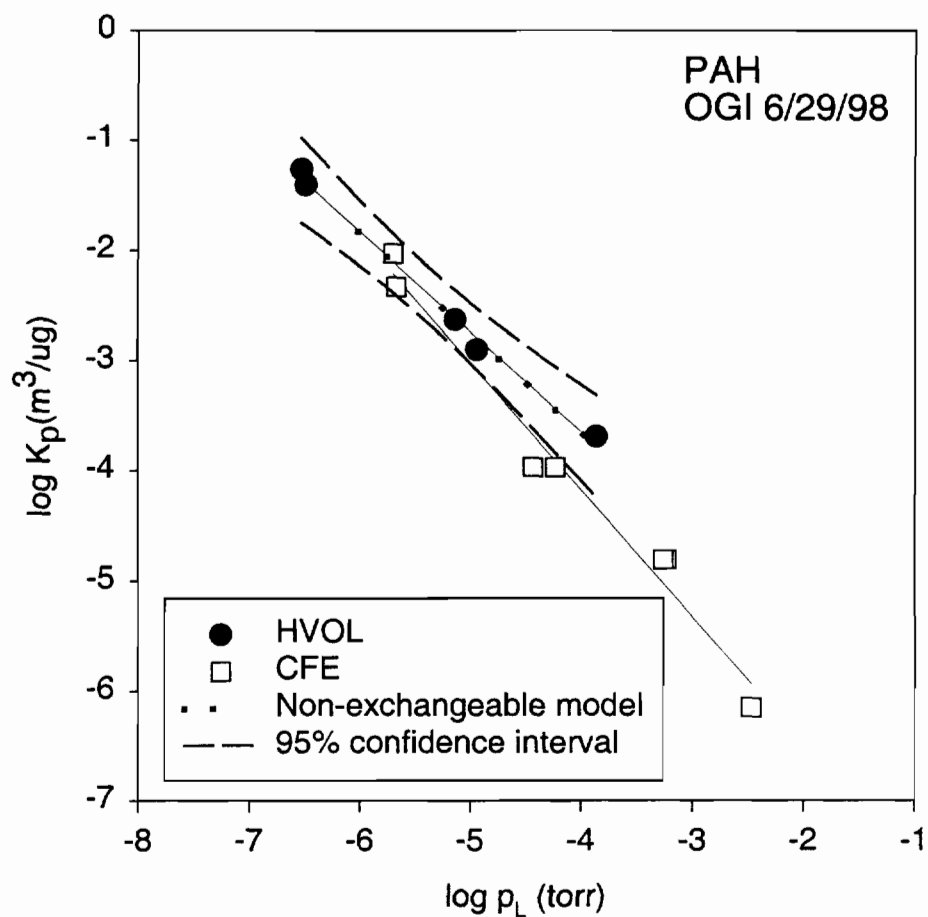
Figure 7.5 Plot of log K_p vs. log p_L^o for the *G/P* partitioning of PAHs as measured using HVOL and CFE. Included is a line corresponding to a fit of the data using the non-exchangeable model of Pankow with an assumption that 0.6% of the particle is non-exchangeable.

fraction of the native particle phase PAH were non-exchangeable, the mass of PAH in that fraction would be insignificant compared to the mass added by the CFE method. The influence of non-exchangeable material on the K_p values of PAHs would be observed in HVOL data but not CFE data. This could be the reason why the slopes of plots of log K_p vs. log p_L^o are shallower for the HVOL data than the CFE data. (Note: for the PAHs the slope of the plot of log K_p vs. log p_L^o from the CFE were all nearly -1 (-1.10 ± 0.06). If the mechanism of partitioning were absorption this suggests that the value of ζ_{om} is the same for low to mid molecular weight PAH. If the mechanism is adsorption then the term (Q_1-Q_v) constant for these compounds. Therefore the shallowness of the slopes of log K_p vs. log p_L^o for the HVOL data cannot be due to variation in ζ_{om} or term (Q_1-Q_v) throughout compound class.)

Pankow (1988) has derived an equation to model the influence of non-exchangeable material on K_p.

$$\log K_{p,\, non\, -\, exchangeable} = \log K_p + \log \frac{100 + \dfrac{X_{ne}}{(K_pTSP)}}{100 - X_{ne}} \qquad (7.7)$$

Where $K_{p,non\text{-}exchangeable}$ ($m^3/\mu g$) is the partition coefficient measured for a particle having a non-exchangeable portion, K_p ($m^3/\mu g$) the partition coefficient for the completely exchangeable fraction of the same particle, TSP ($\mu g/m^3$) the total suspended particulate material, and x the percent of the particle that is non-exchangeable. Data from CFE and HVOL measurements obtained during the same experiment can be used to test this model and estimate the fraction of non-exchangeable material present on the native particles. Data from CFE are not subject to the effects of non-exchangeable material and provide K_p values, data from HVOL provide measured $K_{p,non\text{-}exchangeable}$ and TSP values. The following procedure was done for each of the five experiments where variation in T during HVOL was less than 2 °C: For each PAH measured by HVOL, a K_p value was determined at the T at which the HVOL was conducted (T_{HVOL}) using the log p_L^o of the compound at T_{HVOL} and the m_p and b_p terms from a regression of log K_p vs. log p_L^o from the CFE data. A series of equations of the form of equation 7.7 was compiled; one equation for each compound. The K_p value at T_{HVOL} and the TSP was entered into each

equation. It was assumed that x was the same for all compounds. When a value of x was chosen, each equation in the series returned a predicted value of $K_{p,non-exchangeable}$ for a compound. A residual was defined as

$$\frac{(\text{predicted } K_{p,\ non\ -\ exchangeable} - \text{measured } K_{p,\ non\ -\ exchangeable})^2}{(\text{measured } K_{p,\ non\ -\ exchangeable})^2} \tag{7.8}$$

the difference between the predicted $K_{p,non-exchangeable}$ values and the $K_{p,non-exchangeable}$ values as measured using HVOL. An optimization routine was used to find a single x which minimized the sum of the residuals of all compounds. An example of the fit of the non-exchangeable model to the observed data is shown in Figure 7.5. The non-exchangeable model fit the observed HVOL data within the 95% confidence interval for four of the five samples. Among the different experiments the values of x ranged from 0.6 to 1.73%, averaging 1.24%; x was largest for the particles sampled at the lowest T. At the relatively low $TSPs$ encountered in these experiments, small amounts of non-exchangeable material can greatly influence the K_p value of the lower molecular weight PAHs, resulting the slope of log K_p vs. log p_L^o plots being shallower than -1.

7.3.7 Normalization of PAH and PCDD/Fs K_p values by particle f_{om}. Recent field and laboratory work by Liang, Pankow et al. (1997) and Liang and Pankow (1996) have suggested that the G/P partitioning of PAHs and n-alkanes to urban particulate matter (UPM) is indeed *absorptive* in nature. Such behavior is analogous to the paradigm describing soil water partitioning, whereby the hydrophobic organic compounds are believed to partition into soil organic matter and partitioning is independent of the specific soil type (Chiou, Peters *et al.*, 1979; Kile, Chiou *et al.*, 1995).

For *absorptive* G/P partitioning the magnitude of K_p is affected by the amount of OM present on the particles (Equation 7.3). Particles from different sources and/or locations may have different amounts of OM. Normalizing K_p values by particle f_{om} should reduce this source of variability. In the current study it is likely that differences in the K_p values of compounds with similar p_L^o values at different locations (Figures 7.3a and b) may partially be explained by differences in the OM content of the particles among those locations. If this hypothesis is correct then for SOCs with similar p_L^o values there should be less variation in $K_{p,om}$ values than K_p values among the different

locations. To test this hypothesis the $K_{p,om}$ values of PAHs and PCDD/Fs were calculated from K_p values as measured by CFEs. In each experiment the OC content of the particles collected using HVOL was measured and the fraction of organic carbon (f_{oc}) calculated. These data and a description of the OC measurement technique has been presented by Mader and Pankow (2000). The measured f_{oc} values were converted to f_{om} as follows: When the particle is primary in origin, Countess, *et al.* (1980) observed that the mass of the OM phase is 1.2 times the mass of OC. For a particle that is secondary in nature Izumi and Fukuyama (1990) found the mass of OM phase is 2 times the mass of OC. Particles collected during rain events could only be primary in nature, f_{om} was taken as 1.2 times f_{oc}. For samples taken during stable atmospheric conditions and away from obvious local sources of primary particles f_{om} was taken as 1.8 times f_{oc}. This assumes that 60-80% of the particle is secondary in nature and takes into consideration the presence of some primary OM and the presence of water in the OM matrix. In Denver, particles were collected under stable atmospheric conditions but near sources of primary particles (*e.g.* a roadway). Liang, Pankow et al. (1997) sampled under similar circumstances in Los Angeles and assumed f_{om} was 1.6 times f_{oc}. For the Denver samples f_{om} was taken as 1.6 times f_{oc}.

The log $K_{p,om}$ values of PAHs and PCDD/Fs measured using CFEs are plotted versus log p_L^o in Figures 7.6a and b, respectively. The slope ($m_{p,om}$) and intercept ($b_{p,om}$) values for the regression lines of these data are presented in Tables 7.2 and 7.3. Comparing Figures 7.6a and b to Figures 7.3a and b, there was less variation in the $K_{p,om}$ values of compounds with similar p_L^o values among locations than for K_p values. At a given p_L^o there was approximately an order of magnitude variation in the $\bar{K}_{p,om}$ values of PAH and PCDD/Fs among the different locations.

At the 95% confidence level there was no difference in the $K_{p,om}$ values of PAHs with similar p_L^o values as measured for particles collected at the Beaverton, Denver and Iowa locations. At a given p_L^o the $K_{p,om}$ values of PAHs were larger for partitioning to diesel particles, ETS and LA-SOA than to particles collected to particles collected at the Beaverton, Denver and Iowa locations. For the PCDD/Fs with similar p_L^o values the $K_{p,om}$ values of the PCDD/Fs were the same (95% CI) at the Beaverton and Iowa

locations, but the $K_{p,om}$ of the most non-volatile PCDD/Fs measured were slightly lower at the Denver location than for PCDD/Fs with similar p_L^o values at the Beaverton and Iowa locations.

The reason for the variation in $K_{p,om}$ values of compounds with similar p_L^o values among locations could be the following: error in the conversion factor relating f_{om} to f_{oc} and/or variation in the quantity $\zeta_{om}\,MW_{om}$ among particles from differing origins. It appears that *absorptive partitioning* is important even for particles with small amounts of OM (*i.e.* Iowa particles).

7.3.8 Normalization of PAH and PCDD/F K_p values by particle f_{oc}. In practice, the conversion factor relating f_{om} to f_{oc} requires an assumption regarding the chemical composition of particle OM for which few data exists. It is currently more practical to normalize K_p by f_{oc}:

$$K_{p,oc} = K_p / f_{oc} \qquad\qquad (7.8)$$

Since f_{oc} values do not consider the chemical composition of the absorbing OM, $K_{p,oc}$ values may be less universal than $K_{p,om}$ values.

The log $K_{p,oc}$ values of PAHs and PCDD/Fs measured using CFEs are plotted versus log p_L^o in Figures 7.7a and b, respectively. The slope ($m_{p,oc}$) and intercept ($b_{p,oc}$) values for the regression lines of these data are presented in Tables 7.2 and 7.3. Comparing Figures 7.7a and b to Figures 7.3a and b, there was less variation in the $K_{p,oc}$ values of compounds with similar p_L^o values among locations than for K_p values. At a given p_L^o there was approximately an order of magnitude variation in the $K_{p,oc}$ values of PAH and PCDD/Fs among the different location. To compare the ability f_{oc} vs. f_{om} to account for differences in the magnitude of the K_p value of a given compound among locations, the r^2 value for a regression of log $K_{p,om}$ vs. log p_L^o can be compared to the r^2 value for a regression of log $K_{p,oc}$ vs. log p_L^o using data for given compound class at all locations. For plots of log $K_{p,oc}$ vs. log p_L^o and of log $K_{p,om}$ vs. log p_L^o the values of r^2 were, 0.96 and 0.97 for the PAHs and 0.88 and 0.90 for PCDDFs, respectively. Currently normalization of K_p values by particle f_{oc} is equivalent to normalizing by f_{om}. Significant

Figure 7.6 Log $K_{p,om}$ vs. log p_L^o plots for the *G/P* partitioning of selected compounds at a number of locations. **a.** PAHs **b.** PCDD/Fs.
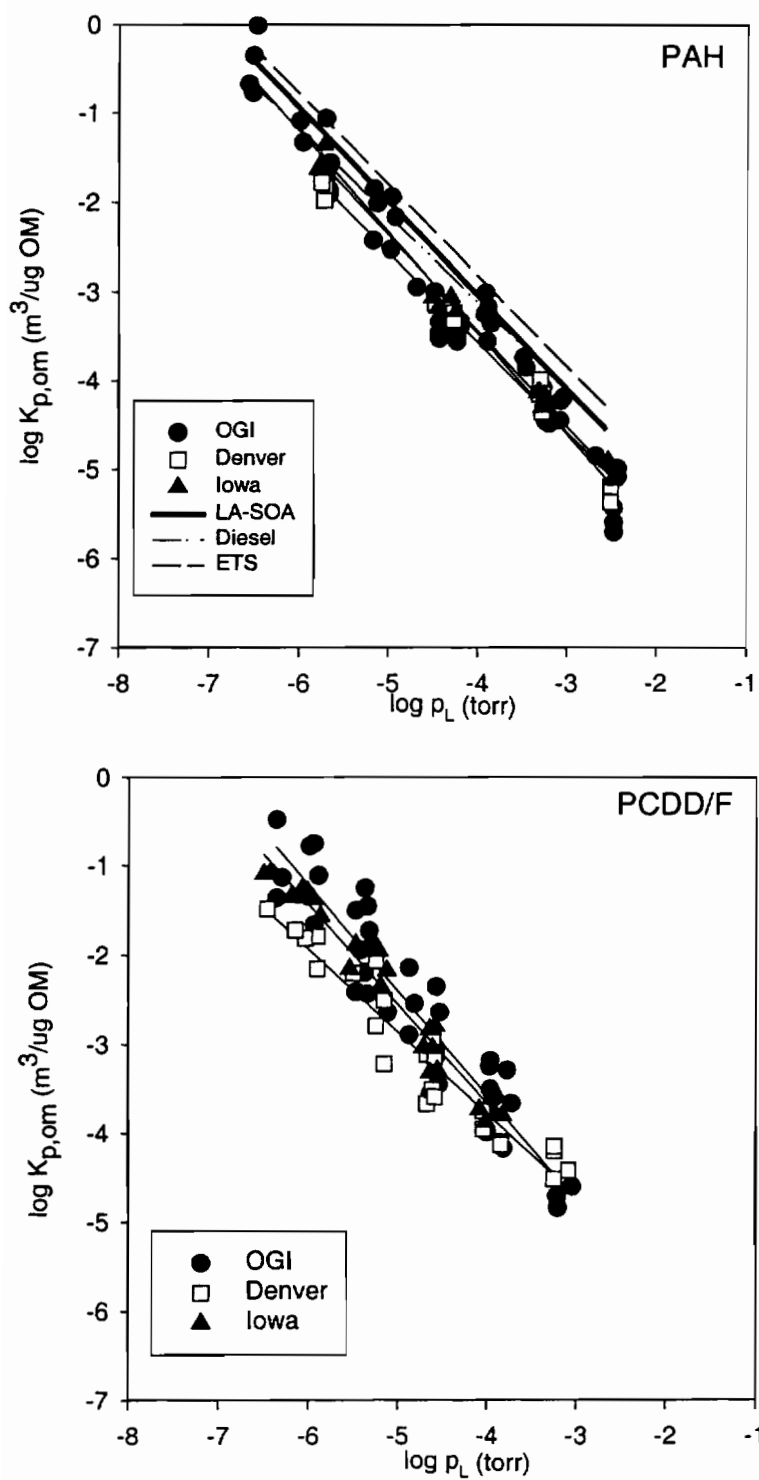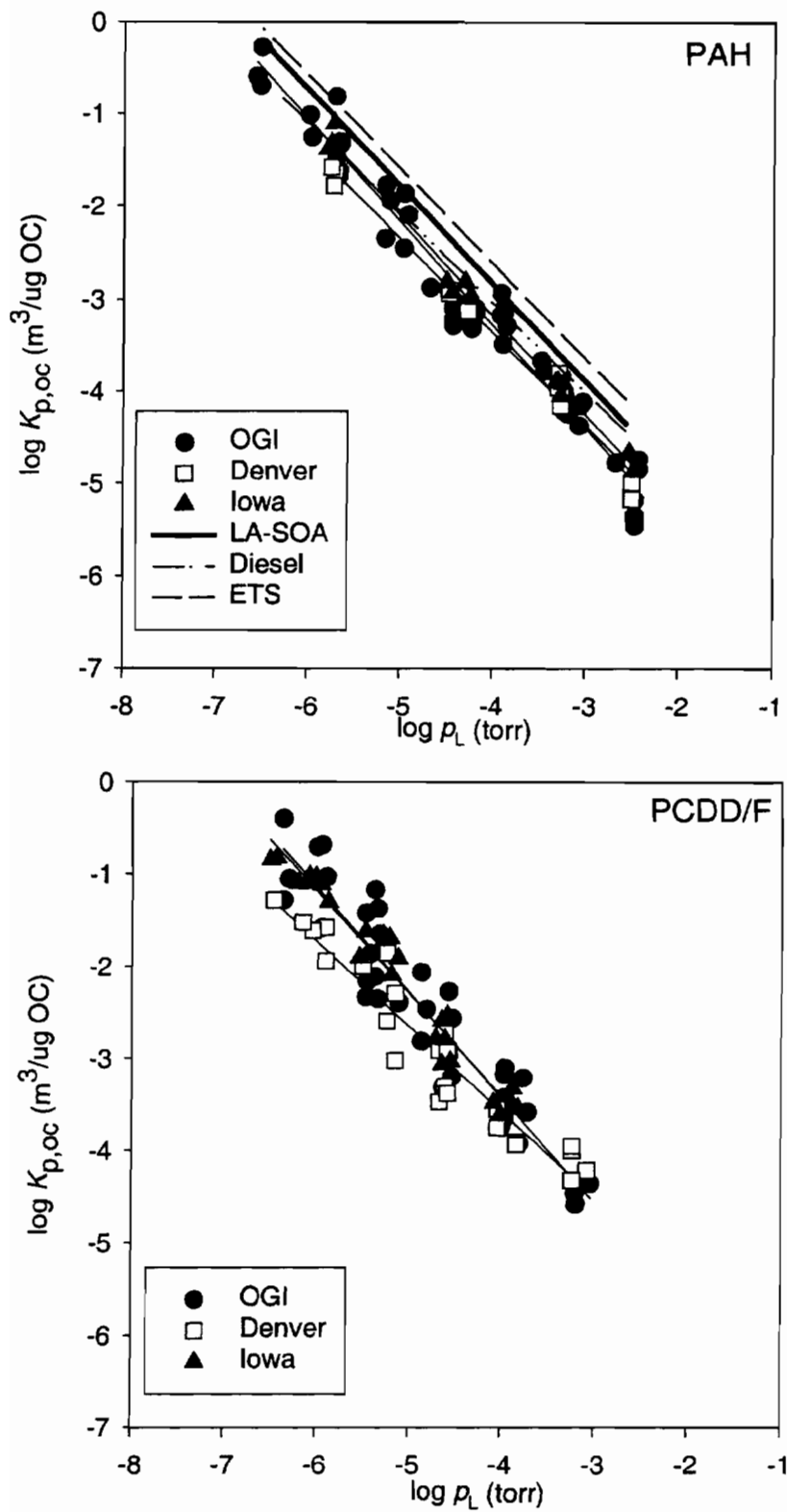
Figure 7.7 Log $K_{p,oc}$ vs. log p_L^o plots for the *G/P* partitioning of selected compounds at a number of locations. **a**. PAHs **b.** PCDD/Fs.

variation in the values of $K_{p,om}$ and $K_{p,oc}$ among locations remain. Future work evaluating the values of ζ_{om} and MW_{om} and the chemical composition of OM is necessary.

7.4 References

Brubaker, W. W., Hites, R. A. 1997. Polychlorinated dibenzo-p-dioxins and dibenzofurans: gas-phase hydroxyl radical reactions and related atmospheric removal. *Environmental Science and Technology* 31, 1805-1810.

Brzuzy, L. P., Hites, R. A. 1995. Estimating the atmospheric deposition of polychlorinated dibenzo-p-dioxins and dibenzofurans from soils. *Environmental Science and Technology* 29, 2090-2098.

Brzuzy, L. P., Hites, R. A. 1996. Global mass balance for polychlorinated dibenzo-p-dioxins and dibenzofurans. *Environmental Science and Technology* 30, 1797-1804.

Chiou, C. T. *et al.* 1979. Physical concept of soil-water equilibria for nonionic organic compounds. *Science* 206, 831-832.

Cotham, W. E., Bidleman, T. F. 1992. Laboratory investigations of the partitioning of organochlorine compounds between the gas phase and atmospheric aerosols on glass fiber filters. *Environmental Science and Technology* 26, 469-478.

Countess, R. J. *et al.* 1980. The Denver winter aerosol: A comprehensive chemical characterization. *Journal of the Air Pollution Control Association* 30, 1194-1200.

Czuczwa, J. M., Hites, R. A. 1984. Environmental fate of combustion-generated polychlorinated dioxins and furans. *Environmental Science and Technology* 18, 444-450.

Czuczwa, J. M., Hites, R. A. 1986. Airborne dioxins and dibenzofurans: Sources and fates. *Environmental Science and Technology* 20, 195-200.

Czuczwa, J. M. *et al.* 1984. Polychlorinated dibenzo-p-dioxins and dibenzofurans in sediments from Siskiwit Lake, Isle Royale. *Science* 226, 568-569.

Duarte-Davidson, R. *et al.* 1996. Exploring the balance between sources deposition and the environmental burden of PCCD/Fs in the UK terrestrial environment: an aid to identifying uncertainties and research needs. *Environmental Science and Technology* 31, 1-11.

Eitzer, B. D., Hites, R. A. 1989. Atmospheric transport and deposition of polychlorinated dibenzo-p-dioxins and dibenzofurans. *Environmental Science and Technology* 23, 1396-1401.

Izumi, K., Fukuyama, T. 1990. Photochemical aerosol formation from aromatic hydrocarbons in the presence of NOx. *Atmospheric Environment* 24a, 1433-1441.

Kamens, R. *et al.* 1995. Some observations on times to equilibrium for semivolatile polycyclic aromatic hydrocarbons. *Environmental Science and Technology* 29, 43-50.

Kile, D. E. *et al.* 1995. Partitioning of nonpolar organic pollutants from water to soil and sediment organic matters. *Environmental Science and Technology* 29, 1401-1406.

Liang, C., Pankow, J. F. 1996. Gas/particle partitioning of organic compounds to environmental tobacco smoke: partition coefficient measurements by desorption and comparison to urban particulate material. *Environmental Science and Technology* 30, 2800-2805.

Liang, C. *et al.* 1997. Gas/particle partitioning of semi-volatile organic compounds to model inorganic, model organic and ambient smog aerosols. *Environmental Science and Technology* 31, 3086-3092.

Maddalena, R. L. *et al.* 1998. Simple and rapid extraction of polycyclic aromatic hydrocarbons collected on polyurethane foam adsorbent. *Atmospheric Environment* 32, 2497-2503.

Mader, B. T., Pankow, J. F. 2000a. Normalization of the gas/particle partition coefficients of PAHs by the fraction particulate organic and elemental carbon. *Atmospheric Environment* submitted March 15, 2000.

Mader, B. T., Pankow, J. F. 2000b. Vapor pressures of polychlorinated dibenzodioxins, polychlorinated dibenzofurans and polycylic aromatic hydrocarbons: measurements and evaluation of estimation techniques. *Environmental Science and Technology* submitted March 15, 2000.

Odum, J. R. *et al.* 1996. Gas/particle partitioning and secondary organic aerosol yields. *Environmental Science and Technology* 30, 2580-2585.

Pankow, J. F. 1987. Review and comparative analysis of the theories on partitioning between the gas and aerosol particulate phases in the atmosphere. *Atmospheric Environment* 21, 2275-2283.

Pankow, J. F. 1988. The calculated effects of non-exchangeable material on the gas-particle distributions of organic compounds. *Atmospheric Environment* 22, 1405-1409.

Pankow, J. F. 1994. An absorption model of gas/particle partitioning of organic compounds in the atmosphere. *Atmospheric Environment* 28, 185-188.

Pankow, J. F. 1994. An absorption model of the gas/aerosol partitioning involved in the formation of secondary organic aerosol. *Atmospheric Environment* 28, 189-193.

Pankow, J. F., Bidleman, T. F. 1991. Effects of temperature, TSP, and percent non-exchangeable material in determining the gas-particle partitioning of organic compounds. *Atmospheric Environment* 25, 2241-2249.

Pankow, J. F., Bidleman, T. F. 1992. Interdependence of the slopes and intercepts from log-log correlations of measured gas-particle partitioning and vapor pressure-I. Theory and analysis of available data. *Atmospheric Environment* 26A, 1071-1080.

Pankow, J. F. *et al.* 1994. Gas particle partitioning of polycyclic aromatic hydrocarbons and alkanes to environmental tobacco smoke. *Environmental Science and Technology* 28, 363.

Smolka, A., Schmidt, K.G. 1997. Gas-particle partitioning before and after flue gas purification by an activated carbon filter. *Chemosphere* 34, 1075-1082.

Welsch-Paulsch, K. *et al.* 1995. Determination of the principal pathways of polychlorinated dibenzo-p-dioxins and dibenzofurans to lolium multiflorum (welsh rye grass). *Environmental Science and Technology* 29, 1090-1098.

CHAPTER 8

CONCLUSION

The overall goal of this research project was to gain a better understanding of how the physical-chemical properties of the SOC and particle phase affect the G/P partitioning of SOCs, and to improve the accuracy and universality of log K_p vs. log p_L^o correlations for PCDD/Fs and PAHs.

G/P distributions of SOCs in the atmosphere are often measured using filter/sorbent samplers. Temperature and relative humidity fluctuations during sampling and the adsorption of gaseous SOCs onto filter surfaces can cause errors in the measured G and P-phase SOC concentrations (c_g and c_p) and K_p values. Controlled field experiments (CFEs) minimize sampling artifacts. CFEs were conducted by equilibrating previously collected ambient particulate materials with SOCs generated in the gas phase using particle free ambient air maintained at a specific temperature (T) and relative humidity (RH) to prevent their diurnal cycling. A backup filter was used to correct for gas adsorption to the filter surface. Results were presented from field trials of CFEs conducted in Beaverton, OR Denver, CO and Hills, IA.

The adsorption of gaseous PCDD/Fs and PAHs to TMF and QFF was studied so that the magnitude of the influence of gas adsorption artifacts on measured values of c_g and c_p and K_p could be evaluated. For TMF's, sorption isotherms of PCDD/Fs and PAH were linear over three orders of magnitude. A 10 degree change in T caused the $K_{p,s}$ values to decrease by factors of 2.4 to 3.4. Changes in RH between 21 and 52% did not affect the measured $K_{p,s}$ values. The dependence of the partitioning on the p_L^o of the subject compounds was investigated. Within each of the three individual compound classes, plots of log $K_{p,s}$ vs. log p_L^o were linear with slopes of approximately −1. The pooled data for the three compound classes yielded a single log $K_{p,s}$ vs. log p_L^o plot for 25

$^{\circ}$C that was correlated nearly as well ($r^2 = 0.96$) as the plots for the individual compound classes ($r^2 \approx 0.95$).

For QFF, within each of the three individual compound classes, plots of log $K_{p,s}$ vs. log p_L° were found to be linear with slopes of approximately –1. At RH = 25%, the pooled log $K_{p,s}$ data at 25 $^{\circ}$C for the three compound classes were correlated with log p_L° nearly as well ($r^2 = 0.95$) as were the data for the individual compound classes ($r^2 \approx 0.97$). In general, the $K_{p,s}$ values for the PAHs and PCDD/Fs studied were found to be about a factor of two larger for partitioning to clean QFFs at RH = 25% than for TMFs at RH = 21-52%. Backup QFFs used in filter/sorbent sampling in suburban areas yielded $K_{p,s}$ values for PAHs at RH = 37% that were significantly lower than for clean QFFs at the same RH. This may have been the result of the adsorption of ambient organic compounds which at least partially blocked the direct adsorption of the SOCs to the QFF surface. Therefore, when QFFs are used to separate atmospheric gas- and particle-phase SOCs, corrections for compound-dependent gas adsorption artifacts for QFFs should probably be carried out using $K_{p,s}$ values that were obtained with ambient backup QFFs.

Using the preceding data, the adsorptive affinity of TMF and QFF for gaseous PCDD/Fs and PAHs was compared and a model developed to predict the magnitude of the influence of gas adsorption artifacts on measurements of c_g, c_p and K_p. The examination was based on values of $K_{p,x}$ (m^3/cm^2), which is the partition coefficient expressed as [ng sorbed/cm^2 of filter face] / [ng/m^3 in gas phase]. At RH values below $\approx$ 54%, the $K_{p,x}$ values for PAHs are lower on TMFs than on ambient backup QFFs. The gas adsorption artifact will therefore be lower with TMFs than with QFFs for these compounds under these conditions. Corrections for this artifact have been made in the past by using a backup filter, and subtracting the mass amount of each compound found on the backup filter from the total (particle phase + sorbed on filter) amount found on the front filter. This procedure assumes that the ng/cm^2 amounts of each SOC sorbed on the front and backup filters are equal. Since the front filter will tend to reach equilibrium with the incoming gaseous SOCs first, that equality might only be achieved after both filters have reached equilibrium with the gaseous SOCs in the sample air. The minimum air sample volume $V_{t,min}$ required to reach gas/solid sorption equilibrium with a pair of

filters is ($K_{p,x} \times 2 \times A_{filter}$) where A_{filter} (cm^2) is the per-filter face area. $K_{p,x}$ values, and therefore $V_{t,min}$ values, depend on the compound, RH, T, and filter type. Compound-dependent $V_{t,min}$ values were determined for both TMFs and QFFs. A model was developed which could be used to predict the magnitude of gas adsorption artifacts on c_g, c_p and K_p values as a function of the compound class, RH, T and filter type. The model accurately fit available measured data. Model results indicate that some of the backup-filter-based corrections described in the literature were carried out using sample volumes that were smaller than the $V_{t,min}$ values for some compounds of interest. For these studies gas adsorption artifacts may have still influenced measurements of c_g and c_p despite corrections made using backup filters.

To construct a correlation of log K_p vs. log p_L^o for a given class of SOCs, p_L^o values as a function of T are required. Moreover information regarding the mechanism of G/P partitioning can be inferred from the value of slope (m_r) of this correlation; the accuracy of the value of m_r depends directly on the accuracy of the p_L^o values used in the correlation. A systematic bias in the measured (or estimated) p_L^o values of a homologues series of compounds can bias the value of m_r. A dynamic gas saturation technique was used to directly measure the vapor pressures of 6 PAHs and 13 PCDD/Fs. The vapor pressures of the 6 PAHs were within a factor 1.5 compared to previously reported values obtained using a similar dynamic gas saturation technique. New measured vapor pressure data for 4 toxicologically significant, 2,3,7,8 substituted PCDD/F congeners and 4 non-2,3,7,8 PCDD/F congeners was significantly different than predicted values from the literature. The vapor pressure data suggests that a miscibility gap exists at room temperature for mixtures of solid phase PAHs and PCDD/Fs. Using the new vapor pressure data, four correlation methods were used to predict the vapor pressures of the PCDD/Fs at 25 °C. A correlation between p_L^o and gas chromatograph retention index (GC-RI) was the most precise and accurate. Parameters were determined for calculating the p_L^o values of 210 PCDD/Fs as function of temperature. Measured PCDD/F p_L^o data was used to evaluate estimates made using a GC-RI method with a single reference compound. A systematic difference between the measured and estimated values was observed and it was suggested that the ratio $\gamma_{test} / \gamma_{reference}$ is variable throughout this class

of compounds. It is suggested that should the GC-RI method be used in future measurements of the p_L^o values of a homologues series of compounds (i.e. chlorinated naphthalenes or chlorinated paraffins), at least one reference compound at each level of chlorination should be used to minimize systematic differences between p_{gc} and p_L^o.

Conventional high volume air sampling was used to measure ambient gas and particle-phase PAHs at an urban, suburban and rural site in Denver CO, Beaverton OR, and Hills IA, respectively. The particle-phase organic (OC) and elemental (EC) carbon was also measured. Among these locations the weight fraction of particle-phase organic (f_{oc}) and elemental carbon (f_{ec}) ranged from 0.018 to 0.20 and from 0 to 0.262, respectively. K_p values were normalized by f_{ec}, where $K_{p,ec} = K_p / f_{ec}$. For samples taken during rain events the variation in the K_p values of PAHs with similar p_L^o values was a factor one and a half among the three samples, but there was no significant difference in the $K_{p,ec}$ values. A correlation between EC and ΣPAH particle-phase concentration was observed for samples taken during rain events in Beaverton.

At the three field locations CFEs were used to determine the K_p values of PCDD/Fs and PAHs. Conventional high volume air sampling (HVOL) was also used to determine the K_p values of the PAHs. HVOL was conducted throughout the night and during rain events with changes of only 2 °C in temperature and 10% the relative humidity (RH); backup filters were used to correct for gas adsorption artifacts. Plots of log K_p vs. log p_L^o made using HVOL data had a slope shallower than -1 but plots made using data from CFEs had a slope nearer to -1. The values of K_p determined from both methods were similar for the low vapor pressure compounds but different for the higher vapor pressure compounds. It was suggested that for PAHs, slopes shallower than -1 may be due to the presence of non-exchangeable material present on the native particles. Model results suggest that the mass percent of the collected particles that was non-exchangeable ranged from 0.6 to 1.73%,

To compensate for differences in the organic matter content and organic carbon content of particles among locations, K_p values were normalized by the weight fraction of particle-phase organic carbon (f_{oc}) and organic matter phase (f_{om}), where $K_{p,om} = K_p / f_{om}$ and $K_{p,oc} = K_p / f_{oc}$. There was less variation in the $K_{p,oc}$ and $K_{p,om}$ values of compounds

with similar p_L^o values among locations than for K_p values. Among the three field locations and three studies from the literature, the K_p values of PAHs with similar p_L^o values varied by over 2.5 orders of magnitude; the $K_{p,om}$ and $K_{p,oc}$ values varied by one order of magnitude. Variation in the $K_{p,om}$ and $K_{p,oc}$ values among locations may be due to error in the conversion factor relating f_{oc} to f_{om} and/or differences in the chemical composition of particulate organic matter phases (OM) among locations and/or sources of particles. It appears that *ab*sorptive partitioning is important even for particles with small amounts of OC ($f_{oc} < 0.02$). Since 1) Particles from different sources and/or locations may have different amounts of OC (and OM) and 2) the OC (and OM) content may vary with time. If a log K_p vs. log p_L^o correlation is to be used to predict *G/P* partitioning behavior of a given class of SOCs at another time and/or location K_p values should normalized by the f_{oc} of the collected particles or if the chemical composition of the particle phase is known by f_{om}.

BIOGRAPHY

The author was raised in Stillwater, Minnesota, a small town on the banks of the St. Croix River. After graduating from Stillwater High School in June of 1989, the author attended college at the University of Minnesota in Minneapolis, Minnesota. He was enrolled in the Institute of Technology and earned a B.S. degree in Chemistry in 1993 graduating cum laude. During his summer vacations from college he worked at a canoe outfitter and as a fishing guide in Northern Minnesota's Boundary Waters Canoe Area Wilderness, his experiences there motivated him to pursue a career in environmental chemistry. At the University of Minnesota, Brian met Prof. Steven J. Eisenreich who encouraged him to join his research group. Brian's Masters thesis work involved the sorption of nonionic hydrophobic organic compounds to mineral surfaces. Brian also spent part of the summer of 1994 at the Canadian Department of Fisheries and Ocean's Experimental Lakes Area research station in Kenora, Ontario. Brian took air, water and lake-sediment samples as part of work related to the study of the biogeochemical cycling of polychlorinated biphenyls (PCBs). He was awarded the "Louis Fontnelli Graduate Student Award" for his achievements in his coursework and research. Brian earned a Masters degree in Civil Engineering from the University of Minnesota in June of 1996.

Brian was interested in the work of Professor James F. Pankow and was fortunate to pursue a Ph.D. in Environmental Science and Engineering at the Oregon Graduate Institute of Science and Technology under his supervision. He spent three and a half years working on the gas/filter and gas/particle partitioning of semivolatile organic compounds. In 1999, Brian traveled to the University of Colorado at Denver and University of Iowa to conduct experiments studying the gas/particle-partitioning behavior of polychlorinated dibenzodioxins, polychlorinated dibenzofurans and polycylic aromatic hydrocarbons. For his achievements in coursework, research and service he was awarded

147

the American Chemical Society's "Graduate Student Award" and "Graduate Student Paper Award" as well as the Oregon Graduate Institute of Science and Technology's "Student Achievement Award" all in 1999. Brian completed the requirements for his Ph.D. in March of 2000.

PUBLICATIONS

Mader, B.T. Pankow, J.F. Gas/solid partitioning of polychlorinated dibenzodioxins (PCDDs), polychlorinated dibenzofurans (PCDFs) and polycyclic aromatic hydrocarbons (PAHs) from the gas phase to filter surfaces 1. Teflon membrane filters. *Atmospheric Environment.* In press 4/15/2000.

Mader, B.T. Pankow, J.F. Gas/solid partitioning of polychlorinated dibenzodioxins (PCDDs), polychlorinated dibenzofurans (PCDFs) and polycyclic aromatic hydrocarbons (PAHs) from the gas phase to filter surfaces 2. Quartz filters. Submitted to *Atmospheric Environment* 4/15/2000.

Mader, B.T. Pankow, J.F. Gas/solid partitioning of polychlorinated dibenzodioxins (PCDDs), polychlorinated dibenzofurans (PCDFs) and polycyclic aromatic hydrocarbons (PAHs) from the gas phase to filter surfaces: 3. Comparison of the gas adsorption artifact potential of Teflon membrane vs.quartz fiber filters and prediction of the magnitude of gas adsorption artifacts. Submitted to *Environmental Science and Technology* 3/15/2000.

Mader, B.T. Pankow, J.F. Vapor pressures of polychlorinated dibenzodioxins (PCDDs), polychlorinated dibenzofurans (PCDFs) and polycylic aromatic hydrocarbons (PAHs): Measurements and evaluation of estimation techniques. Submitted to *Environmental Science and Technology* 3/15/2000.

Mader, B.T. Pankow, J.F. Measurements of ambient gas- and particle-phase polycyclic aromatic hydrocarbons (PAHs) and particle-phase organic (OC) and elemental (EC) carbon: Normalization of the gas/particle partition coefficients of PAHs by the weight fraction of OC and EC. Submitted to *Environmental Science and Technology* 3/15/2000.

Mader, B.T. Pankow, J.F. Controlled field experiments to study the gas/particle partitioning of polychlorinated dibenzodioxins (PCDDs), polychlorinated dibenzofurans (PCDFs) and polycyclic aromatic hydrocarbons (PAHs), to urban, suburban, and rural particulate materials. Submitted to *Environmental Science and Technology* 3/15/2000.

Pankow, J.F.; Mader, B.T.; Isabelle, L.M.; Lou, W.; Pavlick, A.; Liang, C. The conversion of nicotine in tobacco smoke to its volatile and available free base form through the action of gaseous ammonia. *Environmental Science and Technology.* 1997, 31, 2428-2433.

Mader, B.T.; K.U. Goss.; S.J. Eisenreich. Sorption of nonionic, hydrophobic organic chemicals to mineral surfaces. *Environmental Science and Technology.* 1997, 31, 1079-1086.

Mader, B.T.; Pankow, J.F.; Vapor pressures of polychlorinated dibenzodioxins (PCDDs), polychlorinated dibenzofurans (PCDFs) and polycylic aromatic hydrocarbons (PAHs): Measurements and evaluation of estimation techniques. Pre-print ACS extended abstract. Division of Environmental Chemistry, 220th National Meeting of the American Chemical Society. Washington, DC. August 20-24, 2000.

Mader, B.T.; Pankow, J.F.; Controlled field experiments: A unique method to study the fundamental processes controlling the gas-particle partitioning behavior of semivolatile organic compounds (SOCs). Pre-print extended abstract. 18th Annual American Association for Aerosol Research Conference. Tacoma, WA. October 11-15, 1999.

Mader, B.T.; Pankow, J.F.; Controlled field experiments: A unique method to study the fundamental processes controlling the gas-particle partitioning behavior of semivolatile organic compounds (SOCs). Pre-print ACS extended abstract. Division of Environmental Chemistry, 217th National Meeting of the American Chemical Society. Anaheim, CA. March 21-25, 1999. pg. 428-430.